

# The $z$ Transform

## INTRODUCTION

In this chapter and the next, we will examine discrete-time signals and systems using transforms. Thus the subjects covered will largely parallel the analogous material presented in Chapters 4 and 5 for continuous-time signals and systems. Specifically, the *discrete-time Fourier transform (DTFT)* is analogous to the continuous-time Fourier transform covered in Chapter 4, while the  *$z$  transform* is the discrete-time counterpart of the Laplace transform presented in Chapter 5. However, as we saw in the continuous-time case, the notions of regions of convergence and of poles and zeros provide valuable insight into the properties of the Fourier transform, and as might be expected, this is equally true in the discrete-time case. Hence, instead of presenting the discrete-time transforms in an analogous order to Chapters 4 and 5, we will first investigate the  $z$  transform and its properties in this chapter, and then study the discrete-time Fourier transform in depth in Chapter 7.

Many of the properties and uses of the  $z$  transform can be anticipated from the corresponding Laplace transform results. For instance, convolution of signals in the time domain corresponds to multiplication of the associated

$z$  transforms. Also, the system function  $H(z)$  is readily defined for a discrete-time LTI system and plays the same role as  $H(s)$  for continuous-time systems. In particular, the frequency response of the system (DTFT of its impulse response) is a special case of the system function and can be determined to within a scaling constant from the pole/zero plot for  $H(z)$ .

## 6.1

### The Eigenfunctions of Discrete-Time LTI Systems

In Section 3.6 we showed that if the input to an LTI system is written as a linear combination of basis functions  $\phi_k[n]$ , that is,

$$x[n] = \sum_k a_k \phi_k[n], \quad (6.1.1)$$

then the output of the system can be similarly expressed as

$$y[n] = \sum_k a_k \psi_k[n], \quad (6.1.2)$$

where the  $\psi_k[n]$  are output basis functions given by

$$\psi_k[n] = \phi_k[n] * h[n]. \quad (6.1.3)$$

This is, in fact, simply a general statement of the property of linearity. In the special case where the input and output basis functions  $\phi_k[n]$  and  $\psi_k[n]$  have the same form, that is,

$$\psi_k[n] = b_k \phi_k[n] \quad (6.1.4)$$

for constants  $b_k$ , the functions  $\phi_k[n]$  are called *eigenfunctions* of the discrete-time LTI system with corresponding *eigenvalues*  $b_k$ . The eigenfunctions are then basis functions for both the input  $x[n]$  and the output  $y[n]$  because

$$y[n] = \sum_k c_k \phi_k[n], \quad (6.1.5)$$

for constants  $c_k = a_k b_k$ .

In analogy with the continuous-time case, the eigenfunctions of discrete-time LTI systems are the complex exponentials

$$\phi_k[n] = z_k^n \quad (6.1.6)$$

for arbitrary complex constants  $z_k$ . Alternatively, to avoid the implication that the eigenfunctions form a finite or countably infinite set, we will write them as simply

$$\phi[n] = z^n, \quad (6.1.7)$$

where  $z$  is a complex variable. To see that complex exponentials are indeed eigenfunctions of any LTI system, we utilize the convolution sum in Eq. (3.6.10), with  $x[n] = \phi[n] = z^n$ , to write the corresponding output  $y[n] = \psi[n]$  as

$$\begin{aligned}\psi[n] &= \sum_{m=-\infty}^{\infty} h[m]\phi[n-m] \\ &= \sum_{m=-\infty}^{\infty} h[m]z^{n-m} \\ &= z^n \sum_{m=-\infty}^{\infty} h[m]z^{-m} \\ &= H(z)z^n.\end{aligned}\tag{6.1.8}$$

Hence the complex exponential  $z^n$  is an eigenfunction of the system for any value of  $z$ , and  $H(z)$  is the corresponding eigenvalue given by

$$H(z) = \sum_{m=-\infty}^{\infty} h[m]z^{-m}.\tag{6.1.9}$$

The above results motivate the definitions of the  $z$  transform, the discrete-time Fourier transform (DTFT), and the discrete Fourier series (DFS) to be presented in this chapter and the next. In particular, if the basis functions for the input can be enumerated as

$$\phi_k[n] = z_k^n,$$

that is, if  $x[n]$  can be expressed in the form of Eq. (6.1.1) as

$$x[n] = \sum_k a_k z_k^n,\tag{6.1.10}$$

then the corresponding output is simply, from Eqs. (6.1.2) and (6.1.8),

$$y[n] = \sum_k a_k H(z_k) z_k^n.\tag{6.1.11}$$

The discrete Fourier series for periodic signals is of this form, with  $z_k = e^{j2\pi k/N}$ . If, on the other hand, the required basis functions cannot be enumerated, we must utilize the continuum of functions  $\phi[n] = z^n$  to represent  $x[n]$  and  $y[n]$  in the form of integrals. When  $z$  is restricted to have unit magnitude (that is,  $z = e^{j\Omega}$ ), the resulting representation is called the *discrete-time Fourier transform*, while if  $z$  is an arbitrary complex variable, the full  *$z$ -transform* representation results.

**EXAMPLE 6.1** Consider the output of an LTI system having  $h[n] = a^n u[n]$  with  $|a| < 1$  to the sinusoidal input

$$x[n] = 2 \cos \Omega_0 n = e^{j\Omega_0 n} + e^{-j\Omega_0 n}.$$

This input signal is of the form of Eq. (6.1.10), with  $z_1 = e^{j\Omega_0}$  and  $z_2 = e^{-j\Omega_0}$ . Therefore the output is given by Eq. (6.1.11) as simply

$$y[n] = H(e^{j\Omega_0})e^{j\Omega_0 n} + H(e^{-j\Omega_0})e^{-j\Omega_0 n}. \quad (6.1.12)$$

Computing  $H(e^{j\Omega_0})$ , we utilize Eq. (6.1.9) with  $h[n] = a^n u[n]$  and  $z = e^{j\Omega_0}$  to produce

$$\begin{aligned} H(e^{j\Omega_0}) &= \sum_{n=-\infty}^{\infty} h[n]e^{-j\Omega_0 n} = \sum_{n=0}^{\infty} a^n e^{-j\Omega_0 n} \\ &= \sum_{n=0}^{\infty} (ae^{-j\Omega_0})^n = \frac{1}{1 - ae^{-j\Omega_0}} = Ae^{j\phi}. \end{aligned}$$

That is, we define  $A$  and  $\phi$  to be the magnitude and angle, respectively, of the complex number  $H(e^{j\Omega_0})$ . Similarly,  $H(e^{-j\Omega_0})$  is readily determined to be

$$H(e^{-j\Omega_0}) = \frac{1}{1 - ae^{j\Omega_0}} = Ae^{-j\phi}.$$

Hence, from Eq. (6.1.12), the output  $y[n]$  is obtained as

$$\begin{aligned} y[n] &= Ae^{j\phi}e^{j\Omega_0 n} + Ae^{-j\phi}e^{-j\Omega_0 n} \\ &= 2A \cos(\Omega_0 n + \phi). \end{aligned} \quad (6.1.13)$$

Thus, as expected, a sinusoidal input to this (or any other) stable LTI system produces a sinusoidal output with the same frequency  $\Omega_0$  but, in general, a different amplitude  $A$  and phase  $\phi$  that depend upon the *frequency response*  $H(e^{j\Omega_0})$ .

## 6.2

### The Region of Convergence

The function  $H(z)$  in Eq. (6.1.9) is the  $z$  transform of the impulse response  $h[n]$ . Similarly, for a general signal  $x[n]$ , the corresponding  $z$  transform is defined by

$$X(z) = \sum_{n=-\infty}^{\infty} x[n]z^{-n}. \quad (6.2.1)$$

As in the case of the Laplace transform, the  $z$  transform usually converges for only a certain range of values of the complex variable  $z$  known as the

region of convergence (ROC), and this region must be specified along with the algebraic form of  $X(z)$  in order for the  $z$  transform to be complete. This important point is best illustrated by several examples.

**EXAMPLE 6.2** Letting  $x[n]$  be the causal real exponential

$$x[n] = a^n u[n],$$

we have from Eq. (6.2.1) that

$$\begin{aligned} X(z) &= \sum_{n=-\infty}^{\infty} a^n u[n] z^{-n} \\ &= \sum_{n=0}^{\infty} (az^{-1})^n. \end{aligned}$$

As shown in Problem 2.4(b), this summation converges if, and only if,  $|az^{-1}| < 1$ , or equivalently  $|z| > |a|$ , in which case

$$X(z) = \frac{1}{1 - az^{-1}}, \quad |z| > |a|. \quad (6.2.2)$$

Alternatively, by multiplying the numerator and denominator of Eq. (6.2.2) by  $z$ , we may write  $X(z)$  as

$$X(z) = \frac{z}{z - a}, \quad |z| > |a|. \quad (6.2.3)$$

Both forms of  $X(z)$  in Eqs. (6.2.2) and (6.2.3) are useful, depending upon the application. Specifically, when performing the inverse  $z$  transform or designing system implementations, we will find the form in Eq. (6.2.2) to be preferable. However, to determine the poles and zeros of  $X(z)$ , Eq. (6.2.3) is the more useful form. In particular, Eq. (6.2.3) clearly indicates that we have a pole at  $z = a$  and a zero at  $z = 0$ . These pole/zero values can also be obtained from Eq. (6.2.2), but the zero at  $z = 0$  (where  $z^{-1} = \infty$ ) is not quite so obvious from this form for  $X(z)$ . The pole and zero of  $X(z)$  are shown in Fig. 6.1 by an  $x$  and  $o$ , respectively, as before, in four cases: namely,  $0 < a < 1$ ,  $-1 < a < 0$ ,  $a > 1$ , and  $a < -1$ . The region of convergence  $|z| > |a|$  is also indicated by the shaded area. The locus of points for which  $|z| = 1$  (that is,  $z = e^{j\Omega}$ ) is called the *unit circle* and is usually displayed, as shown, on such pole/zero plots. As we will see, the unit circle plays the same role for the  $z$  transform as the  $j\omega$  axis plays for the Laplace transform. Note, in particular, that for a stable system ( $|a| < 1$ ), the unit circle is contained within the ROC, but not otherwise.

Note that the boundary cases for  $a = 1$  and  $a = -1$  correspond simply to the signals  $x[n] = u[n]$  and  $x[n] = (-1)^n u[n]$ , respectively.

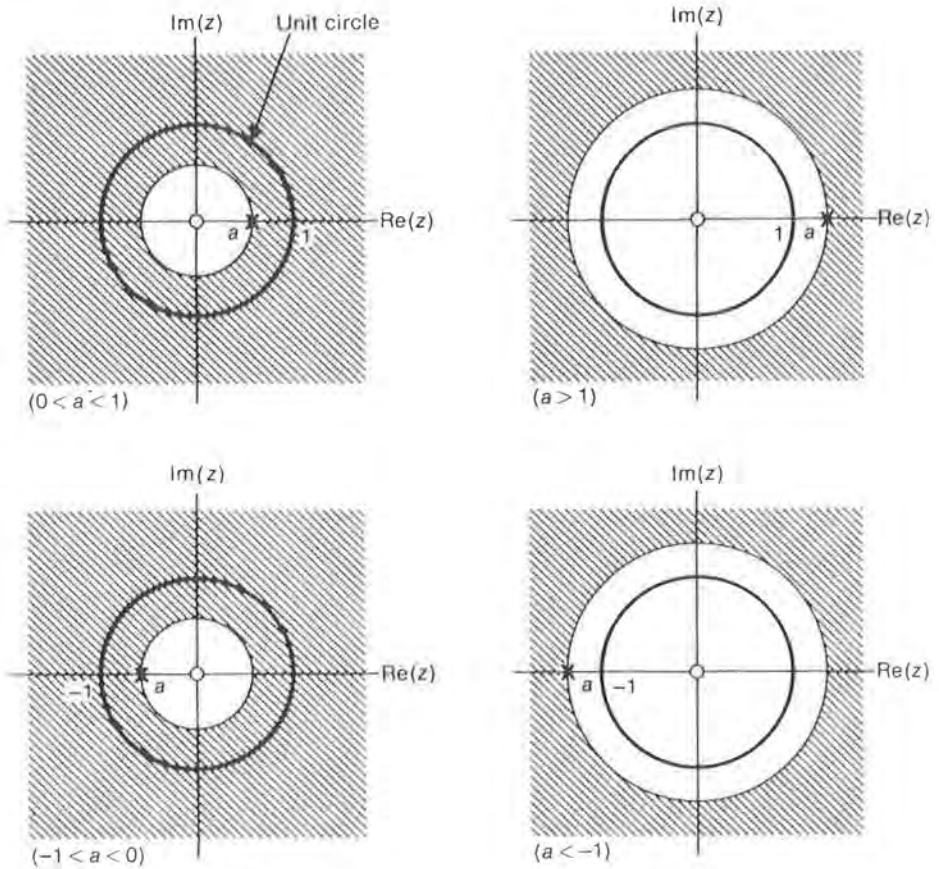


**FIGURE 6.1** Regions of convergence of the form  $|z| > |a|$ .

Therefore, from Eq. (6.2.2) we have the specific  $z$ -transform pairs

$$u[n] \leftrightarrow \frac{1}{1 - z^{-1}}, \quad |z| > 1, \quad (6.2.4)$$

and

$$(-1)^n u[n] \leftrightarrow \frac{1}{1 + z^{-1}}, \quad |z| > 1, \quad (6.2.5)$$

Hence, in each of these cases the pole lies directly on the unit circle at  $z = 1$  or  $z = -1$ , respectively, with the ROC being everywhere outside the unit circle.

**EXAMPLE 6.3** Consider next the anticausal real exponential

$$x[n] = -a^n u[-n - 1],$$

which equals zero for  $n \geq 0$ . The corresponding  $z$  transform is then

$$\begin{aligned} X(z) &= - \sum_{n=-\infty}^{-1} a^n z^{-n} \\ &= - \sum_{n=1}^{\infty} a^{-n} z^n \\ &= -a^{-1}z \sum_{n=0}^{\infty} (a^{-1}z)^n. \end{aligned}$$

As noted earlier from Problem 2.4(b), this summation converges if, and only if  $|a^{-1}z| < 1$ , or equivalently  $|z| < |a|$ , in which case

$$X(z) = \frac{-a^{-1}z}{1 - a^{-1}z} = \frac{1}{1 - az^{-1}}, \quad |z| < |a|. \quad (6.2.6)$$

Alternatively, as before, by multiplying the numerator and denominator of Eq. (6.2.6) by  $z$ , we may also write  $X(z)$  as

$$X(z) = \frac{z}{z - a}, \quad |z| < |a|. \quad (6.2.7)$$

Comparing these results to those in Eqs. (6.2.2) and (6.2.3), we observe that the algebraic form of  $X(z)$  in these two examples is exactly the same and hence that the  $z$  transforms for these two different signals are distinguished only by their differing regions of convergence. Therefore, as in the case of the Laplace transform, if the ROC is not stated explicitly (or at least implied) along with the algebraic form of the  $z$  transform, the transform is, in general, not unique and is thus incomplete. Pole/zero plots for  $X(z)$  with their associated regions of convergence are shown in Fig. 6.2 for four ranges of the parameter  $a$ , as before.

The boundary cases of  $a = 1$  and  $a = -1$  now imply the specific  $z$ -transform pairs

$$-u[-n - 1] \leftrightarrow \frac{1}{1 - z^{-1}}, \quad |z| < 1, \quad (6.2.8)$$

and

$$-(-1)^n u[-n - 1] \leftrightarrow \frac{1}{1 + z^{-1}}, \quad |z| < 1, \quad (6.2.9)$$

and thus the pole lies directly on the unit circle at  $z = 1$  or  $z = -1$ , respectively, in each of these cases, as before. However, in contrast to the corresponding causal transforms, the ROC now consists of all points *inside* the unit circle.

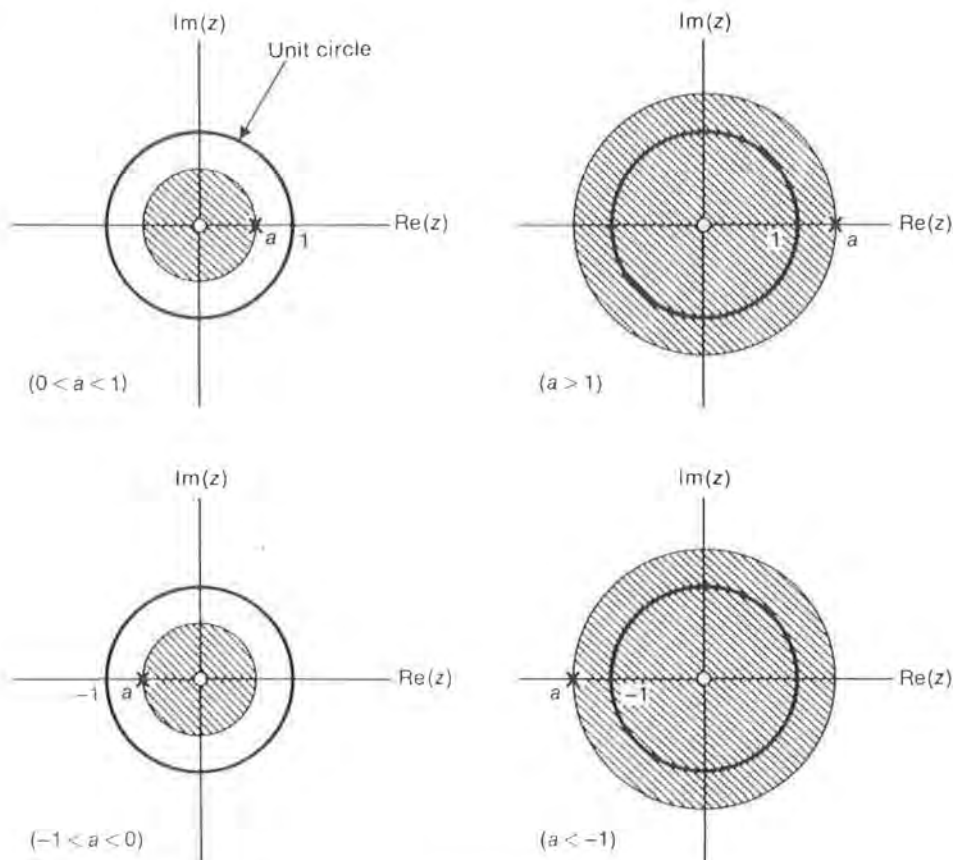


**FIGURE 6.2** Regions of convergence of the form  $|z| < |a|$ .

**EXAMPLE 6.4** Let  $x[n]$  be the sum of two causal exponentials, that is,

$$x[n] = a^n u[n] + b^n u[n], \quad a \neq b.$$

Clearly then,  $X(z)$  is the sum of the corresponding  $z$  transforms, and thus

$$\begin{aligned} X(z) &= \frac{1}{1 - az^{-1}} + \frac{1}{1 - bz^{-1}} \\ &= \frac{2 - (a + b)z^{-1}}{(1 - az^{-1})(1 - bz^{-1})} \\ &= \frac{2z[z - (a + b)/2]}{(z - a)(z - b)}. \end{aligned}$$

The associated region of convergence has the form

$$|z| > \max(|a|, |b|)$$

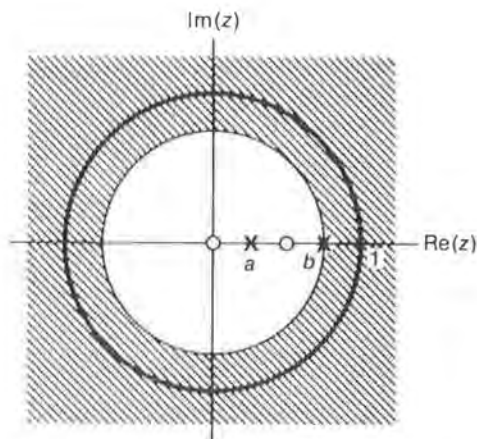


**FIGURE 6.3** Pole/zero plot with ROC for  $[a^n + b^n]u[n]$ ,  $0 < a < b < 1$ .

because both component transforms must converge in order for the overall transform to converge. Hence  $X(z)$  has two poles at  $z = a$  and  $z = b$  and two zeros at  $z = 0$  and  $z = (a + b)/2$ , as depicted in the pole/zero plot in Fig. 6.3 for the case of  $0 < a < b < 1$ .

**EXAMPLE 6.5** Letting  $x[n]$  be the sum of causal and anticausal exponentials

$$x[n] = a^n u[n] + b^n u[-n - 1], \quad a \neq b,$$

we have, from Examples 6.2 and 6.3, that

$$\begin{aligned} X(z) &= \frac{1}{1 - az^{-1}} - \frac{1}{1 - bz^{-1}} \\ &= \frac{(a - b)z^{-1}}{(1 - az^{-1})(1 - bz^{-1})} \\ &= \frac{(a - b)z}{(z - a)(z - b)}, \end{aligned}$$

with an associated region of convergence (if it exists at all) of the form

$$|a| < |z| < |b|.$$

That is, since the ROC for  $a^n u[n]$  is given by  $|z| > |a|$  and the ROC for  $b^n u[-n - 1]$  has the form  $|z| < |b|$ , both conditions must be satisfied in order for  $X(z)$  to exist. Thus, in particular, the transform  $X(z)$  does not converge for any value of  $z$  unless  $|b| > |a|$ . Pole/zero plots for this transform are displayed in Fig. 6.4 for the following three cases:  $1 > b > a > 0$ ,  $b > 1 > a > 0$ , and  $b > a > 1$ .

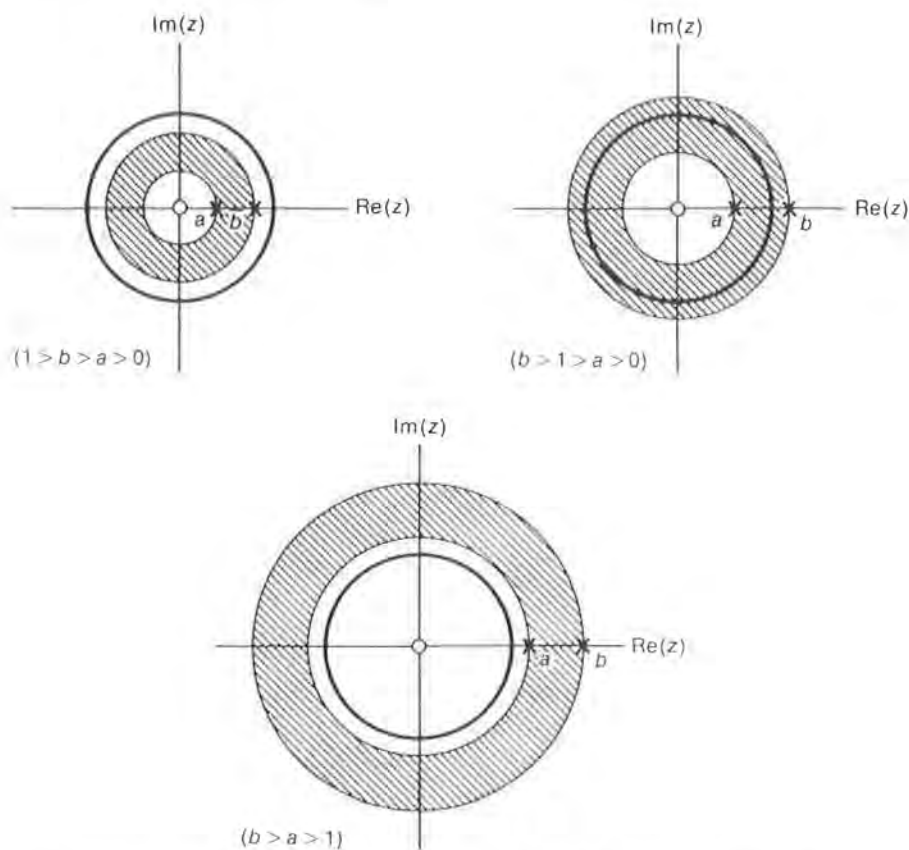


FIGURE 6.4 Pole/zero plots with ROC for  $a^n u[n] + b^n u[-n - 1]$ .

### 6.2.1 ■ ROC Properties

The properties of the region of convergence for the  $z$  transform closely parallel those for the Laplace transform, with vertical lines in the  $s$  plane being analogous to circles in the  $z$  plane and vertical strips in the  $s$  plane corresponding to annular rings in the  $z$  plane. There are, however, a few exceptions concerning convergence at  $z = 0$  and/or  $z = \infty$ . As before, the ROC properties are associated with right-sided, left-sided, two-sided, and finite-duration signals (defined in Section 2.6), as follows:

*Right-Sided Signals.* If  $x[n]$  is right-sided and  $X(z)$  converges for some value of  $z$ , then the ROC must be of the form

$$|z| > r_{\max},$$

or else

$$\infty > |z| > r_{\max},$$

where  $r_{\max}$  is the maximum radius of any of the poles. That is,  $X(z)$  converges everywhere outside the circle  $|z| = r_{\max}$  with the possible exception of  $z = \infty$ . In particular, if  $x[n]$  is causal, the ROC has the simple form  $|z| > r_{\max}$ . However, if  $x[n]$  is right-sided but not causal (that is, if  $x[n] = 0$  for  $n < n_0 < 0$  but  $x[n_0] \neq 0$ ), then  $z = \infty$  is not included in the ROC. This is readily seen from the corresponding  $z$  transform,

$$\begin{aligned} X(z) &= \sum_{n=n_0}^{\infty} x[n]z^{-n} \\ &= x[n_0]z^{-n_0} + x[n_0 + 1]z^{-(n_0+1)} + \cdots, \end{aligned}$$

because the term  $x[n_0]z^{-n_0}$  becomes infinite at  $z = \infty$  if  $n_0$  is negative. Therefore, unlike the Laplace transform case, we can tell that a discrete-time signal is causal (not just right-sided) from the ROC for its  $z$  transform if  $z = \infty$  is included. Examples of regions of convergence for right-sided (causal) signals are shown in Figs. 6.1 and 6.3.

*Left-Sided Signals.* If  $x[n]$  is a left-sided signal and  $X(z)$  converges for some value of  $z$ , then the ROC must be of the form

$$|z| < r_{\min},$$

or else

$$0 < |z| < r_{\min},$$

where  $r_{\min}$  equals the minimum radius of any of the poles. That is,  $X(z)$  converges everywhere inside the circle  $|z| = r_{\min}$  in the  $z$  plane with the possible exception of the point  $z = 0$ . In particular, if  $x[n]$  is anticausal, the ROC has the simple form  $|z| < r_{\min}$ . However, if  $x[n]$  is left-sided but not anticausal (that is, if  $x[n] = 0$  for  $n > n_0 > 0$  but  $x[n_0] \neq 0$ ), then  $z = 0$  is excluded from the ROC. This is readily seen from the corresponding  $z$  transform,

$$\begin{aligned} X(z) &= \sum_{n=-\infty}^{n_0} x[n]z^{-n} \\ &= \cdots + x[n_0 - 1]z^{-(n_0-1)} + x[n_0]z^{-n_0}, \end{aligned}$$

since the term  $x[n_0]z^{-n_0}$  becomes infinite at  $z = 0$  if  $n_0 > 0$ . Hence, unlike the Laplace transform case, we can tell that a discrete-time signal is anticausal (not just left-sided) from the ROC for its  $z$  transform if the point  $z = 0$  is included. Examples of regions of convergence for left-sided (anticausal) signals are shown in Fig. 6.2.

*Finite-Duration Signals.* If  $x[n]$  has finite duration and  $X(z)$  converges for some value of  $z$ , then it converges over the entire  $z$  plane except possibly at  $z = 0$  and/or  $z = \infty$ . This follows from the fact that a finite-duration signal is both right-sided and left-sided, and thus  $X(z)$  must converge both inside and outside of circles of finite radius except possibly at

$z = 0$  and/or  $z = \infty$ . Hence there can be no finite poles in  $X(z)$  except possibly at  $z = 0$  because, by definition,  $X(z)$  does not converge at a pole. These finite-duration properties are illustrated by the following simple examples:

$$\begin{aligned}\delta[n] &\leftrightarrow 1, \quad \text{for all } z; \\ \delta[n-1] &\leftrightarrow z^{-1}, \quad |z| > 0; \\ \delta[n+1] &\leftrightarrow z, \quad |z| < \infty; \\ \delta[n+1] + \delta[n-1] &\leftrightarrow z + z^{-1}, \quad 0 < |z| < \infty.\end{aligned}$$

*Two-Sided Signals.* If  $x[n]$  is two-sided and  $X(z)$  converges for some value of  $z$ , then the ROC must be of the form

$$r_1 < |z| < r_2,$$

where  $r_1$  and  $r_2$  are the radii of (at least) two of the poles. That is, the ROC is an annular ring in the  $z$  plane between the circles  $|z| = r_1$  and  $|z| = r_2$ . This follows from the fact that  $x[n]$  can be written as the sum of the causal signal  $x_1[n] = x[n]u[n]$  and the anticausal signal  $x_2[n] = x[n]u[-n-1]$ , and thus  $X(z) = X_1(z) + X_2(z)$ . Therefore, since  $X_1(z)$  converges for  $|z| > r_1$  and  $X_2(z)$  converges for  $|z| < r_2$ , it follows that  $X(z)$  can only converge if  $r_1 < r_2$ , and then only in the annular ring  $r_1 < |z| < r_2$ . Sample regions of convergence for two-sided signals are shown in Fig. 6.4.

### 6.3

#### The Inverse $z$ Transform

There are several useful procedures for inverting a given  $z$  transform  $X(z)$  to determine the corresponding signal  $x[n]$ . First, as in the case of the Laplace transform, a formal and elegant expression can be derived for the inverse  $z$  transform; but although important theoretically, this formula is cumbersome to use in practice. Hence, in addition to the formal expression, we will present alternative and simpler methods to calculate the inverse  $z$  transform.

The theoretical basis for the inverse  $z$  transform is the Cauchy integral theorem from the theory of complex variables, which states that

$$\frac{1}{2\pi j} \oint_{\Gamma} z^{k-1} dz = \delta[k], \quad (6.3.1)$$

where  $\Gamma$  is a counterclockwise contour of integration enclosing the origin. To employ this theorem, we multiply both sides of the  $z$ -transform definition in Eq. (6.2.1) by  $z^{k-1}/2\pi j$  and integrate along a convenient

contour  $\Gamma$  in the ROC (such as the unit circle), obtaining

$$\begin{aligned} \frac{1}{2\pi j} \oint_{\Gamma} X(z) z^{k-1} dz &= \frac{1}{2\pi j} \oint_{\Gamma} \left[ \sum_{n=-\infty}^{\infty} x[n] z^{-n} \right] z^{k-1} dz \\ &= \sum_{n=-\infty}^{\infty} x[n] \frac{1}{2\pi j} \oint_{\Gamma} z^{-n+k-1} dz \\ &= \sum_{n=-\infty}^{\infty} x[n] \delta[k-n] = x[k]. \end{aligned}$$

Thus, replacing  $k$  by  $n$ , we see that the inverse  $z$  transform may be expressed as

$$x[n] = \frac{1}{2\pi j} \oint_{\Gamma} X(z) z^{n-1} dz. \quad (6.3.2)$$

Clearly, a suitable  $\Gamma$  can always be found for this contour integration since the ROC for  $X(z)$  is an annular ring centered on the origin in the  $z$  plane.

Formal evaluation of Eq. (6.3.2) is based on the Cauchy residue theorem, which, while straightforward conceptually, is cumbersome to use in practice. Fortunately, simpler methods are available to invert the  $z$  transform, especially in the common case when  $X(z)$  is a rational fraction in  $z$ , as we now demonstrate.

### 6.3.1 ■ Power-Series Expansion

The original definition of the  $z$  transform in Eq. (6.2.1) has the form of a power (Laurent) series in the complex variable  $z$ , and thus if we expand  $X(z)$  in a power series,  $x[n]$  must be given by the coefficients of the resulting series. This approach is especially straightforward if  $X(z)$  is a rational fraction, since long division can be used to generate the power series. To utilize this method, we will treat causal and anticausal transforms as special cases. First, if  $X(z)$  is a (causal) rational transform converging for  $|z| > r_{\max}$ , that is, if

$$X(z) = \frac{B(z)}{A(z)}, \quad |z| > r_{\max}, \quad (6.3.3)$$

where  $B(z)$  and  $A(z)$  are polynomials in  $z^{-1}$  of the form

$$B(z) = \sum_{k=0}^M b_k z^{-k}$$

and

$$A(z) = \sum_{k=0}^N a_k z^{-k},$$

we divide  $B(z)$  by  $A(z)$ , starting with the lowest powers of  $z^{-1}$ , as follows:

$$\frac{x[0] + x[1]z^{-1} + x[2]z^{-2} + \dots}{a_0 + a_1z^{-1} + \dots + a_Nz^{-N}} \bigg/ \frac{b_0 + b_1z^{-1} + \dots + b_Mz^{-M}}{b_0 + b_1z^{-1} + \dots + b_Mz^{-M}} \quad (6.3.4)$$

Thus, as shown, each element of the  $x[n]$  sequence is given by the corresponding coefficient of the resulting power series in  $z^{-1}$ .

Similarly, in the anticausal case, if  $X(z)$  is a rational transform converging for  $|z| < r_{\min}$ , that is, if

$$X(z) = \frac{B(z)}{A(z)}, \quad |z| < r_{\min}, \quad (6.3.5)$$

where  $B(z)$  and  $A(z)$  are now polynomials in  $z$  (not  $z^{-1}$ ) of the form

$$B(z) = \sum_{k=0}^M b_k z^k$$

and

$$A(z) = \sum_{k=0}^N a_k z^k,$$

we divide  $B(z)$  by  $A(z)$  starting with the lowest powers of  $z$ , to wit,

$$\frac{x[0] + x[-1]z + x[-2]z^2 + \dots}{a_0 + a_1z + \dots + a_Nz^N} \bigg/ \frac{b_0 + b_1z + \dots + b_Mz^M}{b_0 + b_1z + \dots + b_Mz^M}. \quad (6.3.6)$$

Thus, as indicated, each element of the anticausal sequence is given by the corresponding coefficient of the resulting power series in  $z$ .

Finally, if the region of convergence for  $X(z)$  has the form  $r_1 < |z| < r_2$  (including possibly  $r_1 = 0$  and/or  $r_2 = \infty$ ), we can separate  $X(z)$  into its causal and anticausal parts and proceed as before. That is, given  $X(z)$  with  $r_1 < |z| < r_2$ , let

$$X(z) = X_+(z) + X_-(z), \quad r_1 < |z| < r_2, \quad (6.3.7)$$

where  $X_+(z)$  converges for  $|z| > r_1$  and  $X_-(z)$  converges for  $|z| < r_2$ . Therefore  $X_+(z)$  has the poles of  $X(z)$  that lie inside the circle  $|z| = r_1$ , while  $X_-(z)$  has the poles lying outside the circle  $|z| = r_2$ . Thus the sequences  $x_+[n]$  and  $x_-[n]$  are causal and anticausal, respectively, and can be obtained as described above. The overall inverse transform  $x[n]$  is then simply

$$x[n] = x_+[n] + x_-[n]. \quad (6.3.8)$$

**EXAMPLE 6.6** Given the familiar transform

$$X(z) = \frac{1}{1 - az^{-1}}, \quad |z| > |a|,$$

we apply the causal version of long division in Eq. (6.3.4) to obtain

$$\begin{array}{r} 1 + az^{-1} + a^2z^{-2} + \dots \\ 1 - az^{-1} \overline{)1} \\ \underline{1 - az^{-1}} \\ az^{-1} - a^2z^{-2} \\ \underline{a^2z^{-2}} \\ \dots \end{array}$$

That is,  $X(z)$  is given by the power series

$$X(z) = 1 + az^{-1} + a^2z^{-2} + \dots,$$

from which we determine that  $x[0] = 1$ ,  $x[1] = a$ ,  $x[2] = a^2$ , and so forth, or

$$x[n] = a^n u[n],$$

as expected.

If, on the other hand, the ROC implies that  $x[n]$  is anticausal, that is,

$$X(z) = \frac{1}{1 - az^{-1}}, \quad |z| < |a|,$$

we first multiply the numerator and denominator by  $z$  to obtain

$$X(z) = \frac{z}{z - a}, \quad |z| < |a|,$$

and then employ the anticausal version of long division in Eq. (6.3.6), as follows:

$$\begin{array}{r} -a^{-1}z - a^{-2}z^2 - a^{-3}z^3 - \dots \\ -a + z \overline{)z} \\ \underline{z - a^{-1}z^2} \\ a^{-1}z^2 \\ \underline{a^{-1}z^2 - a^{-2}z^3} \\ a^{-2}z^3 \\ \dots \end{array}$$

That is,  $X(z)$  is given by the power series

$$X(z) = -a^{-1}z - a^{-2}z^2 - a^{-3}z^3 - \dots,$$

from which we determine that  $x[-1] = -a^{-1}$ ,  $x[-2] = -a^{-2}$ ,  $x[-3] = -a^{-3}$ , etc., or

$$x[n] = -a^n u[-n - 1].$$

Hence the expected result is produced in this case as well.

**EXAMPLE 6.7** Given the second order  $z$  transform

$$H(z) = \frac{1}{1 - z^{-1} + 0.5z^{-2}}, \quad |z| > 0.707,$$

the causal version of long division in Eq. (6.3.4) yields the power series

$$\begin{array}{r} 1 + z^{-1} + 0.5z^{-2} - 0.25z^{-4} - 0.25z^{-5} - 0.125z^{-6} + 0.0625z^{-8} + \dots \\ \hline (1 - z^{-1} + 0.5z^{-2}) \overline{)1} \\ \underline{1 - z^{-1} + 0.5z^{-2}} \\ z^{-1} - 0.5z^{-2} \\ \underline{z^{-1} - z^{-2} + 0.5z^{-3}} \\ 0.5z^{-2} - 0.5z^{-3} \\ \underline{0.5z^{-2} - 0.5z^{-3} + 0.25z^{-4}} \\ -0.25z^{-4} \\ \underline{-0.25z^{-4} + 0.25z^{-5} - 0.125z^{-6}} \\ -0.25z^{-5} + 0.125z^{-6} \\ \underline{-0.25z^{-5} + 0.25z^{-6} - 0.125z^{-7}} \\ -0.125z^{-6} + 0.125z^{-7} \\ \underline{-0.125z^{-6} + 0.125z^{-7} - 0.0625z^{-8}} \\ 0.0625z^{-8} \end{array}$$

Therefore, making a table of values for the sequence  $x[n]$ , we have

$n$	0	1	2	3	4	5	6	7	8...
$x[n]$	1	1	1/2	0	-1/4	-1/4	-1/8	0	1/16...

We can continue to generate as many sequence values as desired, but unless a discernible pattern develops as in Example 6.6, the long-division approach becomes tedious if more than a few values of  $x[n]$  are needed. There does, in fact, seem to be some pattern to the above sequence values, but it is difficult to deduce a compact description of (equation for) the sequence. Indeed, this is a major deficiency of the long-division approach that limits its usefulness primarily to simple inverse  $z$  transforms.

**EXAMPLE 6.8** The  $z$  transform

$$X(z) = \frac{-1.25z^{-1}}{1 - 2.75z^{-1} + 1.5z^{-2}}, \quad 0.75 < |z| < 2,$$

corresponds clearly to a two-sided signal because the ROC is an annular ring. Therefore, to invert this transform, we need to separate  $X(z)$  into its causal and anticausal parts. Employing partial-fraction expansion, we find that

$$X(z) = \frac{1}{1 - 0.75z^{-1}} - \frac{1}{1 - 2z^{-1}}, \quad 0.75 < |z| < 2.$$

Hence  $X_+(z)$  and  $X_-(z)$  must be simply

$$X_+(z) = \frac{1}{1 - 0.75z^{-1}}, \quad |z| > 0.75,$$

and

$$X_-(z) = -\frac{1}{1 - 2z^{-1}}, \quad |z| < 2,$$

and thus

$$x[n] = x_+[n] + x_-[n] = (0.75)^n u[n] + 2^n u[-n - 1].$$

Occasionally, an irrational  $z$  transform is encountered, in which case power-series expansion is an especially appropriate method to obtain the inverse  $z$  transform. Specifically,  $X(z)$  is expanded in a Taylor (Maclaurin) series in  $z$  and/or  $z^{-1}$ , and  $x[n]$  is then given by the coefficients of the series. This technique is illustrated by the following important example from the theory of *homomorphic* systems.

**EXAMPLE 6.9** Consider the transform

$$\begin{aligned} X(z) &= \log\left(\frac{1}{1 - az^{-1}}\right) \\ &= -\log(1 - az^{-1}), \quad |z| > |a|. \end{aligned}$$

The Maclaurin series expansion for  $\log(1 - y)$  with  $|y| < 1$  is given by

$$\log(1 - y) = -\sum_{n=1}^{\infty} \frac{1}{n} y^n,$$

and thus, since  $|az^{-1}| < 1$ ,  $X(z)$  has the series expansion

$$X(z) = \sum_{n=1}^{\infty} \frac{1}{n} a^n z^{-n}.$$

Therefore  $x[n]$  is given by the series coefficients as

$$x[n] = \frac{1}{n} a^n u[n - 1].$$

This sequence is known as the *complex cepstrum* of the exponential sequence  $a^n u[n]$ .

### 6.3.2 • Partial-Fraction Expansion

We saw in Example 6.8 that partial-fraction expansion (PFE) is useful in separating a rational  $z$  transform into its causal and anticausal parts. In fact, however, PFE is applicable to all rational  $z$  transforms and provides the

most generally useful inverse- $z$ -transform method for such transforms, as we found in Chapter 5 was also the case for the inverse Laplace transform. For simplicity, we will restrict our coverage here to the case of distinct (nonmultiple) poles and will defer consideration of multiple poles to Appendix 6B. Initially, we also consider only the case of  $N > M$  (that is, more poles than zeros, excluding those at  $z = 0$ ),

Given the rational fraction  $B(z)/A(z)$  with

$$B(z) = \sum_{k=0}^M b_k z^{-k}$$

and

$$A(z) = \sum_{k=0}^N a_k z^{-k},$$

and assuming  $N > M$  and no multiple poles, we can expand  $B(z)/A(z)$  in a PFE of the form

$$\frac{B(z)}{A(z)} = \sum_{k=1}^N \frac{r_k}{1 - p_k z^{-1}}, \quad (6.3.9)$$

with poles  $p_k$  and residues  $r_k$ . Inferring the ROC for each of these  $N$  terms from the overall ROC for  $X(z)$ , we can then invert each term based on the results of earlier examples to obtain the overall inverse  $z$  transform, as done previously to compute the inverse Laplace transform. The following example illustrates this procedure.

**EXAMPLE 6.10** Given the second-order rational fraction

$$\frac{B(z)}{A(z)} = \frac{1 - 1.7z^{-1}}{1 - 2.05z^{-1} + z^{-2}},$$

the corresponding PFE is readily found to be

$$\frac{B(z)}{A(z)} = \frac{2}{1 - 0.8z^{-1}} - \frac{1}{1 - 1.25z^{-1}}.$$

Since there are poles at  $z = 0.8$  and  $z = 1.25$ , there are three possible forms for the ROC: namely,  $|z| > 1.25$ ,  $0.8 < |z| < 1.25$ , and  $|z| < 0.8$ , as depicted in Fig. 6.5.

Assuming first that  $|z| > 1.25$ , we know from the ROC properties in Section 6.2 that the corresponding signal  $x[n]$  must be causal. In particular, from Example 6.2, we have

$$(0.8)^n u[n] \leftrightarrow \frac{1}{1 - 0.8z^{-1}}, \quad |z| > 0.8,$$

and

$$(1.25)^n u[n] \leftrightarrow \frac{1}{1 - 1.25z^{-1}}, \quad |z| > 1.25.$$

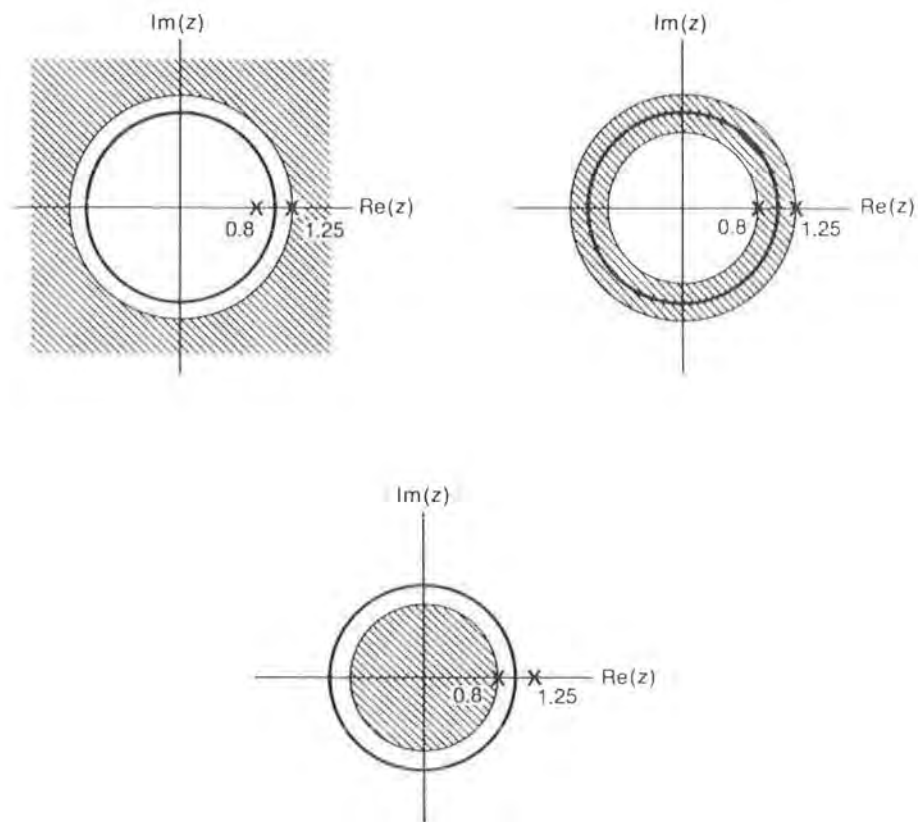


**FIGURE 6.5** Three possible ROCs for given pole plot.

Hence, the combined transform,

$$X(z) = \frac{2}{1 - 0.8z^{-1}} - \frac{1}{1 - 1.25z^{-1}}, \quad |z| > 1.25,$$

implies the causal signal

$$x[n] = \{2(0.8)^n - (1.25)^n\}u[n].$$

On the other hand, if the ROC is  $0.8 < |z| < 1.25$ , we know that  $x[n]$  is two-sided. That is, from Examples 6.2 and 6.3,

$$(0.8)^n u[n] \leftrightarrow \frac{1}{1 - 0.8z^{-1}}, \quad |z| > 0.8,$$

and

$$-(1.25)^n u[-n - 1] \leftrightarrow \frac{1}{1 - 1.25z^{-1}}, \quad |z| < 1.25,$$

and thus the combined transform,

$$X(z) = \frac{2}{1 - 0.8z^{-1}} - \frac{1}{1 - 1.25z^{-1}}, \quad 0.8 < |z| < 1.25,$$

implies the two-sided signal

$$x[n] = 2(0.8)^n u[n] + (1.25)^n u[-n - 1].$$

Lastly, if  $X(z)$  converges for  $|z| < 0.8$ , the signal must be anticausal, and thus, since

$$-(0.8)^n u[-n - 1] \leftrightarrow \frac{1}{1 - 0.8z^{-1}}, \quad |z| < 0.8,$$

and

$$-(1.25)^n u[-n - 1] \leftrightarrow \frac{1}{1 - 1.25z^{-1}}, \quad |z| < 1.25,$$

the combined transform,

$$X(z) = \frac{2}{1 - 0.8z^{-1}} - \frac{1}{1 - 1.25z^{-1}}, \quad |z| < 0.8,$$

corresponds to the anticausal signal

$$x[n] = \{(1.25)^n - 2(0.8)^n\} u[-n - 1].$$

The three forms of the inverse  $z$  transform (causal, two-sided, and anticausal) corresponding to the three ROCs in Fig. 6.5 are shown in Fig. 6.6.

The case of  $N \leq M$  requires an additional step before the PFE can be performed. Illustrating this step for a causal transform, we divide  $B(z)$  by  $A(z)$ , starting with the *highest* powers of  $z^{-1}$ , to produce

$$a_N z^{-N} + \cdots + a_1 z^{-1} + a_0 \Big/ b_M z^{-M} + \cdots + b_1 z^{-1} + b_0 = \frac{g_L z^{-L} + \cdots + g_1 z^{-1} + g_0 + C(z)/A(z)}{b_M z^{-M} + \cdots + b_1 z^{-1} + b_0}, \quad (6.3.10)$$

where  $L = M - N$  and the remainder polynomial  $C(z)$  is of order  $K < N$ . That is,  $X(z)$  is rewritten as

$$X(z) = \frac{B(z)}{A(z)} = G(z) + \frac{C(z)}{A(z)}, \quad |z| > r, \quad (6.3.11)$$

where  $G(z)$  and  $C(z)$  are  $L$ th- and  $K$ th-order polynomials in  $z^{-1}$ , respectively. Then, since  $K < N$ , the rational fraction  $C(z)/A(z)$  can be

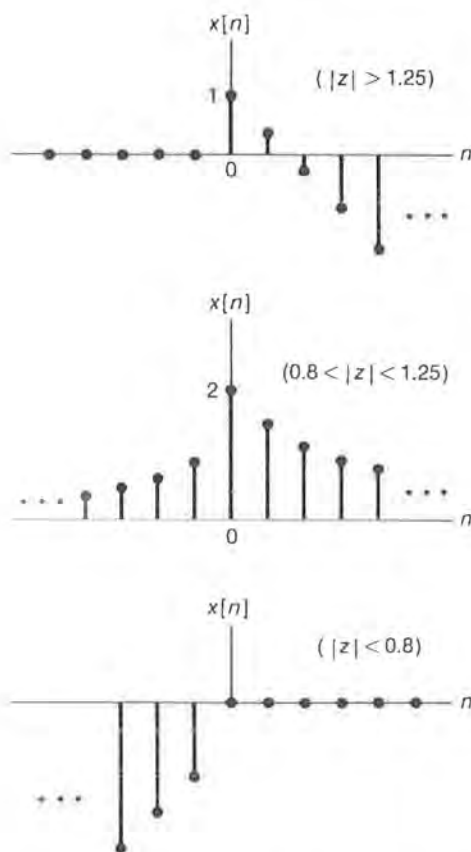


FIGURE 6.6 Signals  $x[n]$  corresponding to ROCs in Fig. 6.5.

expanded in a PFE as in Eq. (6.3.9), that is,

$$\frac{C(z)}{A(z)} = \sum_{k=1}^N \frac{q_k}{1 - p_k z^{-1}} \quad (6.3.12)$$

Finally, from Eqs. (6.3.11) and (6.3.12), the resulting (causal) inverse  $z$  transform can be expressed as

$$x[n] = \sum_{i=0}^L g_i \delta[n - i] + \sum_{k=1}^N q_k (p_k)^n u[n]. \quad (6.3.13)$$

**EXAMPLE 6.11** The  $z$  transform

$$X(z) = \frac{2 - 3.5z^{-1} + 2.5z^{-2} - 0.5z^{-3}}{1 - 1.5z^{-1} + 0.5z^{-2}}, \quad |z| > 1,$$

has  $N = 2$  and  $M = 3$ , and hence the additional step described in Eq.

(6.3.10) is required before the PFE. Performing this division, we have

$$\begin{array}{r}
 -z^{-1} + 2 \\
 0.5z^{-2} - 1.5z^{-1} + 1 \overline{) -0.5z^{-3} + 2.5z^{-2} - 3.5z^{-1} + 2} \\
 \underline{-0.5z^{-3} + 1.5z^{-2} - z^{-1}} \phantom{+ 2} \\
 z^{-2} - 2.5z^{-1} + 2 \\
 \underline{z^{-2} - 3z^{-1} + 2} \\
 0.5z^{-1}
 \end{array}$$

That is, the quotient polynomial  $G(z)$  equals  $-z^{-1} + 2$ , while the remainder polynomial  $C(z)$  is simply  $0.5z^{-1}$ . Next, expanding  $C(z)/A(z)$  in a PFE, we find that

$$\begin{aligned}
 \frac{C(z)}{A(z)} &= \frac{0.5z^{-1}}{1 - 1.5z^{-1} + 0.5z^{-2}} \\
 &= \frac{1}{1 - z^{-1}} - \frac{1}{1 - 0.5z^{-1}}
 \end{aligned}$$

Finally, therefore, the inverse  $z$  transform is obtained from Eq. (6.3.13) as

$$x[n] = 2\delta[n] - \delta[n-1] + \{1 - (0.5)^n\}u[n].$$

Anticausal  $z$  transforms with  $M \geq N$  can be inverted using a similar procedure after expressing  $A(z)$  and  $B(z)$  [and thus  $C(z)$  and  $G(z)$ ] as polynomials in  $z$  rather than  $z^{-1}$ .

## 6.4

### Properties of the $z$ Transform

As in the case of the Fourier and Laplace transforms, there are many properties of the  $z$  transform that are quite useful in system analysis and design. These  $z$ -transform properties closely parallel those for the Laplace transform, as should be expected, since both are usually rational fractions in the complex variable  $s$  or  $z$  and are thus characterized by their poles, zeros, and regions of convergence in the complex plane. In describing these properties, a  $z$ -transform pair is denoted by  $x[n] \leftrightarrow X(z)$ , as before.

#### 6.4.1 • Linearity

Given that the signals  $x_1[n]$  and  $x_2[n]$  have the  $z$  transforms  $X_1(z)$  and  $X_2(z)$ , with regions of convergence  $R_1$  and  $R_2$ , respectively, it is readily

shown that

$$ax_1[n] + bx_2[n] \leftrightarrow aX_1(z) + bX_2(z) \quad (6.4.1)$$

for arbitrary constants  $a$  and  $b$ , with a region of convergence  $R'$  satisfying

$$R' \supset R_1 \cap R_2.$$

As before, the set notation  $A \supset B$  means that set  $A$  contains set  $B$ , while  $B \cap C$  denotes the intersection of sets  $B$  and  $C$ . In words, therefore, the  $z$  transform of a linear combination of two signals  $x_1[n]$  and  $x_2[n]$  is the same linear combination of the corresponding transforms  $X_1(z)$  and  $X_2(z)$ , with a resulting ROC at least as large as the region in common between  $R_1$  and  $R_2$ . Usually, as for the Laplace transform, we have simply  $R' = R_1 \cap R_2$ , but occasionally a pole/zero cancelation is produced in the linear combination that extends the boundary of  $R'$  beyond that for  $R_1 \cap R_2$ . Of course, if  $R_1$  and  $R_2$  do not intersect,  $R'$  equals the empty set, in which case the  $z$  transform for  $ax_1[n] + bx_2[n]$  does not exist.

**EXAMPLE 6.12** From Examples 6.2 and 6.5, we have that the  $z$  transforms of the signals

$$x_1[n] = a^n u[n]$$

and

$$x_2[n] = a^n u[n] + b^n u[-n - 1], \quad a \neq b,$$

are given by

$$X_1(z) = \frac{1}{1 - az^{-1}}, \quad |z| > |a|,$$

and

$$X_2(z) = \frac{(a - b)z^{-1}}{(1 - az^{-1})(1 - bz^{-1})}, \quad |a| < |z| < |b|,$$

respectively. Therefore the  $z$  transform of the sum

$$x[n] = x_1[n] + x_2[n]$$

is given by

$$\begin{aligned} X(z) &= X_1(z) + X_2(z) = \frac{1}{1 - az^{-1}} + \frac{(a - b)z^{-1}}{(1 - az^{-1})(1 - bz^{-1})} \\ &= \frac{(1 - bz^{-1}) + (a - b)z^{-1}}{(1 - az^{-1})(1 - bz^{-1})} \\ &= \frac{1 + (a - 2b)z^{-1}}{(1 - az^{-1})(1 - bz^{-1})}, \quad |a| < |z| < |b|. \end{aligned}$$

Hence, for this linear combination,  $R' = R_1 \cap R_2 = R_2$ .

However, computing the  $z$  transform of the difference

$$x[n] = x_1[n] - x_2[n],$$

we find that

$$\begin{aligned} X(z) &= X_1(z) - X_2(z) = \frac{1}{1 - az^{-1}} - \frac{(a - b)z^{-1}}{(1 - az^{-1})(1 - bz^{-1})} \\ &= \frac{(1 - bz^{-1}) - (a - b)z^{-1}}{(1 - az^{-1})(1 - bz^{-1})} = \frac{1 - az^{-1}}{(1 - az^{-1})(1 - bz^{-1})} \\ &= \frac{1}{1 - bz^{-1}}, \quad |z| < |b|. \end{aligned}$$

That is, the pole at  $z = a$  is canceled by a zero. Therefore, in this case, the region of convergence  $R'$  is larger than  $R_1 \cap R_2$ . This effect is explained in the time domain by noting that the causal term  $a^n u[n]$  cancels out in the difference  $x_1[n] - x_2[n]$ , yielding the anticausal result  $x[n] = -b^n u[-n - 1]$ .

#### 6.4.2 • Time Shift

The  $z$  transform of the shifted signal  $x[n - n_0]$  is, by definition,

$$\mathcal{Z}\{x[n - n_0]\} = \sum_{n=-\infty}^{\infty} x[n - n_0]z^{-n},$$

where  $\mathcal{Z}\{ \}$  denotes the  $z$ -transform operation. Employing the change of variables  $m = n - n_0$ , we find that

$$\begin{aligned} \mathcal{Z}\{x[n - n_0]\} &= \sum_{m=-\infty}^{\infty} x[m]z^{-(m+n_0)} \\ &= z^{-n_0} \sum_{m=-\infty}^{\infty} x[m]z^{-m} \\ &= z^{-n_0} X(z), \end{aligned}$$

with the same ROC as for  $X(z)$  itself except possibly at  $z = 0$  or  $\infty$ . Specifically, for  $n_0 > 0$ , up to  $n_0$  additional poles are introduced at  $z = 0$  and/or deleted at  $z = \infty$  by the factor  $z^{-n_0}$ , and vice versa for  $n_0 < 0$ . Therefore the points  $z = 0$  and  $z = \infty$  can either be added to or deleted from the ROC by time shifting. In the time domain, this reflects the fact that a right-sided but noncausal signal will become causal if delayed sufficiently, while a causal signal will become noncausal if advanced sufficiently. Similarly, a left-sided signal that is not anticausal will become anticausal if advanced sufficiently, but an anticausal signal will not remain anticausal if delayed by a sufficient amount.

In summary, therefore, we have the relationship

$$x[n - n_0] \leftrightarrow z^{-n_0}X(z), \quad R' \supset R \cap 0 < |z| < \infty, \quad (6.4.2)$$

where  $R$  and  $R'$  denote the ROCs before and after the time-shift operation, respectively. In particular, letting  $n_0 = 1$  and  $-1$ , we have the important special cases

$$x[n - 1] \leftrightarrow z^{-1}X(z), \quad R' \supset R \cap |z| > 0, \quad (6.4.3a)$$

and

$$x[n + 1] \leftrightarrow zX(z), \quad R' \supset R \cap |z| < \infty. \quad (6.4.3b)$$

Because of these relationships,  $z^{-1}$  is often called the *unit-delay operator* and  $z$  is called the *unit-advance operator*. [Note that the time-domain effects of the similar Laplace transform operators  $s^{-1}$  and  $s$  are, in fact, quite different from Eq. (6.4.3) since these operators correspond to time-domain integration and differentiation, respectively.]

### 6.4.3 • Modulation

Multiplication of a time-domain signal  $x[n]$  by an exponential  $z_0^n$  for an arbitrary complex number  $z_0$  constitutes the general form of discrete-time modulation. The student can readily verify that

$$z_0^n x[n] \leftrightarrow X(z/z_0), \quad R' = |z_0| R. \quad (6.4.4)$$

In particular, a pole (zero) at  $z = p_k$  in  $X(z)$  moves to  $z = z_0 p_k$  after modulation, and the ROC expands or contracts by the factor  $|z_0|$ . In the important special case of *complex modulation* where  $z_0 = e^{j\Omega_0}$ , Eq. (6.4.4) becomes

$$e^{j\Omega_0 n} x[n] \leftrightarrow X(ze^{-j\Omega_0}), \quad R' = R. \quad (6.4.5)$$

Hence, in this case, all poles and zeros are simply rotated by the angle  $\Omega_0$ , and the ROC is unchanged.

**EXAMPLE 6.13** To find the  $z$  transform of the sequence

$$x[n] = r^n (\cos \Omega_0 n) u[n], \quad r > 0,$$

we note that

$$x[n] = \frac{1}{2}(e^{j\Omega_0 n} + e^{-j\Omega_0 n})r^n u[n]$$

and that

$$r^n u[n] \leftrightarrow \frac{1}{1 - rz^{-1}}, \quad |z| > r.$$

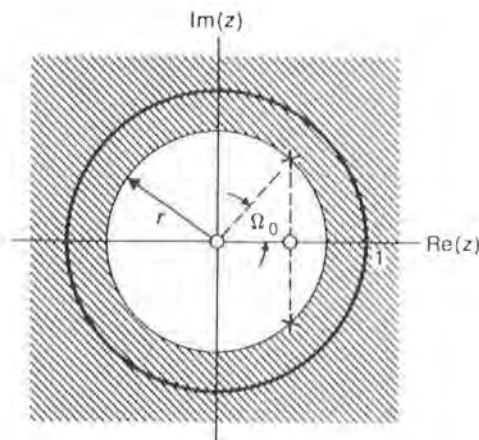


FIGURE 6.7 Pole/zero plot with ROC for  $r^n(\cos \Omega_0 n)u[n]$ .

Therefore, by linearity and the modulation property in Eq. (6.4.5),

$$\begin{aligned} X(z) &= \frac{\frac{1}{2}}{1 - re^{j\Omega_0}z^{-1}} + \frac{\frac{1}{2}}{1 - re^{-j\Omega_0}z^{-1}} \\ &= \frac{1 - r(\cos \Omega_0)z^{-1}}{(1 - re^{j\Omega_0}z^{-1})(1 - re^{-j\Omega_0}z^{-1})} \\ &= \frac{1 - r(\cos \Omega_0)z^{-1}}{1 - 2r(\cos \Omega_0)z^{-1} + r^2z^{-2}}, \quad |z| > r. \end{aligned}$$

The corresponding pole/zero plot is shown in Fig. 6.7.

#### 6.4.4 • Time Reversal

If  $x[n]$  is time-reversed to produce  $x[-n]$ , we readily find from the definition of  $X(z)$  that

$$x[-n] \leftrightarrow X(1/z), \quad R' = 1/R. \quad (6.4.6)$$

Therefore a pole (zero) in  $X(z)$  at  $z = p_k$  moves to  $1/p_k$  after time reversal. The relationship  $R' = 1/R$  reflects the fact that a right-sided signal becomes left-sided if time-reversed, and vice versa.

#### 6.4.5 • Differentiation in $z$

Differentiating both sides of the  $z$ -transform definition in Eq. (6.2.1), we find that

$$\frac{dX(z)}{dz} = \sum_{n=-\infty}^{\infty} -nx[n]z^{-n-1},$$

and thus

$$nx[n] \leftrightarrow -z \frac{dX(z)}{dz}, \quad R' = R. \quad (6.4.7)$$

This relationship is useful in certain derivations, as we show in the following example.

**EXAMPLE 6.14** In Example 6.9 we used power-series expansion to invert the irrational  $z$  transform

$$X(z) = -\log(1 - az^{-1}), \quad |z| > |a|.$$

However, an alternative inversion method is provided by the differentiation property because

$$\frac{dX(z)}{dz} = \frac{-az^{-2}}{1 - az^{-1}}, \quad |z| > |a|,$$

which is a rational fraction. Specifically, from Eq. (6.4.7), we then have

$$nx[n] \leftrightarrow -z \frac{dX(z)}{dz} = \frac{az^{-1}}{1 - az^{-1}}.$$

Writing this result as

$$nx[n] \leftrightarrow (a)z^{-1} \left( \frac{1}{1 - az^{-1}} \right),$$

and utilizing the linearity and time-shift properties, we deduce that

$$nx[n] = (a)a^{n-1}u[n-1] = a^n u[n-1].$$

Therefore the inverse  $z$  transform is given by

$$x[n] = \frac{1}{n} a^n u[n-1],$$

as previously determined.

### 6.4.6 • Convolution of Signals

From Chapter 3 we know that the input and output of a discrete-time LTI system are related by the convolution

$$y[n] = x[n] * h[n] = \sum_{k=-\infty}^{\infty} x[k]h[n-k].$$

Computing the  $z$  transform of  $y[n]$ , we readily find that

$$Y(z) = H(z)X(z), \quad R_y \supset R_h \cap R_x, \quad (6.4.8)$$

as in the analogous Laplace transform property. Usually we have, as before,

simply  $R_y = R_h \cap R_x$ , but if a zero of one transform cancels a pole of the other,  $R_y$  may be larger than  $R_h \cap R_x$ . Generalizing this result to the convolution of arbitrary signals, we have the z-transform pair

$$x_1[n] * x_2[n] \leftrightarrow X_1(z)X_2(z), \quad R' \supset R_1 \cap R_2. \quad (6.4.9)$$

This relationship plays a central role in the theory and design of discrete-time systems, in analogy with the continuous-time case.

**EXAMPLE 6.15** To invert the z transform

$$X(z) = \frac{1}{(1 - az^{-1})^2}, \quad |z| > |a|,$$

which has a double pole at  $z = a$ , we recognize that

$$X(z) = [X_1(z)]^2,$$

where

$$X_1(z) = \frac{1}{1 - az^{-1}}, \quad |z| > |a|.$$

Hence  $x[n]$  is given by the convolution

$$\begin{aligned} x[n] &= x_1[n] * x_1[n] = a^n u[n] * a^n u[n], \\ &= (n + 1)a^n u[n]. \end{aligned}$$

### 6.4.7 • Accumulation

The discrete-time counterpart to integration in the time domain is called *accumulation* and is defined by

$$y[n] = \sum_{k=-\infty}^n x[k].$$

Recognizing that  $y[n]$  can be considered to be the convolution

$$y[n] = x[n] * u[n],$$

we can thus write

$$Y(z) = X(z) \frac{1}{1 - z^{-1}}, \quad R_y \supset R_x \cap |z| > 1. \quad (6.4.10)$$

(Note that the comparable Laplace transform operator for integration is  $1/s$ .)

**EXAMPLE 6.16** In Example 3.14, the step response of the system

$$h[n] = a^n u[n]$$

was determined in the time domain from the relationship

$$s[n] = h[n] * u[n],$$

or equivalently,

$$s[n] = \sum_{k=-\infty}^n h[k].$$

Using now, instead, the accumulation property of the  $z$  transform to compute  $s[n]$ , we have

$$\begin{aligned} S(z) &= \frac{1}{(1 - az^{-1})(1 - z^{-1})} \\ &= \frac{r_1}{1 - az^{-1}} + \frac{r_2}{1 - z^{-1}}, \quad |z| > \max(1, |a|). \end{aligned}$$

Determining the residues  $r_1$  and  $r_2$  of this PFE, we find that

$$r_1 = \frac{-a}{1-a} \quad r_2 = \frac{1}{1-a}.$$

Therefore, the step response is given by

$$s[n] = \frac{1 - a^{n+1}}{1 - a} u[n],$$

in agreement with Eq. (3.6.12).

#### 6.4.8 ■ Summary of Transform Properties

Table 6.1 contains a summary of the properties presented in this section for the  $z$  transform. Some common signals and their  $z$  transforms are then given in Table 6.2.

**TABLE 6.1** Properties of the  $z$  Transform

Property	Time domain	Transform	ROC
Linearity	$ax_1[n] + bx_2[n]$	$aX_1(z) + bX_2(z)$	$R' \supset R_1 \cap R_2$
Time shift	$x[n - n_0]$	$z^{-n_0}X(z)$	$R' \supset R \cap$ $0 <  z  < \infty$
Modulation	$z_0^n x[n]$	$X(z/z_0)$	$R' =  z_0  R$
	$e^{j\Omega_0 n} x[n]$	$X(ze^{-j\Omega_0})$	$R' = R$
Time reversal	$x[-n]$	$X(1/z)$	$R' = 1/R$
Differentiation	$nx[n]$	$-z \frac{dX(z)}{dz}$	$R' = R$
Convolution	$x_1[n] * x_2[n]$	$X_1(z)X_2(z)$	$R' \supset R_1 \cap R_2$
Accumulation	$\sum_{k=-\infty}^n x[k]$	$X(z) \frac{1}{1 - z^{-1}}$	$R' \supset R \cap  z  > 1$

**TABLE 6.2** Common  $z$  Transforms

Signal	Time domain	Transform	ROC
Impulse	$\delta[n]$	1	All $z$
	$\delta[n - n_0], n_0 > 0$	$z^{-n_0}$	$ z  > 0$
	$\delta[n + n_0], n_0 > 0$	$z^{n_0}$	$ z  < \infty$
Unit step	$u[n]$	$\frac{1}{1 - z^{-1}}$	$ z  > 1$
	$-u[-n - 1]$	$\frac{1}{1 - z^{-1}}$	$ z  < 1$
Exponential	$a^n u[n]$	$\frac{1}{1 - az^{-1}}$	$ z  >  a $
	$-a^n u[-n - 1]$	$\frac{1}{1 - az^{-1}}$	$ z  <  a $
Weighted exponential	$(n + 1)a^n u[n]$	$\frac{1}{(1 - az^{-1})^2}$	$ z  >  a $
Causal sine	$(\sin \Omega_0 n)u[n]$	$\frac{(\sin \Omega_0)z^{-1}}{1 - 2(\cos \Omega_0)z^{-1} + z^{-2}}$	$ z  > 1$
Causal cosine	$(\cos \Omega_0 n)u[n]$	$\frac{1 - (\cos \Omega_0)z^{-1}}{1 - 2(\cos \Omega_0)z^{-1} + z^{-2}}$	$ z  > 1$
Damped sine	$r^n (\sin \Omega_0 n)u[n]$	$\frac{r(\sin \Omega_0)z^{-1}}{1 - 2r(\cos \Omega_0)z^{-1} + r^2 z^{-2}}$	$ z  > r$
Damped cosine	$r^n (\cos \Omega_0 n)u[n]$	$\frac{1 - r(\cos \Omega_0)z^{-1}}{1 - 2r(\cos \Omega_0)z^{-1} + r^2 z^{-2}}$	$ z  > r$

## 6.5

### The System Function for LTI Systems

The  $z$  transform  $H(z)$  of an impulse response  $h[n]$ , that is,

$$H(z) = \sum_{n=-\infty}^{\infty} h[n]z^{-n}, \quad (6.5.1)$$

is known as the *system function* (or sometimes the *transfer function*) of the corresponding discrete-time LTI system. Recall from Section 6.1 that  $H(z)$  can also be considered to be the eigenvalue associated with the eigenfunction  $z^n$  (for values of  $z$  in the ROC). Since  $h[n]$  completely characterizes the LTI system with respect to its input/output relationship, and since  $h[n]$  can

be recovered from  $H(z)$  via the inverse  $z$  transform, the system function  $H(z)$  must also completely characterize the LTI system. Many useful insights into the properties and design of an LTI system are provided by  $H(z)$ , as was seen in Chapter 5 for the analogous Laplace transform  $H(s)$ . The utility of the system function derives, of course, from the relationship

$$Y(z) = H(z)X(z), \quad R_y \supset R_h \cap R_x, \quad (6.5.2)$$

since  $y[n] = h[n] * x[n]$ . Several simple but important system functions implied by the properties in Table 6.1 are as follows:

$$\text{Unit Delay} \quad H(z) = z^{-1}, \quad |z| > 0.$$

$$\text{Unit Advance} \quad H(z) = z, \quad |z| < \infty.$$

$$\text{Accumulator} \quad H(z) = \frac{1}{1 - z^{-1}}, \quad |z| > 1.$$

**EXAMPLE 6.17** To find the output  $y[n]$  of the system

$$h[n] = 0.5^n u[n]$$

for the anticausal input

$$x[n] = 2^n u[-n] = 0.5^{-n} u[-n],$$

we can either directly convolve  $h[n]$  and  $x[n]$ , or we can find and then invert the  $z$  transform  $Y(z)$ . Taking the latter approach, we have

$$H(z) = \frac{1}{1 - 0.5z^{-1}}, \quad |z| > 0.5,$$

and

$$X(z) = \frac{1}{1 - 0.5z} = \frac{-2z^{-1}}{1 - 2z^{-1}}, \quad |z| < 2,$$

and thus

$$\begin{aligned} Y(z) &= H(z)X(z) = \frac{-2z^{-1}}{(1 - 0.5z^{-1})(1 - 2z^{-1})} \\ &= \frac{4/3}{1 - 0.5z^{-1}} - \frac{4/3}{1 - 2z^{-1}}, \quad 0.5 < |z| < 2. \end{aligned}$$

Therefore, inverting  $Y(z)$ , we determine that

$$\begin{aligned} y[n] &= (4/3)\{0.5^n u[n] + 2^n u[-n - 1]\} \\ &= (4/3)\{0.5^n u[n] + 0.5^{-n} u[-n - 1]\} \\ &= (4/3)0.5^{|n|}. \end{aligned}$$

### 6.5.1 • Frequency Response

A special input signal of particular interest is the complex sinusoid

$$x[n] = e^{j\Omega n}$$

for arbitrary radian frequency  $\Omega$ . Since this signal is an eigenfunction for any LTI system, we have immediately from Eqs. (6.1.8) and (6.1.9), with  $z = e^{j\Omega}$ , that the corresponding output signal is also a complex sinusoid of the form

$$y[n] = H(e^{j\Omega})e^{j\Omega n},$$

where

$$H(e^{j\Omega}) = \sum_{n=-\infty}^{\infty} h[n]e^{-j\Omega n}. \quad (6.5.3)$$

The function (eigenvalue)  $H(e^{j\Omega})$ , if it converges, is known as the *frequency response* of the discrete-time LTI system and plays the same role as  $H(j\omega)$  in the continuous-time case. Note that if the ROC for the system function  $H(z)$  contains the unit circle, then  $H(e^{j\Omega})$  does converge and equals  $H(z)$  evaluated on the unit circle.

The frequency response  $H(e^{j\Omega})$  is the discrete-time Fourier transform (DTFT) of the impulse response  $h[n]$  and, as such, will be investigated in depth in Chapter 7. However, certain of its properties can be determined now from our knowledge of the system function  $H(z)$ . For instance, since  $H(e^{j\Omega})$  equals  $H(z)$  evaluated on a circle in the  $z$  plane, it must be a periodic function of the frequency  $\Omega$ . In particular, since  $e^{j\Omega}$  is a periodic function of  $\Omega$  with period  $2\pi$ ,  $H(e^{j\Omega})$  must also be a periodic function of  $\Omega$  with period  $2\pi$ . Specific values of the frequency response of interest are the *dc response*  $H(e^{j0}) = H(1)$  and the response  $H(e^{j\pi}) = H(-1)$  at the *Nyquist frequency*  $\Omega = \pi$ . In addition, for real-valued  $h[n]$ , we have

$$h[n] = h^*[n],$$

and thus, from Eq. (6.5.3),

$$H(e^{-j\Omega}) = H^*(e^{j\Omega}). \quad (6.5.4)$$

That is,  $H(e^{j\Omega})$  is a conjugate-symmetric function of frequency. Therefore the *magnitude response*  $|H(e^{j\Omega})|$  is an even function of  $\Omega$ , while the *phase response*  $\angle H(e^{j\Omega})$  is an odd function of  $\Omega$ , that is,

$$|H(e^{j\Omega})| = |H(e^{-j\Omega})|, \quad h[n] \text{ real}, \quad (6.5.5)$$

and

$$\angle H(e^{j\Omega}) = -\angle H(e^{-j\Omega}), \quad h[n] \text{ real}.$$

**EXAMPLE 6.18** The exponential impulse response

$$h[n] = a^n u[n], \quad |a| < 1,$$

implies the familiar system function

$$H(z) = \frac{1}{1 - az^{-1}}, \quad |z| > |a|.$$

Hence, since the ROC contains the unit circle for  $|a| < 1$ , the frequency response exists and equals simply

$$H(e^{j\Omega}) = \frac{1}{1 - ae^{-j\Omega}}.$$

Computing the corresponding magnitude response, we have

$$\begin{aligned} |H(e^{j\Omega})| &= [H(e^{j\Omega})H^*(e^{j\Omega})]^{1/2} \\ &= \left[ \frac{1}{(1 - ae^{-j\Omega})(1 - ae^{j\Omega})} \right]^{1/2} \\ &= \left[ \frac{1}{1 - 2a(\cos \Omega) + a^2} \right]^{1/2}, \end{aligned}$$

which is clearly an even function of  $\Omega$  since  $\cos \Omega$  is even. To obtain the phase response, we write  $H(e^{j\Omega})$  as

$$H(e^{j\Omega}) = \frac{1}{1 - a(\cos \Omega) + ja(\sin \Omega)},$$

and thus

$$\angle H(e^{j\Omega}) = -\arctan \left[ \frac{a(\sin \Omega)}{1 - a(\cos \Omega)} \right],$$

which is indeed an odd function of  $\Omega$ . Plots of  $|H(e^{j\Omega})|$  and  $\angle H(e^{j\Omega})$  are shown in Fig. 6.8 for  $a > 0$ . Note that both functions are periodic in

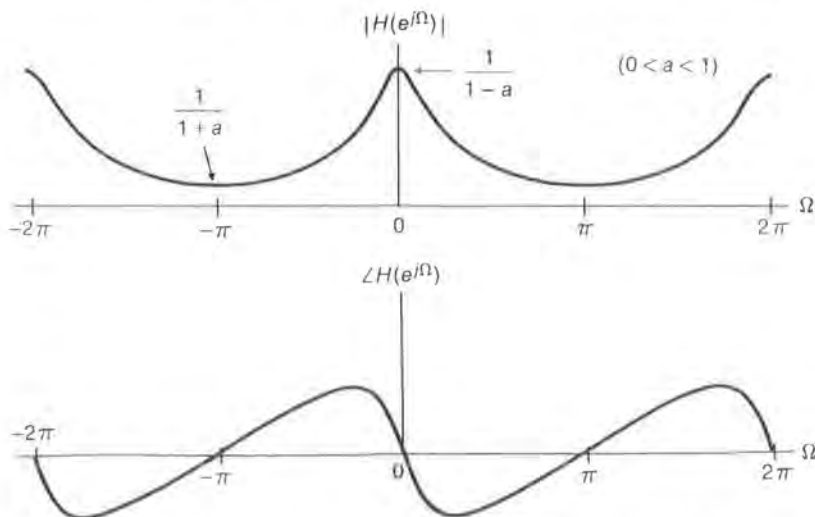


FIGURE 6.8 Magnitude and phase responses for  $H(z) = 1/(1 - az^{-1})$ .

$\Omega$  with period  $2\pi$ , as required. Therefore only one period of the frequency response is usually displayed in such plots—either for the interval  $0 \leq \Omega \leq 2\pi$  or for  $-\pi \leq \Omega \leq \pi$ .

### 6.5.2 • Causal and Anticausal Systems

In Chapter 3 we investigated several important attributes of discrete-time systems in terms of associated conditions on the impulse response  $h[n]$ . In this and following sections, we will reconsider these attributes in terms of the system function  $H(z)$  and, where appropriate, the frequency response  $H(e^{j\Omega})$ .

As previously argued, the system function  $H(z)$  for a causal impulse response  $h[n]$  must have an ROC of the form

$$|z| > r_{\max},$$

that is, outside a circle containing all of the system poles in the  $z$  plane. Similarly, an anticausal impulse response implies an ROC for  $H(z)$  of the form

$$|z| < r_{\min},$$

that is, inside a circle containing no poles.

### 6.5.3 • Stable Systems

In Section 3.7 we found that an LTI system is BIBO stable if and only if the impulse response  $h[n]$  is absolutely summable, that is,

$$\sum_{n=-\infty}^{\infty} |h[n]| < \infty. \quad (6.5.6)$$

But this is also a sufficient condition for  $H(z)$  to converge on the unit circle, as we now show. Using Eq. (6.5.3) to bound  $|H(e^{j\Omega})|$ , we have

$$\begin{aligned} |H(e^{j\Omega})| &= \left| \sum_{n=-\infty}^{\infty} h[n]e^{-j\Omega n} \right| \\ &\leq \sum_{n=-\infty}^{\infty} |h[n]e^{-j\Omega n}| \\ &= \sum_{n=-\infty}^{\infty} |h[n]|. \end{aligned} \quad (6.5.7)$$

Therefore, if the inequality in expression (6.5.6) holds,  $H(z)$  converges for  $z = e^{j\Omega}$ . That is, *for a stable discrete-time system, the ROC for  $H(z)$  must contain the unit circle, and the frequency response  $H(e^{j\Omega})$  thus exists.* The four possible forms for the ROC of a stable system function are illustrated in Fig. 6.9, corresponding to right-sided, left-sided, two-sided, and finite-

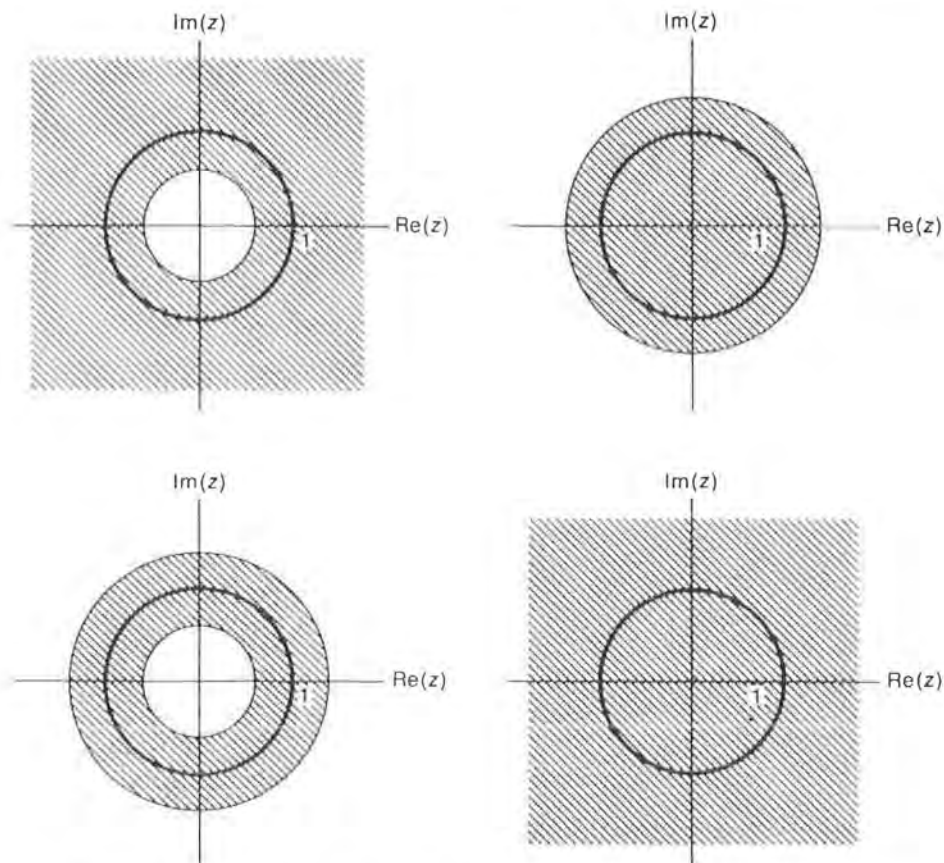


FIGURE 6.9 Four possible forms for ROC of a stable system.

duration impulse responses  $h_1[n]$ , respectively. (The points  $z = 0$  and/or  $z = \infty$  may or may not be included.) Note that if the system is both causal and stable, all of the poles must lie inside the unit circle because the ROC is of the form  $|z| > r_{\max}$  and thus, since the unit circle is included in the ROC, we must have  $r_{\max} < 1$ .

#### 6.5.4 • System Interconnection

For two LTI systems  $h_1[n]$  and  $h_2[n]$  in cascade, the overall impulse response  $h[n]$  is given by the convolution

$$h[n] = h_1[n] * h_2[n].$$

Therefore, from the convolution property in Eq. (6.4.9), the corresponding system functions must be related by the product

$$H(z) = H_1(z)H_2(z), \quad R \supset R_1 \cap R_2. \quad (6.5.8)$$

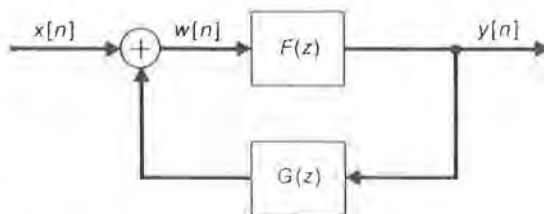


FIGURE 6.10 Feedback interconnection of subsystems  $F(z)$  and  $G(z)$ .

As noted earlier, the overall ROC will actually be  $R = R_1 \cap R_2$  unless one or more poles defining an ROC boundary are canceled by zeros when  $H_1(z)$  and  $H_2(z)$  are multiplied.

Similarly, the impulse response of a parallel combination of two LTI systems is given by

$$h[n] = h_1[n] + h_2[n],$$

and thus from the linearity property in Eq. (6.4.1),

$$H(z) = H_1(z) + H_2(z), \quad R \supset R_1 \cap R_2. \quad (6.5.9)$$

Again, the overall ROC will be larger than the intersection  $R_1 \cap R_2$  only if a pole/zero cancellation produced by adding  $H_1(z)$  and  $H_2(z)$  extends the ROC boundary.

Finally, the feedback interconnection of systems is depicted in Fig. 6.10 for (causal) subsystems  $F(z)$  and  $G(z)$ . As will be shown in Problem 6.37, the overall system function  $H(z)$  for this feedback system is given by

$$H(z) = \frac{F(z)}{1 - F(z)G(z)}, \quad |z| > r_{\max}. \quad (6.5.10)$$

Again therefore, as for continuous-time systems,  $H(z)$  is given by the *feedforward gain*  $F(z)$  divided by 1 minus the *loop gain*  $F(z)G(z)$ . The feedback interconnection is also fundamental in discrete-time control theory and signal processing.

In addition, as for continuous-time systems, certain block-diagram manipulations can be useful in analyzing or reconfiguring discrete-time systems. These simple manipulations, illustrated in Fig. 5.13, will not be shown again here because they are exactly analogous in the discrete-time case, as were the above relationships for cascade, parallel, and feedback interconnections. The purpose of the manipulations is to move branch or summing nodes behind or ahead of adjacent system blocks, as desired.

### 6.5.5 • Invertible Systems

It was argued in Section 3.7.6 that, if an LTI system  $h[n]$  is invertible, there must exist an inverse system with impulse response  $h_I[n]$  such that

$$h[n] * h_I[n] = \delta[n]. \quad (6.5.11)$$

Expressing this relationship in terms of  $z$  transforms, we thus have

$$H(z)H_I(z) = 1,$$

or

$$H_I(z) = \frac{1}{H(z)}. \quad (6.5.12)$$

That is,  $H_I(z)$  is the algebraic inverse of  $H(z)$ , as for the analogous Laplace transforms  $H(s)$  and  $H_I(s)$ . Therefore, if  $H(z)$  is the rational fraction  $B(z)/A(z)$ , then  $H_I(z)$  is the rational fraction  $A(z)/B(z)$ , and the poles of  $H(z)$  are the zeros of  $H_I(z)$ , and vice versa. Note then that, in general, the inverse system  $H_I(z)$  for a given  $H(z)$  is not unique because multiple ROCs can be defined for a rational fraction  $A(z)/B(z)$  having at least one pole at other than  $z = 0$  or  $z = \infty$ . Usually, however, only one of the possible inverse systems will be useful in practice because of additional requirements on  $H_I(z)$ , such as stability and/or causality.

**EXAMPLE 6.19** Given the accumulator system function

$$H(z) = \frac{1}{1 - z^{-1}}, \quad |z| > 1,$$

the associated inverse system is simply

$$H_I(z) = 1 - z^{-1}, \quad |z| > 0, \quad (6.5.13)$$

corresponding to the impulse response

$$h_I[n] = \delta[n] - \delta[n - 1].$$

This system is known as a *first-difference operator* and is the only possible inverse system in this case because  $H_I(z)$  has only a pole at  $z = 0$ . Checking that Eq. (6.5.11) is indeed satisfied by  $h_I[n]$ , we have

$$\begin{aligned} h[n] * h_I[n] &= u[n] * \{\delta[n] - \delta[n - 1]\} \\ &= u[n] - u[n - 1] = \delta[n]. \end{aligned}$$

Similarly, the inverse system for the unit delay

$$H(z) = z^{-1}, \quad |z| > 0,$$

is the unit advance

$$H_I(z) = z, \quad |z| < \infty,$$

and vice versa.

**EXAMPLE 6.20** Given the stable and causal system

$$H(z) = \frac{1 + 0.8z^{-1}}{1 - 0.5z^{-1}}, \quad |z| > 0.5,$$

we can identify two corresponding inverse systems, as follows:

$$H_{r1}(z) = \frac{1 - 0.5z^{-1}}{1 + 0.8z^{-1}}, \quad |z| > 0.8,$$

and

$$H_{r2}(z) = \frac{1 - 0.5z^{-1}}{1 + 0.8z^{-1}}, \quad |z| < 0.8.$$

In most practical applications, however, only  $H_{r1}(z)$  is useful because it is both stable and causal, while  $H_{r2}(z)$  is neither.

On the other hand, for the stable and causal system

$$H(z) = \frac{1 - 2z^{-1}}{1 - 0.5z^{-1}}, \quad |z| > 0.5,$$

the two possible inverse systems are

$$H_{r1}(z) = \frac{1 - 0.5z^{-1}}{1 - 2z^{-1}}, \quad |z| > 2,$$

and

$$H_{r2}(z) = \frac{1 - 0.5z^{-1}}{1 - 2z^{-1}}, \quad |z| < 2.$$

Hence, in this case, we must choose between stability and causality for the inverse system because  $H_{r1}(z)$  is causal but not stable, while  $H_{r2}(z)$  is stable but not causal.

## 6.6

### Difference Equations

As discussed previously in Chapter 3, most discrete-time LTI systems of practical interest can be described by finite-order linear difference equations with constant coefficients of the form

$$\sum_{k=0}^N a_k y[n-k] = \sum_{k=0}^M b_k x[n-k], \quad (6.6.1)$$

where the order of the system is the larger of  $N$  and  $M$ . From our previous results for continuous-time systems described by linear differential equations, we might expect that the system function  $H(z)$  corresponding to Eq. (6.6.1) is a rational fraction in  $z$ , and this is indeed true as we now show. Note first, since  $Y(z) = H(z)X(z)$ , that the system function  $H(z)$  can be

expressed as the ratio

$$H(z) = \frac{Y(z)}{X(z)}, \quad (6.6.2)$$

where we defer for the moment a discussion of the corresponding ROC. Next, taking the  $z$  transform of both sides of Eq. (6.6.1), we have

$$\mathcal{Z}\left\{\sum_{k=0}^N a_k y[n-k]\right\} = \mathcal{Z}\left\{\sum_{k=0}^M b_k x[n-k]\right\}$$

or, by the linearity property of the  $z$  transform,

$$\sum_{k=0}^N a_k \mathcal{Z}\{y[n-k]\} = \sum_{k=0}^M b_k \mathcal{Z}\{x[n-k]\}.$$

Then, using the time-shift property of the  $z$  transform, we have

$$\sum_{k=0}^N a_k z^{-k} Y(z) = \sum_{k=0}^M b_k z^{-k} X(z)$$

or, factoring  $Y(z)$  and  $X(z)$  from the summations,

$$Y(z) \sum_{k=0}^N a_k z^{-k} = X(z) \sum_{k=0}^M b_k z^{-k}.$$

Finally, dividing through this equation by  $X(z) \sum_{k=0}^N a_k z^{-k}$ , we produce

$$H(z) = \frac{Y(z)}{X(z)} = \frac{\sum_{k=0}^M b_k z^{-k}}{\sum_{k=0}^N a_k z^{-k}}, \quad (6.6.3)$$

which is the expected rational fraction  $B(z)/A(z)$ . Unlike the analogous Laplace transform  $H(s)$ , however, there is no restriction that  $M \leq N$  for actual systems or filters. Note that the ROC for  $H(z)$  is not specified by Eq. (6.6.3) or by the original difference equation in Eq. (6.6.1), but must be inferred from auxiliary information or requirements on the system such as stability or causality.

**EXAMPLE 6.21** In the first-order linear difference equation

$$y[n] - ay[n-1] = x[n],$$

we have  $N = 1$  and  $M = 0$ , with  $a_0 = 1$ ,  $a_1 = -a$ , and  $b_0 = 1$ , implying the familiar rational fraction

$$\frac{B(z)}{A(z)} = \frac{1}{1 - az^{-1}}$$

The actual system function can thus be either

$$H_1(z) = \frac{1}{1 - az^{-1}}, \quad |z| > |a|,$$

or

$$H_2(z) = \frac{1}{1 - az^{-1}}, \quad |z| < |a|,$$

corresponding to the causal and anticausal impulse responses

$$h_1[n] = a^n u[n]$$

and

$$h_2[n] = -a^n u[-n - 1],$$

respectively. (The student should check that the given first-order difference equation is indeed satisfied for all  $n$  by either  $y[n] = h_1[n]$  or  $y[n] = h_2[n]$ , with  $x[n] = \delta[n]$ .) Of course,  $H_1(z)$  is stable if and only if (iff)  $|a| < 1$ , while  $H_2(z)$  is stable iff  $|a| > 1$ . Since  $h_1[n]$  and  $h_2[n]$  are both nonzero for an infinite time duration (one for  $n \geq 0$  and the other for  $n < 0$ ), they are classified as *infinite-impulse-response (IIR)* filters. Clearly, any filter with at least one nonzero, finite pole (i.e., a pole at other than  $z = 0$  or  $z = \infty$ ) that is not canceled by a zero will be IIR because such poles imply exponential components in  $h[n]$ .

The choice between  $H_1(z)$  and  $H_2(z)$  is dictated by auxiliary information or requirements on the system implying stability and/or causality. From the difference equation alone, we can only conclude that the ROC is either  $|z| > |a|$  or  $|z| < |a|$ , implying  $H_1(z)$  or  $H_2(z)$ , respectively. In particular, we have the following cases:

1. If the system is causal, it must be  $H_1(z)$ .
2. If the system is anticausal, it must be  $H_2(z)$ .
3. If the system is stable and  $|a| < 1$ , it must be  $H_1(z)$ .
4. If the system is stable and  $|a| > 1$ , it must be  $H_2(z)$ .
5. If the system is unstable and  $|a| > 1$ , it must be  $H_1(z)$ .
6. If the system is unstable and  $|a| < 1$ , it must be  $H_2(z)$ .
7. If  $h[0] = 1$ , it must be  $H_1(z)$  because  $\lim_{z \rightarrow \infty} H_1(z) = 1$ . (See Problem 6.9.)
8. If  $h[0] = 0$ , it must be  $H_2(z)$  because  $\lim_{z \rightarrow 0} H_2(z) = 0$ .

**EXAMPLE 6.22** The first-difference operator was defined in Example 6.19 by the system function

$$H(z) = 1 - z^{-1}, \quad |z| > 0.$$

Recognizing that  $H(z)$  is a first-order rational fraction of the form in

Eq. (6.6.3), with  $b_0 = 1$ ,  $b_1 = -1$ , and  $a_0 = 1$  (and thus  $M = 1$  and  $N = 0$ ), we can write the corresponding difference equation from Eq. (6.6.1) as simply

$$y[n] = x[n] - x[n - 1].$$

Since the associated impulse response

$$h[n] = \delta[n] - \delta[n - 1]$$

is nonzero for only a finite time duration, this filter is classified as a *finite-impulse-response (FIR)* filter. Note, in particular, that in contrast with the IIR case, this filter has only a pole at  $z = 0$ .

The first-difference operator is somewhat analogous to a continuous-time differentiator because the first derivative can be defined as the limit of the first difference

$$y(t) = \frac{x(t) - x(t - \Delta t)}{\Delta t}$$

as  $\Delta t \rightarrow 0$ . In fact, substituting  $z = e^{j\Omega}$  into  $H(z)$  to determine the frequency response  $H(e^{j\Omega})$ , we find that

$$\begin{aligned} H(e^{j\Omega}) &= 1 - e^{-j\Omega} = e^{-j\Omega/2}(e^{j\Omega/2} - e^{-j\Omega/2}) \\ &= 2je^{-j\Omega/2} \sin \Omega/2. \end{aligned}$$

Distinguishing the linear-phase (delay) factor  $e^{-j\Omega/2}$  from the rest of  $H(e^{j\Omega})$ , we thus have

$$H(e^{j\Omega}) = e^{-j\Omega/2} I(\Omega),$$

where

$$I(\Omega) = 2j(\sin \Omega/2).$$

Note that since  $\sin \theta \approx \theta$  for  $\theta < \pi/6$ , the purely imaginary factor  $I(\Omega)$  satisfies

$$I(\Omega) \approx j\Omega, \quad \Omega < \pi/3,$$

and thus approximates the ideal differentiator response  $H(j\omega) = j\omega$  for small  $\omega$ .

### 6.6.1 • First- and Second-Order Filters

As noted in Eq. (2.4.14), discrete-time sinusoids with frequencies  $\Omega_1$  and  $\Omega_2$  separated by some multiple of  $2\pi$  (that is,  $\Omega_1 - \Omega_2 = 2\pi k$ ) are indistinguishable. This fact helps explain why any discrete-time frequency response  $H(e^{j\Omega})$  must be periodic in  $\Omega$  with period  $2\pi$ . Therefore, considering the frequency response in Fig. 6.8 for the system

$$H_1(z) = \frac{1}{1 - az^{-1}}, \quad |z| > |a|, \quad (6.6.4)$$

with  $0 < a < 1$  over the unique interval  $-\pi \leq \Omega \leq \pi$ , we see that it can be identified as a lowpass filter (LPF). Recall also from Example 6.21 that this is classified as a first-order IIR filter. On the other hand, the simple first-order FIR filter

$$H_2(z) = 1 + z^{-1}, \quad |z| > 0, \quad (6.6.5)$$

is also a discrete-time LPF because

$$\begin{aligned} H_2(e^{j\Omega}) &= 1 + e^{-j\Omega} = e^{-j\Omega/2}(e^{j\Omega/2} + e^{-j\Omega/2}) \\ &= 2e^{-j\Omega/2} \cos \Omega/2, \end{aligned} \quad (6.6.6)$$

and thus

$$|H_2(e^{j\Omega})| = 2 \cos \Omega/2, \quad -\pi \leq \Omega \leq \pi, \quad (6.6.7)$$

and

$$\angle H_2(e^{j\Omega}) = -\Omega/2, \quad -\pi < \Omega < \pi,$$

as depicted in Fig. 6.11. Observe, however, that  $|H_2(e^{j\Omega})|$  is a *wideband* response because its 3-dB point occurs at  $\Omega = \pi/2$ , whereas the bandwidth of  $|H_1(e^{j\Omega})|$  can be narrow or wide depending upon the value of  $a$ . Note also the abrupt  $180^\circ$  phase shift in  $\angle H_2(e^{j\Omega})$  at  $\Omega = \pm\pi$  because the factor  $\cos \Omega/2$  in Eq. (6.6.6) changes sign at those frequencies. An improved first-order LPF with controllable bandwidth is obtained by cascading  $H_1(z)$  and  $H_2(z)$  to produce

$$H_1(z)H_2(z) = \frac{1 + z^{-1}}{1 - az^{-1}}, \quad |z| > |a|.$$

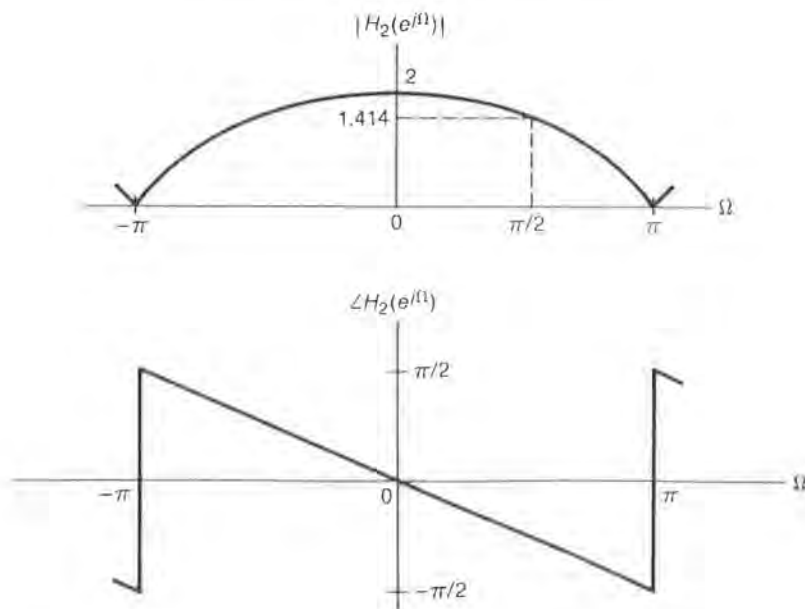


FIGURE 6.11 Magnitude and phase responses for  $H_2(z) = 1 + z^{-1}$ .

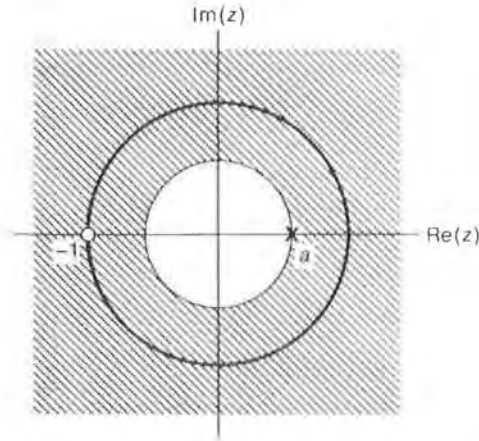


FIGURE 6.12 Pole/zero plot for improved first-order LPF.

Actually, since we often want unity gain at dc [that is,  $H(e^{j0}) = H(1) = 1$ ], let

$$H(z) = \frac{(1-a)(1+z^{-1})}{2(1-az^{-1})}, \quad |z| > |a|. \quad (6.6.8)$$

This filter is again IIR because it has a finite, nonzero pole at  $z = a$ , but it also has a zero at  $z = -1$ , as illustrated in Fig. 6.12 for  $a > 0$ . The corresponding magnitude response is proportional to  $|H_1(e^{j\Omega})| |H_2(e^{j\Omega})|$  and is shown in Fig. 6.13 for various values of  $a$  in the range  $-1 < a < 1$ . Note that the bandwidth of the filter increases as the parameter  $a$  decreases, but that we always have  $H(e^{j\pi}) = H(-1) = 0$  at the Nyquist frequency  $\Omega = \pi$  due to the zero at  $z = -1$ .

A first-order highpass filter with controllable bandwidth can be produced by replacing  $z$  by  $-z$  in Eq. (6.6.8), that is,

$$H(z) = \frac{(1-a)(1-z^{-1})}{2(1+az^{-1})}, \quad |z| > |a|.$$

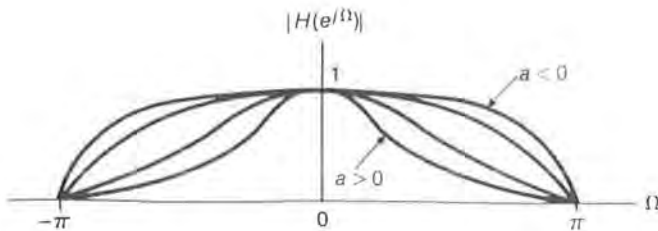


FIGURE 6.13 Magnitude responses from Fig. 6.12 as  $a$  varies.

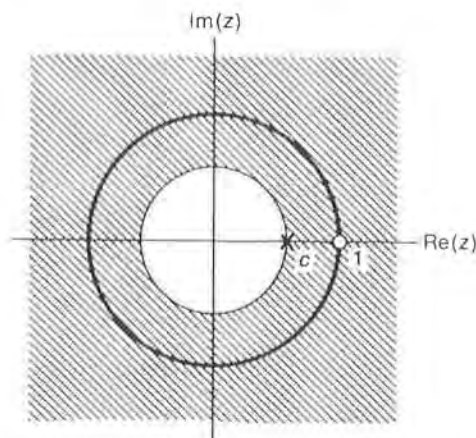


FIGURE 6.14 Pole/zero plot for first-order HPF.

or, letting  $c = -a$ ,

$$H(z) = \frac{(1+c)(1-z^{-1})}{2(1-cz^{-1})}, \quad |z| > |c|. \quad (6.6.9)$$

Note, in particular, that the dc gain is now  $H(e^{j0}) = H(1) = 0$ , but that  $H(e^{j\pi}) = H(-1) = 1$ . The corresponding pole/zero plot is shown in Fig. 6.14 for  $c > 0$ .

To see the overall effect of this transformation on  $H(e^{j\Omega})$ , note that the effect of replacing  $z$  by  $-z$  is simply to replace  $e^{j\Omega}$  by  $-e^{j\Omega} = e^{j(\Omega+\pi)}$ , and thus the HPF frequency response corresponds to the LPF frequency response shifted by  $\pi$  radians, as shown in Fig. 6.15.

Consider next the causal second-order system function

$$H(z) = \frac{b_0}{1 + a_1 z^{-1} + a_2 z^{-2}}, \quad |z| > r_{\max}, \quad (6.6.10)$$

corresponding to the second-order linear difference equation

$$y[n] + a_1 y[n-1] + a_2 y[n-2] = b_0 x[n].$$

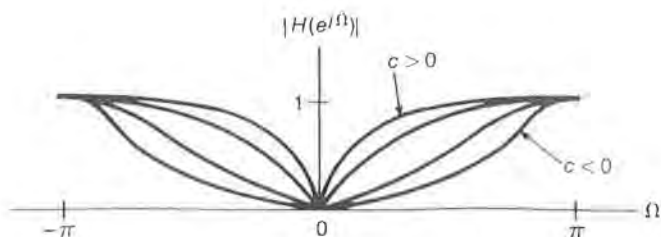


FIGURE 6.15 Magnitude responses from Fig. 6.14 as  $c$  varies.

The poles of the system equal the roots of the denominator quadratic, that is,

$$p_1, p_2 = \frac{-a_1 \pm \sqrt{a_1^2 - 4a_2}}{2} \quad (6.6.11)$$

and hence the poles are complex-conjugates if  $a_1^2 < 4a_2$ , and real otherwise. Rewriting  $H(z)$  in terms of its poles as

$$\begin{aligned} H(z) &= \frac{b_0}{(1 - p_1 z^{-1})(1 - p_2 z^{-1})} \\ &= \frac{b_0}{1 - (p_1 + p_2)z^{-1} + p_1 p_2 z^{-2}}, \end{aligned} \quad (6.6.12)$$

we note that the denominator coefficients  $a_1$  and  $a_2$  in Eq. (6.6.10) can be expressed in terms of  $p_1$  and  $p_2$  as simply

$$a_1 = -(p_1 + p_2) \quad (6.6.13a)$$

and

$$a_2 = p_1 p_2. \quad (6.6.13b)$$

Therefore, since the poles of a stable and causal system must be inside the unit circle, that is,

$$|p_1| < 1 \quad \text{and} \quad |p_2| < 1,$$

the coefficients  $a_1$  and  $a_2$  will satisfy

$$|a_1| < 2 \quad \text{and} \quad |a_2| < 1$$

if the system is stable. Actually, however, necessary and sufficient conditions for the stability of  $H(z)$  are given by (see Problem 6.23)

$$|a_1| < 1 + a_2 \quad (6.6.14a)$$

and

$$|a_2| < 1. \quad (6.6.14b)$$

The corresponding *stability triangle* of stable coefficient values in the  $a_1, a_2$  plane is illustrated in Fig. 6.16, which also shows the regions associated with real and complex-conjugate poles.

In the *underdamped* case of complex-conjugate poles

$$p_1, p_2 = r e^{\pm j\Omega_0},$$

with  $r > 0$  and  $0 < \Omega_0 < \pi$ , it is often convenient to rewrite  $H(z)$  in the form

$$H(z) = \frac{b_0}{1 - 2r(\cos \Omega_0)z^{-1} + r^2 z^{-2}}, \quad |z| > r, \quad (6.6.15)$$

where  $r$  is thus the radius of the poles in the  $z$  plane and  $\pm\Omega_0$  are the associated pole angles, as depicted in Fig. 6.17 for the stable case of  $r < 1$ .

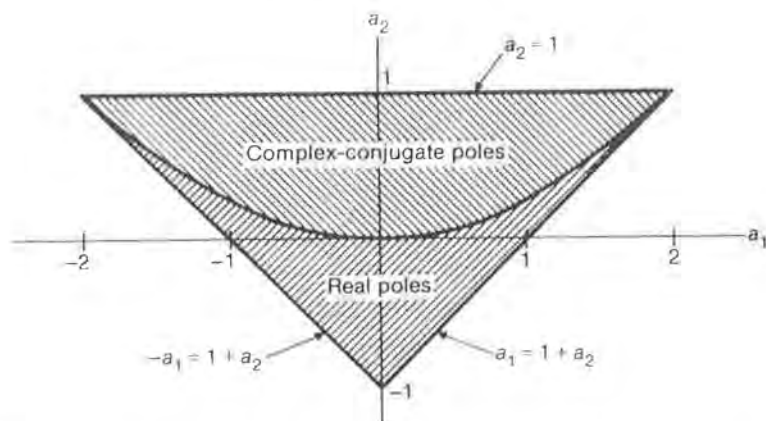


FIGURE 6.16 Stability triangle for denominator coefficients  $a_1$  and  $a_2$ .

If we use the time-shift property and let  $b_0 = (\sin \Omega_0)^{-1}$ , the corresponding impulse response is readily determined from Table 6.2 to be

$$h[n] = r^n [\sin \Omega_0(n+1)]u[n], \quad (6.6.16)$$

which is a damped sinusoid for  $r < 1$ . Second-order LPF, HPF, BPF, and BSF responses based on underdamped denominators of the form in Eq. (6.6.15) will be analyzed in the next section and in Problems 6.26 and 6.29.

By analogy with second-order continuous-time systems, the boundary case of  $\Omega_0 = 0$ , corresponding to the system function

$$H(z) = \frac{b_0}{(1 - rz^{-1})^2}, \quad |z| > r, \quad (6.6.17)$$

is called *critically damped*. In this case,  $H(z)$  has a double pole at  $z = r$ ,

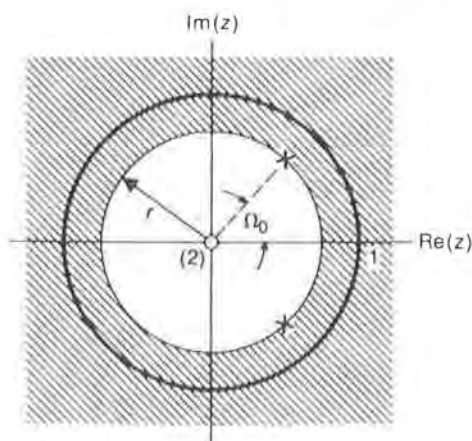


FIGURE 6.17 Pole/zero plot for underdamped second-order system.

and  $h[n]$  is given by

$$h[n] = b_0(n+1)r^n u[n]. \quad (6.6.18)$$

Also, as for continuous-time systems, the case of unequal real-valued poles  $p_1$  and  $p_2$  [see Eq. (6.6.12)] is called *overdamped*.

### 6.6.2 • Geometric Evaluation of the Frequency Response

The geometric method introduced in Section 5.5.2 to estimate and sketch the magnitude and phase responses of continuous-time systems from pole/zero plots of  $H(s)$  works equally well for discrete-time systems using pole/zero plots of  $H(z)$ . First, factoring the numerator and denominator polynomials of the rational fraction in Eq. (6.6.3) into products of first-order factors of the form

$$H(z) = \frac{C \prod_{k=1}^M (1 - z_k z^{-1})}{\prod_{k=1}^N (1 - p_k z^{-1})}, \quad (6.6.19)$$

where  $z_k$  and  $p_k$  are the zeros and poles, respectively, of  $H(z)$  and  $C = b_0/a_0$ , we may write  $H(z)$  in the equivalent form

$$H(z) = \frac{Cz^{N-M} \prod_{k=1}^M (z - z_k)}{\prod_{k=1}^N (z - p_k)}. \quad (6.6.20)$$

The corresponding frequency response  $H(e^{j\Omega})$  is then simply

$$H(e^{j\Omega}) = \frac{C e^{j\Omega(N-M)} \prod_{k=1}^M (e^{j\Omega} - z_k)}{\prod_{k=1}^N (e^{j\Omega} - p_k)}. \quad (6.6.21)$$

Therefore, for a given frequency  $\Omega$ , each complex-valued numerator term  $(e^{j\Omega} - z_k)$  can be thought of as a vector in the complex ( $z$ ) plane from the zero  $z_k$  to the point  $e^{j\Omega}$  on the unit circle; and likewise, each denominator term  $(e^{j\Omega} - p_k)$  is effectively a vector from the pole  $p_k$  to the point  $e^{j\Omega}$ . Also, the  $N - M$  zeros (or  $M - N$  poles if  $M > N$ ) at  $z = 0$  produce an additional factor  $e^{j\Omega(N-M)}$  in the frequency response.

Utilizing Eq. (6.6.21) to write the magnitude response  $|H(e^{j\Omega})|$ , we thus have

$$|H(e^{j\Omega})| = \frac{|C| \prod_{k=1}^M |e^{j\Omega} - z_k|}{\prod_{k=1}^N |e^{j\Omega} - p_k|}. \quad (6.6.22)$$

That is, the magnitude response at the frequency  $\Omega$  equals the scaled product of the lengths of all vectors  $(e^{j\Omega} - z_k)$  from the zeros to the point  $e^{j\Omega}$  divided by the product of the lengths of all vectors  $(e^{j\Omega} - p_k)$  from the poles to the point  $e^{j\Omega}$ , with the scaling constant being  $|C| = |b_0/a_0|$ . Similarly, the phase response  $\angle H(e^{j\Omega})$  can be written from Eq. (6.6.21) as

$$\angle H(e^{j\Omega}) = \sum_{k=1}^M \angle(e^{j\Omega} - z_k) - \sum_{k=1}^N \angle(e^{j\Omega} - p_k) + (N - M)\Omega + \angle C; \quad (6.6.23)$$

and thus  $\angle H(e^{j\Omega})$  is simply the sum of the angles of all numerator vectors  $(e^{j\Omega} - z_k)$  minus the sum of the angles of all denominator vectors  $(e^{j\Omega} - p_k)$  plus a linear-phase term  $(N - M)\Omega + \angle C$ .

**EXAMPLE 6.23** The reader can readily check that the first-order LPF and HPF magnitude responses in Figs. 6.13 and 6.15, respectively, are indeed consistent with the pole/zero plots in Figs. 6.12 and 6.14 for various (stable) values of the parameters  $a$  and  $c$ . The 3-dB bandwidth of these filters is also easily approximated in narrowband cases using geometric analysis, as follows: From Eq. (6.6.8), we can write the LPF frequency response  $H(e^{j\Omega})$  as

$$\begin{aligned} H(e^{j\Omega}) &= C \frac{(1 + e^{-j\Omega})}{(1 - ae^{-j\Omega})} \\ &= C \frac{(e^{j\Omega} + 1)}{(e^{j\Omega} - a)}, \end{aligned} \quad (6.6.24)$$

where  $C = (1 - a)/2$  for unity gain at dc. The vectors  $(e^{j\Omega} + 1)$ ,  $(e^{j\Omega} - a)$ , and also  $(1 - a)$  are depicted in Fig. 6.18 for  $0 \ll a < 1$ .

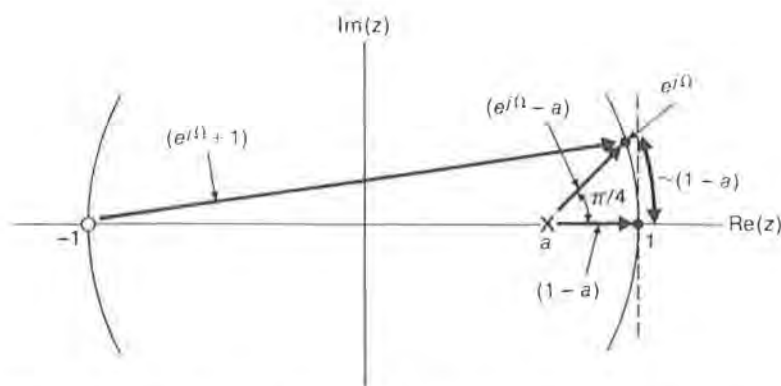


**FIGURE 6.18** Geometric approximation of 3-dB bandwidth for first-order LPF.

Since the dc gain of the LPF is unity, the 3-dB point occurs at the value  $\Omega_b$  for which  $H(e^{j\Omega_b}) = 1/\sqrt{2}$ .

Approximating the unit circle in the vicinity of  $z = 1$  by the dotted vertical line shown in the figure, we note that the vectors  $(e^{j\Omega} - a)$  and  $(1 - a)$  and the dotted line approximate an isosceles triangle for  $0 \ll a < 1$  when the angle of  $(e^{j\Omega} - a)$  is  $\pi/4$ , as illustrated. Hence, since the vector  $(e^{j\Omega} - a)$  forms the approximate hypotenuse of this triangle, its length can be estimated as  $\sqrt{2}(1 - a)$  at this angle, while, on the other hand, the length of the numerator vector  $(e^{j\Omega} + 1)$ , which equals 2 for  $\Omega = 0$ , is only slightly less in this case.

We thus find that  $\Omega \approx \Omega_b$  for this geometric situation because, from Eq. (6.6.22),

$$|H(e^{j\Omega})| \approx |C| \frac{2}{\sqrt{2}(1 - a)} = \frac{1}{\sqrt{2}}.$$

Finally, to estimate the value of  $\Omega_b$ , we note that the two sides of an isosceles triangle have equal lengths and that the length of an arc on the unit circle equals the associated angle (in radians). Therefore the vertical side of the triangle has length  $1 - a$ , and for  $0 \ll a < 1$ , the associated angle (bandwidth)  $\Omega_b$  is also approximately

$$\Omega_b \approx 1 - a, \quad (6.6.25)$$

as depicted in the figure.

A similar geometric derivation can be employed to estimate the bandwidth of a first-order HPF in the narrowband case. Expressing the HPF frequency response from Eq. (6.6.9) as

$$\begin{aligned} H(e^{j\Omega}) &= C \frac{(1 - e^{-j\Omega})}{(1 - ce^{-j\Omega})} \\ &= C \frac{(e^{j\Omega} - 1)}{(e^{j\Omega} - c)}, \end{aligned} \quad (6.6.26)$$

where  $C = (1 + c)/2$ , the vectors  $(e^{j\Omega} - 1)$ ,  $(e^{j\Omega} - c)$ , and also  $(1 - c)$  are shown in Fig. 6.19 for  $0 \ll c < 1$ . Again, since the maximum gain of the HPF is unity (at  $\Omega = \pi$ ), the 3-dB point occurs at the value  $\Omega_b$  for which  $H(e^{j\Omega_b}) = 1/\sqrt{2}$ . Note that the vector  $(e^{j\Omega} - 1)$  is almost vertical and thus forms an approximate isosceles triangle with the other two vectors when the angle of  $(e^{j\Omega} - c)$  is  $\pi/4$ , as illustrated. Therefore the length of  $(e^{j\Omega} - 1)$  is approximately  $1 - c$ , while the length of the hypotenuse  $(e^{j\Omega} - c)$  is approximately  $\sqrt{2}(1 - c)$ . Note also that  $C \approx 1$  for  $0 \ll c < 1$ . Hence, from Eq. (6.6.22), the magnitude response in this situation is approximated by

$$|H(e^{j\Omega})| \approx \frac{1 - c}{\sqrt{2}(1 - c)} = \frac{1}{\sqrt{2}},$$

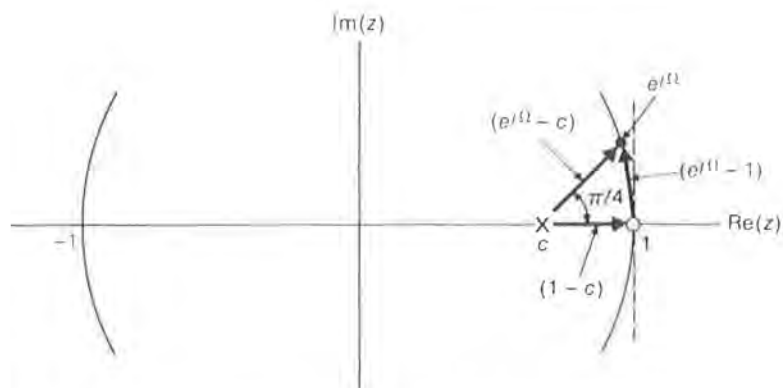


**FIGURE 6.19** Geometric approximation of 3-dB bandwidth for first-order HPF.

and thus  $\Omega \approx \Omega_b$ . As before, the associated value of the angle  $\Omega_b$  (bandwidth of the stopband) is then simply

$$\Omega_b \approx 1 - c. \quad (6.6.27)$$

#### APPLICATION 6.1 Second-Order IIR Filters

The second-order underdamped system function

$$H(z) = \frac{1 + b_1 z^{-1} + b_2 z^{-2}}{1 - 2r(\cos \Omega_0)z^{-1} + r^2 z^{-2}}, \quad |z| > r, \quad (6.6.28)$$

can provide an LPF, HPF, BPF, or BSF response, depending upon the values of the numerator coefficients  $b_1$  and  $b_2$ , as illustrated by the following cases:

*LPF Case.* For  $b_1 = 2$  and  $b_2 = 1$ , Eq. (6.6.28) becomes

$$\begin{aligned} H(z) &= \frac{1 + 2z^{-1} + z^{-2}}{1 - 2r(\cos \Omega_0)z^{-1} + r^2 z^{-2}} \\ &= \frac{(1 + z^{-1})^2}{1 - 2r(\cos \Omega_0)z^{-1} + r^2 z^{-2}}, \quad |z| > r, \end{aligned} \quad (6.6.29)$$

and hence there is a double zero at  $z = -1$ . Therefore  $H(e^{j\pi}) = 0$ , implying an LPF response. Sketching the corresponding pole/zero plot and magnitude response, we can actually identify two possible cases, as illustrated in Fig. 6.20. In particular, if the poles are close enough to the unit circle to produce discernible peaks in  $|H(e^{j\Omega})|$ , the response is nonmonotonic in the passband, as shown in Fig. 6.20(a). By analogy with the corresponding continuous-time case, such filters are called *highly underdamped*. On the other hand, if the radius ( $r$ ) of the poles is

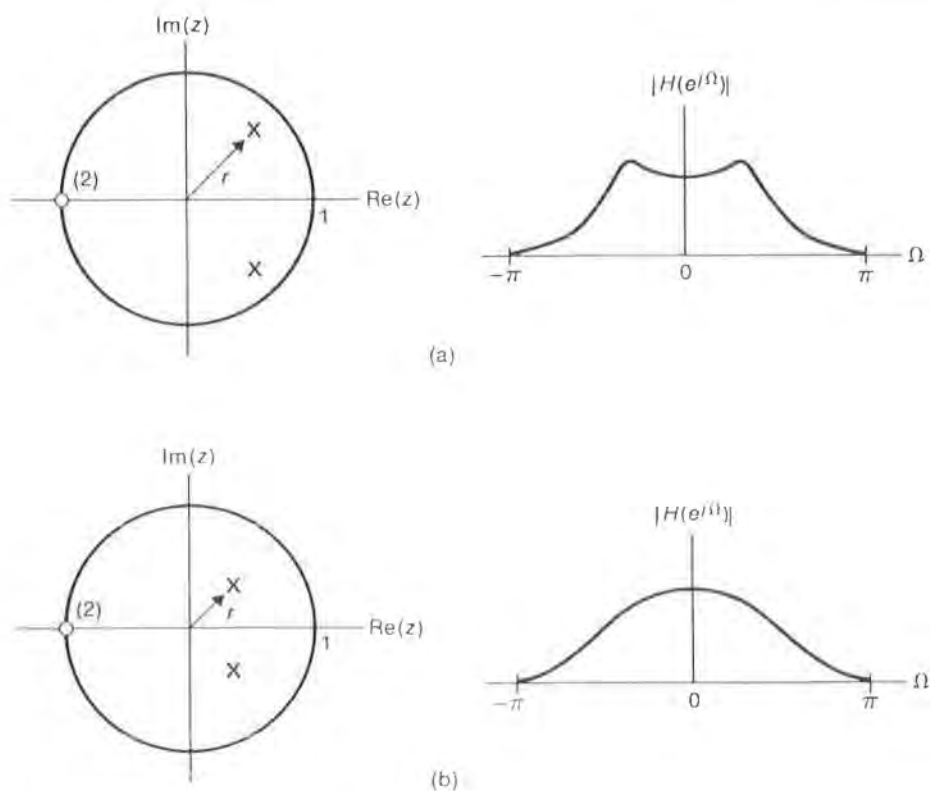


**FIGURE 6.20** Pole/zero plots and magnitude responses for second-order LPF.

sufficiently small, distinct peaks due to the poles are not discernible in  $|H(e^{j\Omega})|$ , and the response decreases monotonically, as depicted in Fig. 6.20(b).

*HPF Case.* For  $b_1 = -2$  and  $b_2 = 1$ , we have instead

$$\begin{aligned}
 H(z) &= \frac{1 - 2z^{-1} + z^{-2}}{1 - 2r(\cos \Omega_0)z^{-1} + r^2z^{-2}} \\
 &= \frac{(1 - z^{-1})^2}{1 - 2r(\cos \Omega_0)z^{-1} + r^2z^{-2}}, \quad |z| > r.
 \end{aligned} \tag{6.6.30}$$

Thus there is a double zero at  $z = +1$ , implying an HPF response with  $H(e^{j0}) = 0$ . As in the LPF case, we have again depicted two possible forms for the associated magnitude response in Fig. 6.21. That is, if the poles are close enough to the unit circle to produce discernible peaks in  $|H(e^{j\Omega})|$ , the response is nonmonotonic in the passband, as shown in Fig. 6.21(a), and the filter is said to be *highly underdamped*. However,

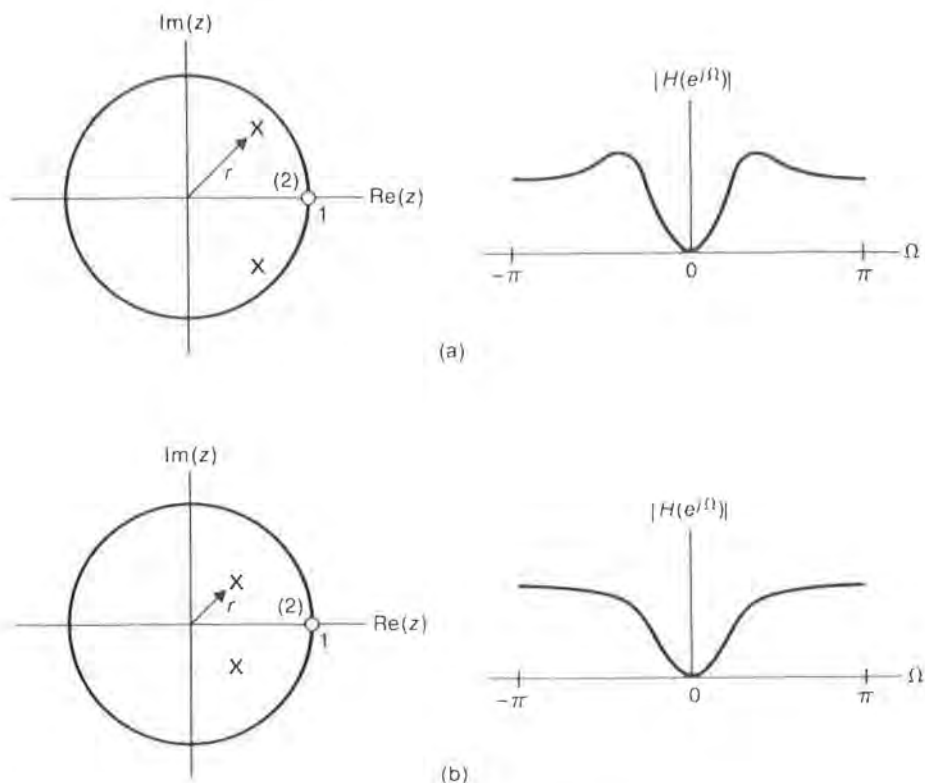


**FIGURE 6.21** Pole/zero plots and magnitude responses for second-order HPF.

if the radius ( $r$ ) of the poles is sufficiently small, distinct peaks due to the poles are not evident in  $|H(e^{j\Omega})|$ , and the response increases monotonically, as illustrated in Fig. 6.21(b).

*BPF Case.* For  $b_1 = 0$  and  $b_2 = -1$ , Eq. (6.6.28) becomes

$$\begin{aligned}
 H(z) &= \frac{1 - z^{-2}}{1 - 2r(\cos \Omega_0)z^{-1} + r^2 z^{-2}} \\
 &= \frac{(1 - z^{-1})(1 + z^{-1})}{1 - 2r(\cos \Omega_0)z^{-1} + r^2 z^{-2}}, \quad |z| > r,
 \end{aligned} \tag{6.6.31}$$

implying single zeros at both  $z = 1$  and  $z = -1$ , and thus  $H(e^{j0}) = H(e^{j\pi}) = 0$ . Figure 6.22 depicts the corresponding pole/zero plot and magnitude response. Note that the center frequency for the BPF response is approximately  $\Omega_0$  since the denominator vector from the pole at  $re^{j\Omega_0}$  to the point  $e^{j\Omega}$  on the unit circle is shortest when  $\Omega = \Omega_0$ . The associated 3-dB bandwidth is readily shown to be about  $2(1 - r)$  radians for narrowband filters, that is,  $0 \ll r < 1$  (see Problem 6.26).

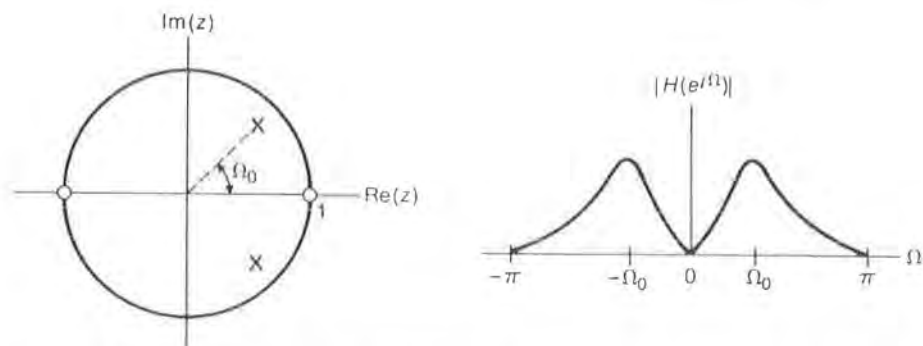


FIGURE 6.22 Pole/zero plot and magnitude response for second-order BPF.

*BSF Case.* For  $b_1 = -2(\cos \Omega_0)$  and  $b_2 = 1$ , Eq. (6.6.28) takes the form

$$H(z) = \frac{1 - 2(\cos \Omega_0)z^{-1} + z^{-2}}{1 - 2r(\cos \Omega_0)z^{-1} + r^2z^{-2}}, \quad |z| > r, \quad (6.6.32)$$

implying complex-conjugate zeros on the unit circle at angles of  $\pm\Omega_0$ , as shown in Fig. 6.23. That is,  $H(e^{j\Omega_0}) = H(e^{-j\Omega_0}) = 0$ . Note then that the pole angles and the zero angles are the same. Using the geometric method to sketch the resulting *notch-filter* response in Fig. 6.23, we produce  $|H(e^{j\Omega})|$  as shown. Note that at  $\Omega = 0$ , and also at  $\Omega = \pi$ , the numerator and denominator vectors all have about the same length, and hence  $H(e^{j0}) \approx H(e^{j\pi}) \approx 1$ . As in the BPF case, the associated 3-dB bandwidth (of the stopband) is readily shown to be about  $2(1 - r)$  radians for BSF responses with narrow stopbands, that is,  $0 \ll r < 1$  (see Problem 6.26).

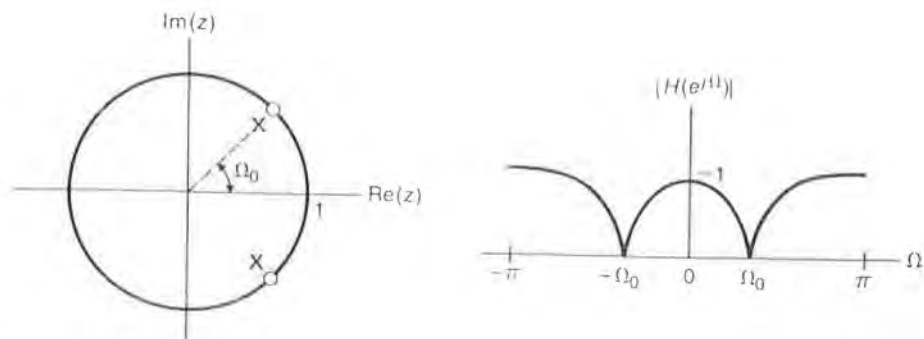


FIGURE 6.23 Pole/zero plot and magnitude response for second-order BSF.

**APPLICATION 6.2** Linear-Phase FIR Filters

Letting  $a_0 = 1$  and  $a_k = 0$  for all  $k > 0$  in the general difference equation in Eq. (6.6.1), we produce the *nonrecursive* difference equation

$$y[n] = \sum_{k=0}^M b_k x[n-k], \quad (6.6.33)$$

and thus, setting  $x[n] = \delta[n]$ , we find that the corresponding impulse response is simply

$$h[n] = \sum_{k=0}^M b_k \delta[n-k].$$

That is,

$$h[n] = \begin{cases} b_n, & n = 0, 1, \dots, M \\ 0, & \text{otherwise.} \end{cases} \quad (6.6.34)$$

Therefore any discrete-time system satisfying a finite-order nonrecursive difference equation is FIR. (As might then be expected, a *recursive* difference equation having  $a_k \neq 0$  for some  $k > 0$  usually implies an IIR system, but pole/zero cancelations can still cause such systems to be FIR.) Because of their special properties, discrete-time FIR filters find wide application in digital signal processing and communications.

The most important class of FIR filters in practice are those having piecewise linear-phase responses. Assuming  $h[n]$  to be real, such *linear-phase* filters have either even or odd symmetry about the midpoint of  $h[n]$ , that is,

$$b_n = b_{M-n} \quad (6.6.35)$$

or

$$b_n = -b_{M-n}. \quad (6.6.36)$$

Examples of even- and odd-symmetric impulse responses are shown in Fig. 6.24 for even and odd values of  $M$ . Note that the center of symmetry (shown by a dotted line) occurs at the coefficient  $b_{M/2}$  for  $M$  even, but between two coefficients for  $M$  odd. Note also that  $b_{M/2}$  must equal zero for odd symmetry and  $M$  even.

To show the linear-phase property of such filters, we first express the FIR system function  $H(z)$  as

$$\begin{aligned} H(z) &= \sum_{n=0}^M b_n z^{-n} \\ &= b_c z^{-M/2} + \sum_{n=0}^L (b_n z^{-n} + b_{M-n} z^{-(M-n)}) \end{aligned} \quad (6.6.37)$$

where  $L$  is the integer part of  $(M-1)/2$  and  $b_c$  is the central coefficient (if there is one), that is,

$$b_c = \begin{cases} b_{M/2}, & M \text{ even} \\ 0, & M \text{ odd.} \end{cases}$$

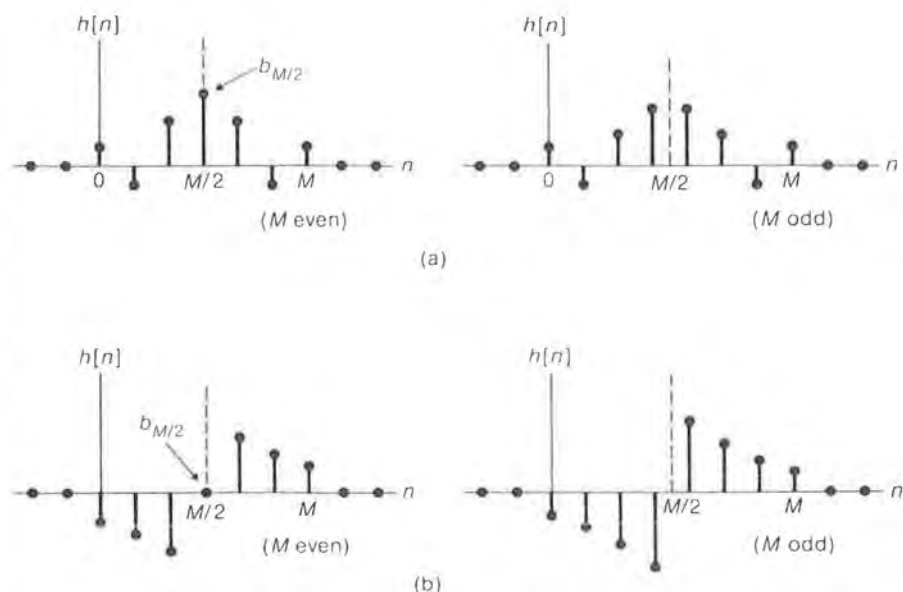


**FIGURE 6.24** Four cases of symmetry for linear-phase FIR filters: (a) even symmetry and (b) odd symmetry.

In the even-symmetry case ( $b_n = b_{M-n}$ ), we then have

$$\begin{aligned}
 H(e^{j\Omega}) &= b_c e^{-j\Omega M/2} + \sum_{n=0}^{L-1} b_n (e^{-j\Omega n} + e^{-j\Omega(M-n)}) \\
 &= e^{-j\Omega M/2} \left\{ b_c + \sum_{n=0}^{L-1} b_n (e^{j\Omega(M/2-n)} + e^{-j\Omega(M/2-n)}) \right\} \quad (6.6.38) \\
 &= e^{-j\Omega M/2} \left\{ b_c + \sum_{n=0}^{L-1} 2b_n \cos \left[ \Omega \left( \frac{M}{2} - n \right) \right] \right\} \\
 &= e^{-j\Omega M/2} R(\Omega),
 \end{aligned}$$

where  $R(\Omega)$  is a purely real function of  $\Omega$ . Therefore the associated magnitude and phase responses are simply

$$|H(e^{j\Omega})| = |R(\Omega)|$$

and

$$\angle H(e^{j\Omega}) = \frac{-\Omega M}{2} + \angle R(\Omega), \quad (6.6.39)$$

where  $\angle R(\Omega) = 0$  if  $R(\Omega) > 0$ , and  $\angle R(\Omega) = \pm\pi$  if  $R(\Omega) < 0$ . Hence the phase response is a piecewise linear function having a discontinuity of  $\pi$  radians at each zero crossing of  $R(\Omega)$ . A simple example of such a linear-phase filter is the LPF described by Eqs. (6.6.6) and (6.6.7) and depicted in Fig. 6.11.

A similar derivation for odd symmetry ( $b_n = -b_{M-n}$ ) leads to the result

$$\begin{aligned} H(e^{j\Omega}) &= je^{-j\Omega M/2} \sum_{n=0}^{L-1} 2b_n \sin \left[ \Omega \left( \frac{M}{2} - n \right) \right] \\ &= je^{-j\Omega M/2} R(\Omega) \\ &= e^{j(\pi/2 - \Omega M/2)} R(\Omega) \end{aligned} \quad (6.6.40)$$

for real  $R(\Omega)$ . Therefore the associated magnitude response is again simply

$$|H(e^{j\Omega})| = |R(\Omega)|,$$

but the phase response has an additional component of  $\pi/2$  ( $90^\circ$ ), that is,

$$\angle H(e^{j\Omega}) = \frac{\pi}{2} - \frac{\Omega M}{2} + \angle R(\Omega). \quad (6.6.41)$$

A simple example of this case is the first-difference operator  $H(z) = 1 - z^{-1}$  from Example 6.22, which has the frequency response

$$H(e^{j\Omega}) = 2je^{-j\Omega/2} \sin \frac{\Omega}{2}. \quad (6.6.42)$$

The corresponding magnitude and phase responses are then

$$|H(e^{j\Omega})| = 2 \left| \sin \frac{\Omega}{2} \right|$$

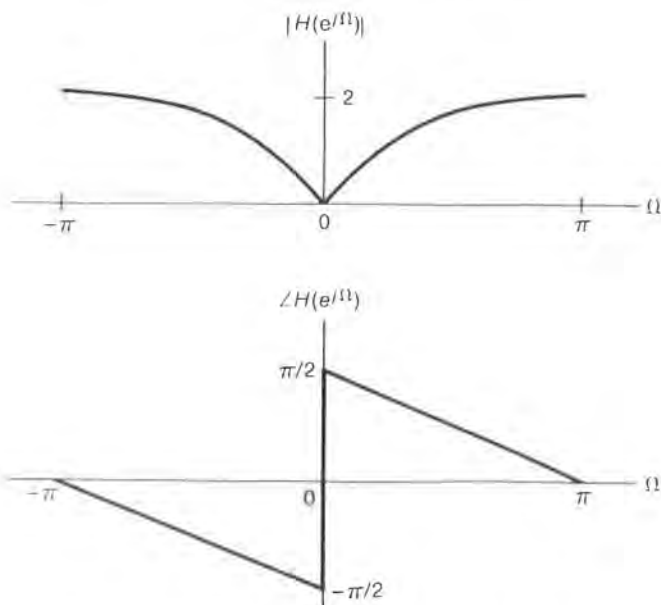


FIGURE 6.25 Magnitude and phase responses for  $H(z) = 1 - z^{-1}$ .

and

$$\angle H(e^{j\Omega}) = \begin{cases} \pi/2 - \Omega/2, & 0 < \Omega \leq \pi, \\ -\pi/2 - \Omega/2, & -\pi \leq \Omega < 0, \end{cases}$$

as shown in Fig. 6.25. Note, in particular, the phase discontinuity of  $-\pi$  radians at  $\Omega = 0$  due to the real factor  $R(\Omega) = 2 \sin \Omega/2$ , which changes sign at  $\Omega = 0$ .

**EXAMPLE 6.24** A crude but common technique for smoothing a noisy data sequence is to average the sequence over  $M + 1$  adjacent data samples, that is,

$$y[n] = \frac{1}{M + 1} \sum_{k=0}^M x[n - k]. \quad (6.6.43)$$

Hence,  $y[n]$  is computed as the average of  $x[n]$  and the  $M$  preceding samples  $x[n - 1]$ ,  $x[n - 2]$ ,  $\dots$ ,  $x[n - M]$ . The corresponding impulse response is thus

$$h[n] = \frac{1}{M + 1} \sum_{k=0}^M \delta[n - k] = \frac{1}{M + 1} (u[n] - u[n - M - 1]),$$

implying the system function

$$H(z) = \frac{1}{M + 1} \sum_{k=0}^M z^{-k} = \frac{1 - z^{-(M+1)}}{(M + 1)(1 - z^{-1})}. \quad (6.6.44)$$

The zeros of  $H(z)$  occur at values of  $z$  satisfying

$$z^{-(M+1)} = 1$$

and thus equal the  $(M + 1)$ st roots of unity, that is,

$$z_k = e^{j2\pi k/(M+1)}, \quad k = 1, 2, \dots, M. \quad (6.6.45)$$

The zero at  $z = 1$  for  $k = 0$  is not included in Eq. (6.6.45) because, as seen from Eq. (6.6.44), this zero is canceled by a pole at  $z = 1$ .

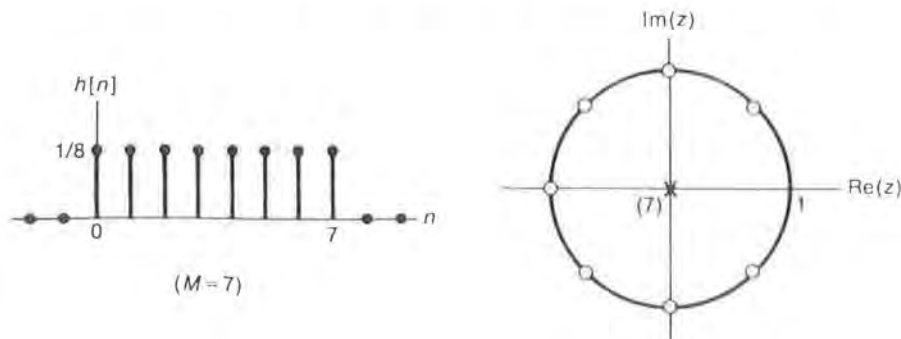


FIGURE 6.26 Impulse response and pole/zero plot for simple-averaging filter.

Therefore  $H(z)$  has  $M$  zeros on the unit circle spaced by  $2\pi/(M + 1)$  radians and  $M$  poles at  $z = 0$ , as illustrated in Fig. 6.26 for  $M = 7$ . Note that  $M$  zeros are expected since this is an  $M$ th-order FIR filter, and the  $M$  poles at  $z = 0$  result from the fact that the filter is causal. Also, since  $h[n]$  has even symmetry about its midpoint, this is a linear-phase FIR filter.

To determine the magnitude and phase responses, we set  $z = e^{j\Omega}$  in Eq. (6.6.44) to produce

$$\begin{aligned} H(e^{j\Omega}) &= \frac{1 - e^{-j\Omega(M+1)}}{(M+1)(1 - e^{-j\Omega})} \\ &= \frac{e^{-j\Omega(M+1)/2}(e^{j\Omega(M+1)/2} - e^{-j\Omega(M+1)/2})}{(M+1)e^{-j\Omega/2}(e^{j\Omega/2} - e^{-j\Omega/2})} \\ &= \frac{e^{-j\Omega M/2} \sin[\Omega(M+1)/2]}{(M+1) \sin(\Omega/2)} \\ &= e^{-j\Omega M/2} R(\Omega), \end{aligned}$$

which is consistent with Eq. (6.6.38). Figure 6.27 shows  $|H(e^{j\Omega})|$  and  $\angle H(e^{j\Omega})$  for  $M = 7$ . Hence the *simple-averaging* filter defined by Eq. (6.6.43) has a lowpass response and a bandwidth of about  $\pi/(M + 1)$ . Note that the zeros on the unit circle in the  $z$  plane produce *zeros of transmission* in  $|H(e^{j\Omega})|$  at  $\Omega = \pm 2\pi k/(M + 1)$ ,  $k = 1, 2, \dots, M$ , and that phase discontinuities of  $\pi$  radians occur in  $\angle H(e^{j\Omega})$  at the same frequencies.

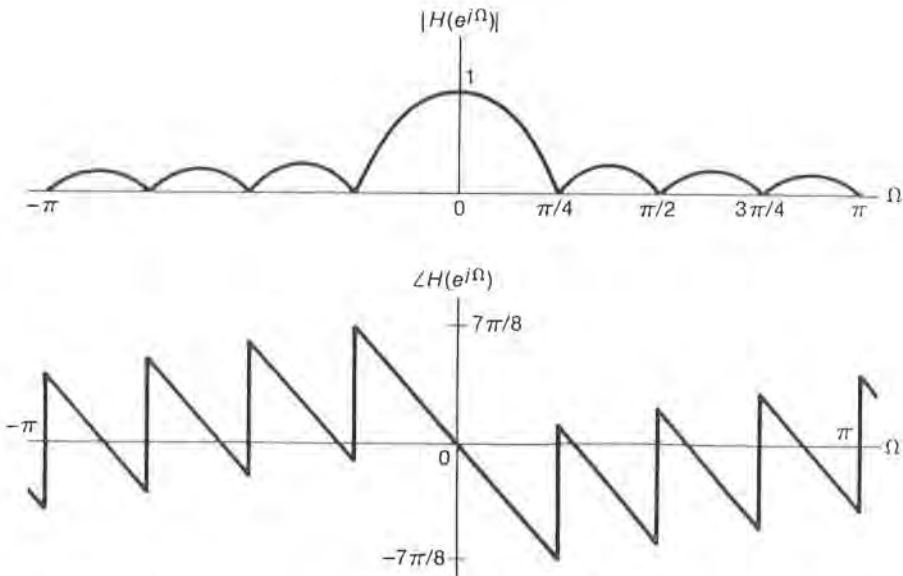


FIGURE 6.27 Magnitude and phase responses for simple-averaging filter.

## 6.7

## Structures for Discrete-Time Filters

In Section 3.8 block diagrams were employed to show the structure of discrete-time filter implementations as described by the corresponding difference equations. The structure corresponding directly to the general difference equation in Eq. (6.6.1) was called the *direct form* and is shown again in Fig. 6.28, with  $z^{-1}$  denoting each unit delay. (Interestingly, the corresponding block diagrams for continuous-time systems in Section 5.6 have  $s^{-1} = 1/s$  in place of  $z^{-1}$ , although the time-domain equivalents of these operators are completely different.)

Note that the structure in Fig. 6.28 consists effectively of the cascade of two subsystems. The first subsystem corresponds to the nonrecursive difference equation

$$v[n] = \sum_{k=0}^M b_k x[n - k] \quad (6.7.1)$$

and is thus FIR, while, in general, the second subsystem is IIR because it

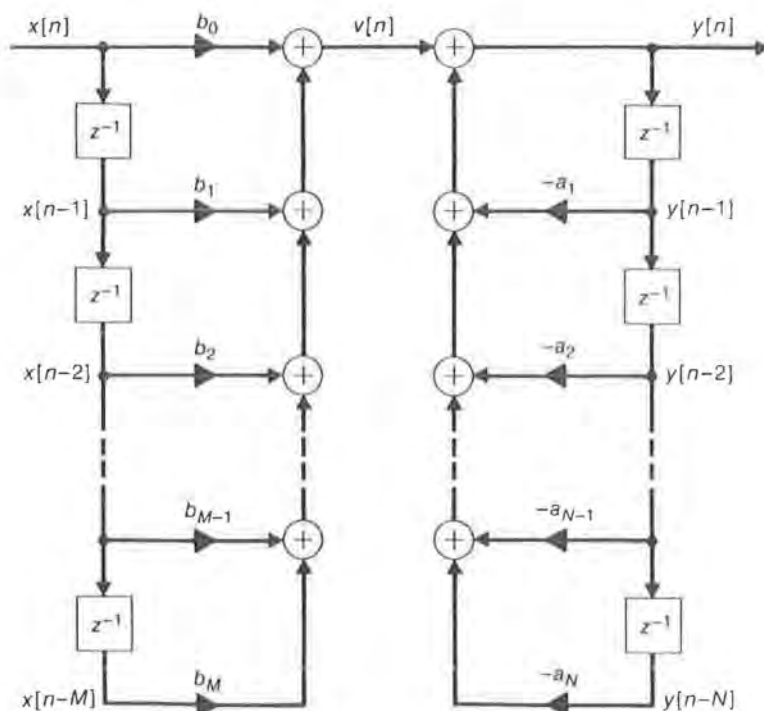


FIGURE 6.28 General discrete-time direct-form structure.

implements the recursive difference equation

$$y[n] = v[n] - \sum_{k=1}^N a_k y[n-k]. \quad (6.7.2)$$

Calling these subsystems  $H_1(z)$  and  $H_2(z)$ , respectively, we thus have

$$H(z) = H_1(z)H_2(z) = \frac{B(z)}{A(z)},$$

where

$$H_1(z) = B(z) = \sum_{k=0}^M b_k z^{-k} \quad (6.7.3)$$

and

$$H_2(z) = \frac{1}{A(z)} = \frac{1}{\sum_{k=0}^N a_k z^{-k}}, \quad (6.7.4)$$

with  $a_0 = 1$ . In the special case of  $N = 0$  (i.e., no feedback), we have simply  $A(z) = 1$ , and the direct form reduces to the *transversal* structure shown in Fig. 6.29, implementing the FIR system function  $H(z) = B(z)$ .

As noted in Section 3.8, the direct form in Fig. 6.28 is not *canonical* because the number of delays ( $M + N$ ) is not minimum unless  $M = 0$  or  $N = 0$ . Reversing the order of  $H_1(z)$  and  $H_2(z)$  and eliminating the redundant delays, as shown in Fig. 3.43, we produce the *canonical direct form II*, shown in Fig. 6.30 for  $M = N$ . Note that, in addition to  $N$  delays, this canonical form includes  $(2N + 1)$  multipliers and  $2N$  adders, in general, for an  $N$ th-order filter.

For example, direct-form-II implementations of the first-order LPF and HPF from Eqs. (6.6.8) and (6.6.9), respectively, are shown in Fig. 6.31. In each case, an additional scaling multiplier has been included at the input for unity gain. Note that the signs of the feedback multipliers ( $a$  and  $c$ ) and the corresponding terms in the denominators of  $H(z)$  are different, as opposed to the feedforward multipliers ( $\pm 1$ ) and the corresponding numerator terms.

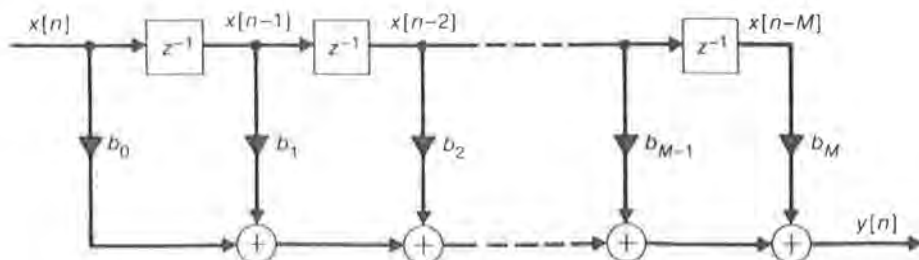


FIGURE 6.29 Transversal (direct-form) structure for FIR filter.

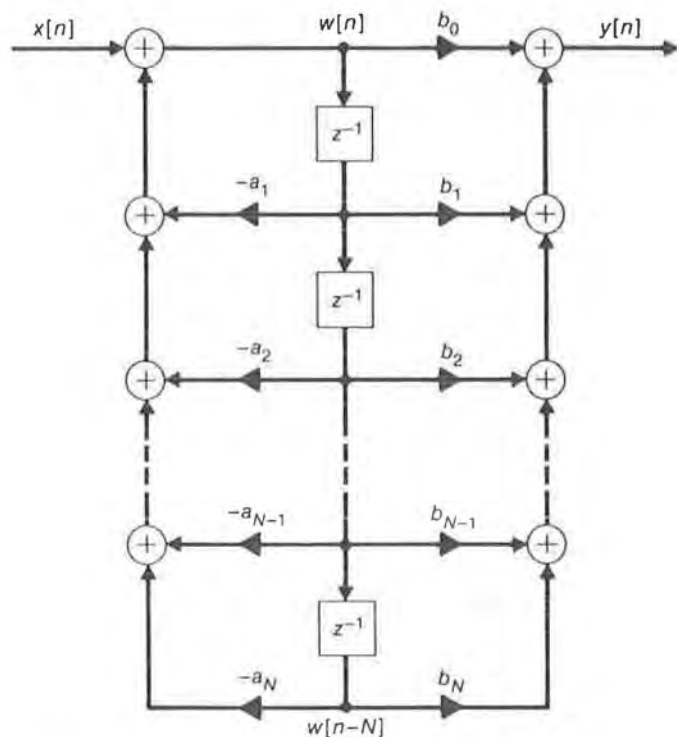


FIGURE 6.30 General discrete-time direct-form-II structure.

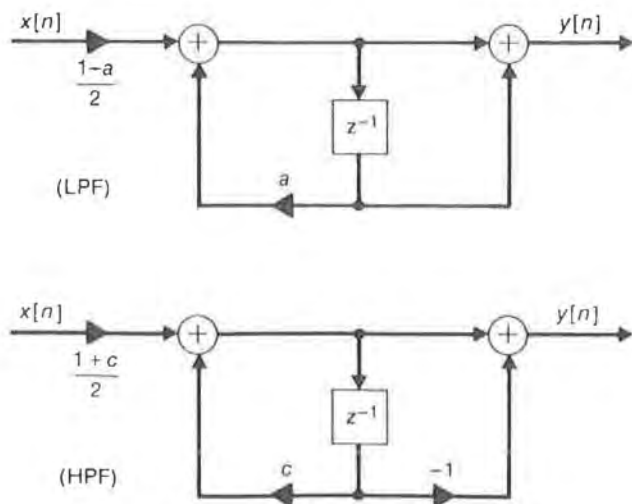


FIGURE 6.31 First-order LPF and HPF direct-form-II structures.

There are many other structures (canonical and otherwise) that are useful for implementing discrete-time filters. These structures have various desirable properties such as modularity and/or reduced sensitivity to quantization effects in digital realizations (*digital filters*). Two canonical structures having both of these properties are the *parallel form* and the *cascade form*. To derive the parallel form, we expand  $H(z)$  in the partial-fraction expansion

$$H(z) = g_0 + \sum_{k=1}^N \frac{q_k}{1 - p_k z^{-1}} \quad (6.7.5)$$

(assuming no multiple poles), where  $g_0 = 0$  if  $M < N$ . This form for  $H(z)$  implies a parallel combination of  $N$  first-order subfilters. However, since, in general, the poles  $p_k$  and residues  $q_k$  are complex-valued, complex multipliers would be required in the corresponding implementation. In particular, if we assume that  $h[n]$  is real-valued,  $H(z)$  can be rewritten as

$$H(z) = g_0 + \sum_{k=1}^L \left( \frac{q_k}{1 - p_k z^{-1}} + \frac{q_k^*}{1 - p_k^* z^{-1}} \right) + \sum_{k=2L+1}^N \frac{q_k}{1 - p_k z^{-1}},$$

where  $p_k, k = 1, \dots, L, (L \leq N/2)$  are complex-valued and  $p_k, k = 2L + 1, \dots, N$ , are real-valued. To avoid the unnecessary complication of complex multipliers, we combine the terms in the first summation to obtain

$$H(z) = g_0 + \sum_{k=1}^L \frac{\gamma_{0k} + \gamma_{1k} z^{-1}}{1 + \alpha_{1k} z^{-1} + \alpha_{2k} z^{-2}} + \sum_{k=2L+1}^N \frac{q_k}{1 - p_k z^{-1}}, \quad (6.7.6)$$

where

$$\begin{aligned} \alpha_{1k} &= -2 \operatorname{Re}\{p_k\} & \alpha_{2k} &= |p_k|^2 \\ \gamma_{0k} &= 2 \operatorname{Re}\{q_k\} & \gamma_{1k} &= -2 \operatorname{Re}\{p_k^* q_k\}. \end{aligned}$$

Hence all of the coefficients in Eq. (6.7.6) are real-valued. Using direct-form-II networks to realize each of the terms in Eq. (6.7.6), we produce *parallel form II*, which is shown in Fig. 6.32 for  $N$  odd and  $L = (N - 1)/2$ . Note that the parallel form is also canonical since, in general, it has  $N$  delays,  $(2N + 1)$  multipliers, and  $2N$  adders. If several poles are real-valued (that is, if  $N - 2L \geq 2$ ), some or all of the associated first-order terms in Eq. (6.7.6) are often combined into second-order terms to produce additional second-order *sections* in the parallel form, which increases the modularity of the corresponding hardware or software implementations.

To obtain the cascade form, we instead factor  $H(z)$  into a product of first-order terms of the form

$$H(z) = b_0 \prod_{k=1}^N \frac{1 - z_k z^{-1}}{1 - p_k z^{-1}}, \quad (6.7.7)$$

where for simplicity we have assumed that  $M = N$  and  $a_0 = 1$ . (Multiple poles and/or zeros are allowed). This expression for  $H(z)$  implies a cascade

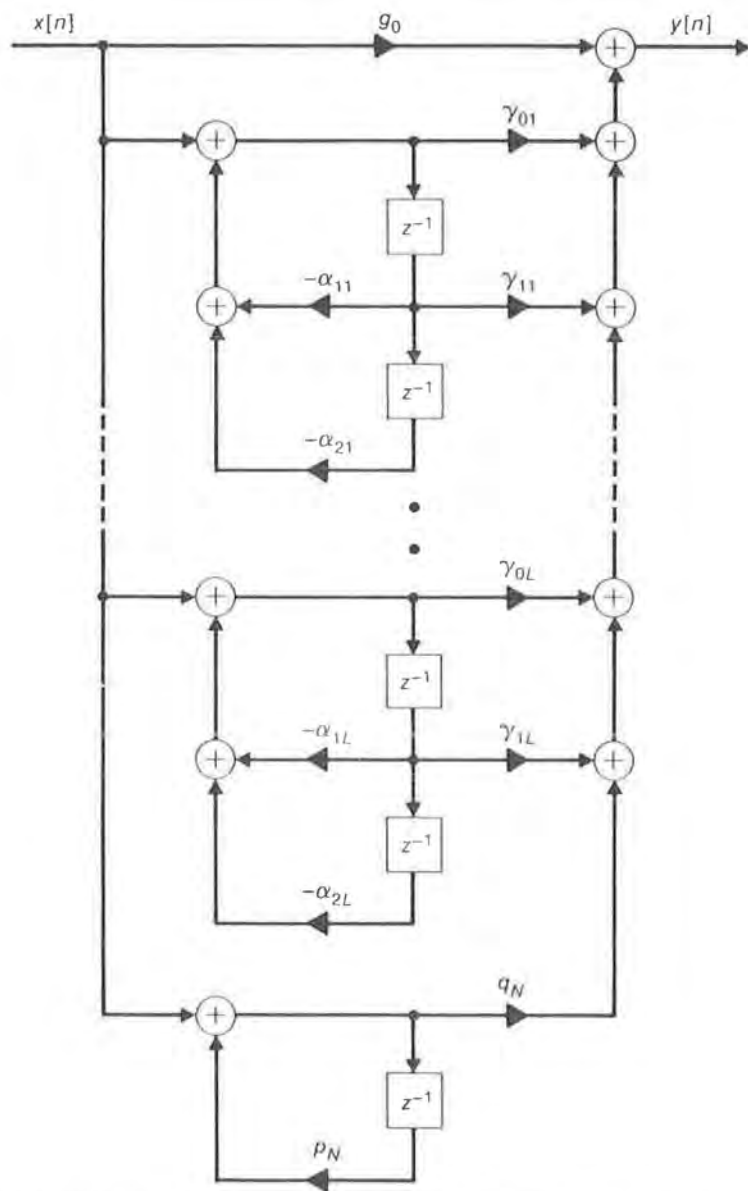
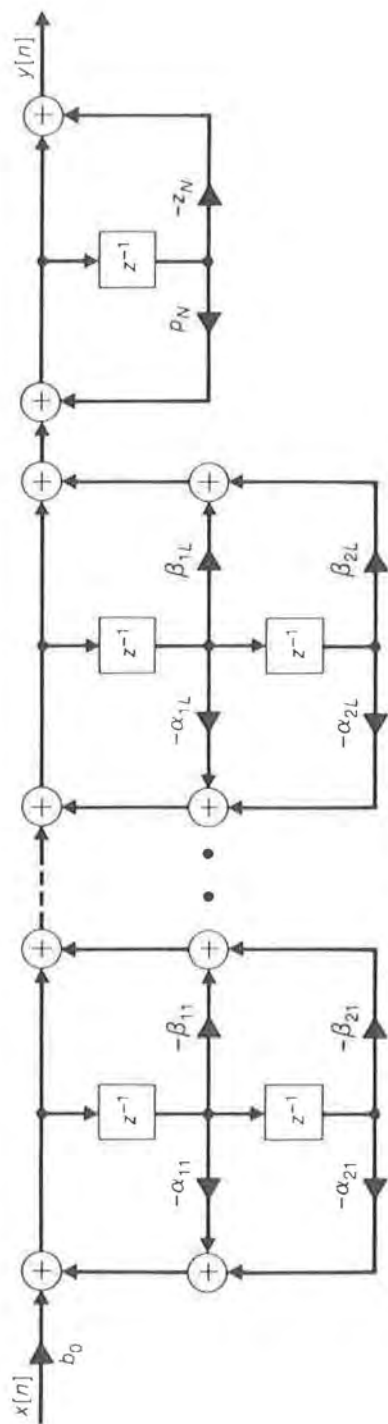


FIGURE 6.32  $N$ th-order parallel-form-II structure for  $N$  odd.

combination of  $N$  first-order subfilters, but again complex-valued  $p_k$  and  $z_k$  would necessitate complex multipliers. Therefore, rewriting  $H(z)$  as

$$H(z) = b_0 \frac{\prod_{k=1}^K (1 - z_k z^{-1})(1 - z_k^* z^{-1}) \prod_{k=2K+1}^N (1 - z_k z^{-1})}{\prod_{k=1}^L (1 - p_k z^{-1})(1 - p_k^* z^{-1}) \prod_{k=2L+1}^N (1 - p_k z^{-1})},$$



**FIGURE 6.33** Nth-order cascade-form-II structure for N odd.

where  $z_k, k = 1, \dots, K$ , and  $p_k, k = 1, \dots, L$ , ( $K, L \leq N/2$ ) are complex-valued and  $z_k, k = 2K + 1, \dots, N$ , and  $p_k, k = 2L + 1, \dots, N$ , are real-valued, we can combine the complex factors to obtain

$$H(z) = b_0 \frac{\prod_{k=1}^K (1 + \beta_{1k} z^{-1} + \beta_{2k} z^{-2}) \prod_{k=2K+1}^N (1 - z_k z^{-1})}{\prod_{k=1}^L (1 + \alpha_{1k} z^{-1} + \alpha_{2k} z^{-2}) \prod_{k=2L+1}^N (1 - p_k z^{-1})}, \quad (6.7.8)$$

where

$$\begin{aligned} \alpha_{1k} &= -2 \operatorname{Re}\{p_k\} & \alpha_{2k} &= |p_k|^2 \\ \beta_{1k} &= -2 \operatorname{Re}\{z_k\} & \beta_{2k} &= |z_k|^2. \end{aligned}$$

Therefore, since all of the coefficients in this expression are real-valued,  $H(z)$  can be implemented as a cascade of first- and second-order sections with real multipliers. Again, if there are several real-valued poles and/or zeros (i.e., if  $N - 2L \geq 2$  and/or  $N - 2K \geq 2$ ), the corresponding factors are usually combined in pairs to produce additional second-order sections. Realizing the resulting first- and second-order sections using direct-form-II networks, we produce *cascade form II*, illustrated in Fig. 6.33 for  $N$  odd. Note that the cascade form is also, in general, canonical.

A useful property of the cascade form is that for zeros on the unit circle,  $|z_k| = 1$  and thus  $\beta_{2k} = 1$  (or  $\beta_{2k} = -1$  for zeros at  $z = \pm 1$ ). Furthermore,  $\beta_{1k} = 2, -2$ , or  $0$  for zeros at  $z = -1, z = 1$ , or  $z = \pm 1$ , respectively. Since these integer values for  $\beta_{2k}$  and  $\beta_{1k}$  do not require actual multiplication (only shifting in binary for  $\beta_{1k} = \pm 2$ ), substantial savings in component count or execution time are often realized by employing the cascade form.

Many other structures have been developed to implement discrete-time filters with various trade-offs involving modularity, sensitivity, and number of components (primarily multipliers). These structures have names such as *state-space structures*, *normal forms*, *lattice structures*, and *wave digital filters*. By far the most popular structure in practice, however, is the cascade form because it is modular, has low sensitivity, and is canonical.

## SUMMARY

In this chapter we have seen that the  $z$  transform plays an analogous role in the analysis and design of discrete-time signals and systems to that of the Laplace transform in the continuous-time case. Hence, as might be expected, the properties of these transforms and their regions of convergence are closely parallel, with the counterpart of vertical lines in the  $s$  plane being circles in the  $z$  plane. Of particular importance is the

characterization of an LTI system in terms of its system function  $H(z)$  and the associated poles and zeros in the  $z$  plane. Also, the frequency response  $H(e^{j\Omega})$  of a (stable) system is given by  $H(z)$  evaluated on the unit circle and can be determined geometrically from the pole/zero plot. Discrete-time filters are classified as having either finite or infinite (duration) impulse responses, with IIR filters satisfying recursive difference equations and FIR filters satisfying nonrecursive difference equations (although recursive realizations also exist for FIR filters). An important subclass of FIR filters are those having piecewise linear phase responses, corresponding to even or odd symmetry in the impulse response. Several canonical filter structures were presented.

## APPENDIX 6A

### The Unilateral $z$ Transform

The  $z$  transform defined in Eq. (6.2.1) is sometimes referred to as the two-sided or *bilateral  $z$  transform (BZT)* to distinguish it from the one-sided or *unilateral  $z$  transform (UZT)* defined by

$$X(z) = \sum_{n=0}^{\infty} x[n]z^{-n}. \quad (6.A.1)$$

The UZT is useful for calculating the response of a causal system to a causal input when the system is described by a linear difference equation with constant coefficients but nonzero initial conditions. That is, the system need not be at initial rest. Specifically, the zero-input response  $y_{zi}[n]$ , as well as the zero-state response  $y_{zs}[n]$ , is readily determined using the UZT (see Section 3.8). Note that such analysis is not anticipated by the relationship  $Y(z) = H(z)X(z)$  using the BZT because this assumes that the system is LTI, not merely incrementally linear. (On the other hand, if the nonzero initial conditions are replaced by an equivalent nonzero input  $x[n]$  for  $-\infty < n < 0$ , then the BZT can be employed.)

The basic properties of the UZT that are useful in this application relate to the transforms of the delayed signals  $x[n - k]$  and are listed in Table 6A. These properties may be derived as follows: Computing the UZT of the unit delay  $x[n - 1]$ , we have

$$\begin{aligned} \sum_{n=0}^{\infty} x[n - 1]z^{-n} &= x[-1] + \sum_{n=1}^{\infty} x[n - 1]z^{-n} \\ &= x[-1] + z^{-1} \sum_{m=0}^{\infty} x[m]z^{-m} \\ &= x[-1] + z^{-1}X(z), \end{aligned} \quad (6.A.2)$$

**TABLE 6A** Unilateral  $z$  Transforms

Delayed signal	Transform
$x[n-1]$	$z^{-1}X(z) + x[-1]$
$x[n-2]$	$z^{-2}X(z) + x[-1]z^{-1} + x[-2]$
$x[n-3]$	$z^{-3}X(z) + x[-1]z^{-2} + x[-2]z^{-1} + x[-3]$
$x[n-k]$	$z^{-k}X(z) + x[-1]z^{-(k-1)} + \cdots + x[-(k-1)]z^{-1} + x[-k]$

as indicated in Table 6A. Likewise,

$$\begin{aligned} \sum_{n=0}^{\infty} x[n-2]z^{-n} &= x[-2] + \sum_{n=1}^{\infty} x[n-2]z^{-n} \\ &= x[-2] + z^{-1} \sum_{m=0}^{\infty} x[m-1]z^{-m} \quad (6.A.3) \\ &= x[-2] + z^{-1}x[-1] + z^{-2}X(z), \end{aligned}$$

and so forth.

**EXAMPLE 6.25** Repeating Example 3.16 using the UZT, we have the linear difference equation

$$y[n] - ay[n-1] = x[n] = b^n u[n],$$

with  $y[-1] = Y_I$ . Applying the UZT to both sides of this equation, we obtain

$$Y(z) - az^{-1}Y(z) - ay[-1] = \frac{1}{1 - bz^{-1}}$$

or

$$(1 - az^{-1})Y(z) - aY_I = \frac{1}{1 - bz^{-1}},$$

and thus

$$Y(z) = \frac{1}{(1 - az^{-1})(1 - bz^{-1})} + \frac{aY_I}{1 - az^{-1}},$$

from which

$$y[n] = \frac{b^{n+1} - a^{n+1}}{b - a} + Y_I a^{n+1}, \quad n \geq 0.$$

In particular, note that

$$y_{zs}[n] = \frac{b^{n+1} - a^{n+1}}{b - a},$$

while

$$y_{zi}[n] = Y_I a^{n+1}.$$

**EXAMPLE 6.26** The response of an all-pole discrete-time system with zero input for  $n \geq 0$ , but nonzero initial conditions, can be modeled as the impulse response of a pole/zero system at initial rest. To see this, consider the second-order difference equation

$$y[n] + a_1 y[n-1] + a_2 y[n-2] = x[n], \quad (6.A.4)$$

with  $x[n] = 0$ ,  $n \geq 0$ , and initial conditions  $y[-1] = Y_{I1}$  and  $y[-2] = Y_{I2}$ , corresponding to the LTI system

$$H(z) = \frac{1}{1 + a_1 z^{-1} + a_2 z^{-2}},$$

with an unknown input for  $n < 0$ . Taking the UZT of both sides of Eq. (6.A.4), we obtain

$$Y(z) + a_1 \{z^{-1} Y(z) + y[-1]\} + a_2 \{z^{-2} Y(z) + z^{-1} y[-1] + y[-2]\} = 0$$

or

$$Y(z)[1 + a_1 z^{-1} + a_2 z^{-2}] = -[a_1 Y_{I1} + a_2 Y_{I2}] - a_2 Y_{I1} z^{-1},$$

from which

$$Y(z) = \frac{b_0 + b_1 z^{-1}}{1 + a_1 z^{-1} + a_2 z^{-2}},$$

where  $b_0 = -[a_1 Y_{I1} + a_2 Y_{I2}]$  and  $b_1 = -a_2 Y_{I1}$ . Hence  $Y(z)$  has the form of a system function with the same poles as  $H(z)$ , plus a zero at  $z = -b_1/b_0$ , and  $y[n]$  can be thought of as the corresponding impulse response.

## APPENDIX 6B

### Partial-Fraction Expansion for Multiple Poles

The partial-fraction expansions of  $B(z)/A(z)$  in Eq. (6.3.9) or  $C(z)/A(z)$  in Eq. (6.3.12) assumed that there are no multiple poles, i.e., that the roots of  $A(z)$  are distinct. If this is not the case, the PFE must be modified to include higher-order terms of the form in Table 6B with inverse transforms

TABLE 6B Higher-Order PFE Terms

PFE Term	ROC	Inverse transform
$\frac{1}{(1 - az^{-1})^2}$	$ z  >  a $	$(n + 1)a^n u[n]$
$\frac{1}{(1 - az^{-1})^2}$	$ z  <  a $	$-(n + 1)a^n u[-n - 1]$
$\frac{1}{(1 - az^{-1})^3}$	$ z  >  a $	$\frac{1}{2!}(n + 1)(n + 2)a^n u[n]$
$\frac{1}{(1 - az^{-1})^3}$	$ z  <  a $	$-\frac{1}{2!}(n + 1)(n + 2)a^n u[-n - 1]$
$\frac{1}{(1 - az^{-1})^4}$	$ z  >  a $	$\frac{1}{3!}(n + 1)(n + 2)(n + 3)a^n u[n]$
$\frac{1}{(1 - az^{-1})^4}$	$ z  <  a $	$-\frac{1}{3!}(n + 1)(n + 2)(n + 3)a^n u[-n - 1]$

as given (see Problem 6.10). That is, writing  $B(z)/A(z)$  from Eq. (6.3.11) as

$$\frac{B(z)}{A(z)} = G(z) + \frac{C(z)}{(1 - az^{-1})^{K_a}(1 - bz^{-1})^{K_b}(1 - cz^{-1})^{K_c} \dots}, \quad (6.B.1)$$

where  $K_a$  is the multiplicity of the pole at  $z = a$ ,  $K_b$  is the multiplicity of the pole at  $z = b$ , etc., the rational fraction  $C(z)/A(z)$  can be expanded in the PFE

$$\begin{aligned} \frac{C(z)}{A(z)} = & \frac{r_{a1}}{1 - az^{-1}} + \frac{r_{a2}}{(1 - az^{-1})^2} + \dots + \frac{r_{aK_a}}{(1 - az^{-1})^{K_a}} \\ & + \frac{r_{b1}}{1 - bz^{-1}} + \frac{r_{b2}}{(1 - bz^{-1})^2} + \dots + \frac{r_{bK_b}}{(1 - bz^{-1})^{K_b}} + \dots \end{aligned} \quad (6.B.2)$$

[Note that  $C(z) = B(z)$  unless  $G(z) \neq 0$ .]

There are several methods to determine the residues  $r_{a1}, r_{b1}, \dots$ , associated with these higher-order terms, as in the case of Laplace transforms, and we will demonstrate two in the following examples. The method of *successive PFEs* is simple and often applicable but requires that

$$M \leq N_p \quad (6.B.3)$$

or

$$M' \leq N_p \quad (\text{if } M \geq N), \quad (6.B.4)$$

where  $M$  and  $M'$  are the orders of  $B(z)$  and  $C(z)$ , respectively, and  $N_p$  is the number of distinct poles. In particular, this method can always be used

if there is only one double pole ( $N_p = N - 1$ ) since  $M' < N$ . On the other hand, the *derivative* method always works but is more complicated.

**EXAMPLE 6.27** *Successive PFEs*

Given the  $z$  transform

$$X(z) = \frac{3 - 2z^{-1}}{(1 - z^{-1})(1 - 0.5z^{-1})^3}, \quad 0.5 < |z| < 1,$$

we note that  $M = 1$  and  $N_p = 2$ , and thus Eq. (6.B.3) is satisfied. Rewriting  $X(z)$  as the product

$$X(z) = \left[ \frac{3 - 2z^{-1}}{(1 - z^{-1})(1 - 0.5z^{-1})} \right] \frac{1}{(1 - 0.5z^{-1})^2},$$

with the first factor containing only single poles, we expand that factor in a PFE to produce

$$\begin{aligned} X(z) &= \left[ \frac{2}{1 - z^{-1}} + \frac{1}{1 - 0.5z^{-1}} \right] \frac{1}{(1 - 0.5z^{-1})^2} \\ &= \frac{2}{(1 - z^{-1})(1 - 0.5z^{-1})^2} + \frac{1}{(1 - 0.5z^{-1})^3}. \end{aligned}$$

Since the first term in this expression is still not of the form in Eq. (6.B.2), we repeat the above steps for that term, as follows:

$$\begin{aligned} X(z) &= \left[ \frac{2}{(1 - z^{-1})(1 - 0.5z^{-1})} \right] \frac{1}{(1 - 0.5z^{-1})} + \frac{1}{(1 - 0.5z^{-1})^3} \\ &= \left[ \frac{4}{1 - z^{-1}} - \frac{2}{1 - 0.5z^{-1}} \right] \frac{1}{(1 - 0.5z^{-1})} + \frac{1}{(1 - 0.5z^{-1})^3} \\ &= \frac{4}{(1 - z^{-1})(1 - 0.5z^{-1})} - \frac{2}{(1 - 0.5z^{-1})^2} + \frac{1}{(1 - 0.5z^{-1})^3} \\ &= \frac{8}{1 - z^{-1}} - \frac{4}{1 - 0.5z^{-1}} - \frac{2}{(1 - 0.5z^{-1})^2} + \frac{1}{(1 - 0.5z^{-1})^3}, \end{aligned}$$

which has the form of Eq. (6.B.2). Therefore, since  $0.5 < |z| < 1$ , the corresponding inverse transform is given by

$$\begin{aligned} x[n] &= -8u[-n - 1] \\ &\quad + \{-4 - 2(n + 1) + 0.5(n + 1)(n + 2)\}(0.5)^n u[n]. \end{aligned}$$

**EXAMPLE 6.28** *Derivative Method*

Given the  $z$  transform

$$X(z) = \frac{5 - 12z^{-1} + 8.5z^{-2} - 2z^{-3}}{(1 - z^{-1})^3(1 - 0.5z^{-1})}, \quad |z| > 1,$$

we now have  $M = 3$ ,  $N = 4$ , and  $N_p = 2$ . Hence, neither Eq. (6.B.3) nor Eq. (6.B.4) is satisfied, and the method of successive PFEs cannot be employed. However,  $X(z)$  can still be expanded in the form

$$\frac{5 - 12z^{-1} + 8.5z^{-2} - 2z^{-3}}{(1 - z^{-1})^3(1 - 0.5z^{-1})} = \frac{r_1}{1 - z^{-1}} + \frac{r_2}{(1 - z^{-1})^2} + \frac{r_3}{(1 - z^{-1})^3} + \frac{r_4}{1 - 0.5z^{-1}} \quad (6.B.5)$$

as follows: First, letting  $z^{-1} = -v$ , we rewrite Eq. (6.B.5) in the more convenient form

$$\frac{5 + 12v + 8.5v^2 + 2v^3}{(1 + v)^3(1 + 0.5v)} = \frac{r_1}{1 + v} + \frac{r_2}{(1 + v)^2} + \frac{r_3}{(1 + v)^3} + \frac{r_4}{1 + 0.5v} \quad (6.B.6)$$

Then, multiplying both sides of Eq. (6.B.6) by  $(1 + 0.5v)$  and setting  $v = -2$ , we find that

$$r_4 = \left. \frac{5 + 12v + 8.5v^2 + 2v^3}{(1 + v)^3} \right|_{v=-2} = 1.$$

Next, multiplying both sides of Eq. (6.B.6) by  $(1 + v)^3$ , we obtain the expression

$$\frac{5 + 12v + 8.5v^2 + 2v^3}{1 + 0.5v} = r_1(1 + v)^2 + r_2(1 + v) + r_3 + \frac{r_4(1 + v)^3}{1 + 0.5v} \quad (6.B.7)$$

from which we have

$$r_3 = \left. \frac{5 + 12v + 8.5v^2 + 2v^3}{1 + 0.5v} \right|_{v=-1} = -1.$$

To determine  $r_2$ , we differentiate both sides of Eq. (6.B.7), yielding

$$\frac{12 + 17v + 6v^2}{1 + 0.5v} - \frac{5 + 12v + 8.5v^2 + 2v^3}{2(1 + 0.5v)^2} = 2r_1(1 + v) + r_2 + r_4(1 + v)^2 F(v), \quad (6.B.8)$$

where  $F(v)$  is some function of  $v$ , and thus

$$r_2 = \left. \frac{12 + 17v + 6v^2}{1 + 0.5v} - \frac{5 + 12v + 8.5v^2 + 2v^3}{2(1 + 0.5v)^2} \right|_{v=-1} = 3.$$

Finally, to obtain  $r_2$ , we differentiate Eq. (6.B.8), producing

$$\frac{17 + 12v}{1 + 0.5v} - \frac{12 + 17v + 6v^2}{2(1 + 0.5v)^2} - \frac{12 + 17v + 6v^2}{2(1 + 0.5v)^2} + \frac{2(5 + 12v + 8.5v^2 + 2v^3)}{4(1 + 0.5v)^3} = 2r_1 + r_4(1 + v)G(v)$$

for some  $G(v)$ , and thus

$$2r_1 = \frac{17 + 12v}{1 + 0.5v} - \frac{12 + 17v + 6v^2}{(1 + 0.5v)^2} + \frac{2(5 + 12v + 8.5v^2 + 2v^3)}{4(1 + 0.5v)^3} \Big|_{v=-1} = 4$$

or

$$r_1 = 2.$$

Therefore, substituting these residue values into Eq. (6.B.5), we produce

$$X(z) = \frac{2}{1 - z^{-1}} + \frac{3}{(1 - z^{-1})^2} - \frac{1}{(1 - z^{-1})^3} + \frac{1}{1 - 0.5z^{-1}}, \quad |z| > 1,$$

from which

$$x[n] = \{2 + 3(n + 1) - 0.5(n + 1)(n + 2) + (0.5)^n\}u[n].$$

## PROBLEMS

**6.1** Find the eigenvalues  $H(z)$  associated with the following LTI systems  $h[n]$  and eigenfunctions  $\phi[n] = z^n$ . State any restrictions on the (complex) values of  $z$  for  $H(z)$  to converge.

- (a)  $h[n] = u[n]$ . (b)  $h[n] = u[n] - u[n - N]$ .  
 (c)  $h[n] = a^n u[-n]$ . (d)  $h[n] = (\cos \Omega_0 n)u[n]$ .

**6.2** Find the  $z$  transform  $X(z)$  and the associated region of convergence for each of the following signals and draw the corresponding pole/zero plot.

- (a)  $x[n] = (\sin \Omega_0 n)u[n]$ . (b)  $x[n] = (\cos \Omega_0 n)u[-n - 1]$ .  
 (c)  $x[n] = \delta[n + N] - \delta[n - N]$ . (d)  $x[n] = a^{|n|}$ ,  $|a| < 1$ .  
 (e)  $x[n] = a^{n-1}u[n - 1]$ . (f)  $x[n] = a^{n+1}u[n + 1]$ .

- 6.3 Find  $X(z)$ , including the ROC, for the signal

$$x[n] = Ar^n \cos(\Omega_0 n + \theta)u[n].$$

Plot the corresponding pole/zero plot for  $\theta = 0$  and for  $\theta = -\pi/2$  with  $0 < r < 1$ .

- 6.4 Invert the following  $z$  transforms, using *both* long division and partial-fraction expansion, and plot the pole/zero diagram with ROC for each  $X(z)$ .

$$(a) X(z) = \frac{1}{1 - a^2 z^{-2}},$$

$$|z| > |a|.$$

$$(b) X(z) = \frac{1}{1 - a^2 z^{-2}},$$

$$|z| < |a|.$$

$$(c) X(z) = \frac{1}{1 + a^2 z^{-2}},$$

$$|z| > |a|.$$

$$(d) X(z) = \frac{1}{1 + a^2 z^{-2}},$$

$$|z| < |a|.$$

$$(e) X(z) = \frac{1}{1 - a^4 z^{-4}},$$

$$|z| > |a|.$$

$$(f) X(z) = \frac{1}{1 - a^4 z^{-4}},$$

$$|z| < |a|.$$

- 6.5 Invert each of the following  $X(z)$  to find the associated signal  $x[n]$ .

$$(a) X(z) = \frac{2 - z^{-1}}{1 - z^{-1} - 0.75z^{-2}}, \quad |z| > 1.5,$$

$$(b) X(z) = \frac{2 - z^{-1}}{1 - z^{-1} - 0.75z^{-2}}, \quad 0.5 < |z| < 1.5,$$

$$(c) X(z) = \frac{2 - z^{-1}}{1 - z^{-1} - 0.75z^{-2}}, \quad |z| < 0.5,$$

$$(d) X(z) = \frac{1 - z^{-1} - 0.75z^{-2}}{2 - z^{-1}}, \quad |z| > 0.5,$$

$$(e) X(z) = \frac{1 - z^{-1} - 0.75z^{-2}}{2 - z^{-1}}, \quad 0 < |z| < 0.5.$$

- 6.6 Invert each of the following irrational  $z$  transforms.

$$(a) X(z) = e^{a/z}, \quad |z| > 0.$$

$$(b) X(z) = -\log(1 - az), \quad |z| < 1/|a|.$$

- 6.7 Show the following properties for the  $z$  transforms of even and odd discrete-time functions.

$$(a) \text{ If } x[n] \text{ is even, that is, } x[n] = x[-n], \text{ then } X(z) = X(z^{-1}).$$

$$(b) \text{ If } x[n] \text{ is odd, that is, } x[n] = -x[-n], \text{ then } X(z) = -X(z^{-1}).$$

$$(c) \text{ If } x[n] \text{ is odd, then there is a zero in } X(z) \text{ at } z = 1.$$

- (d) If  $x[n]$  is even or odd, then for each pole in  $X(z)$  at  $z = p_k$ , there is also a pole at  $z = 1/p_k$ .
- (e) If  $x[n]$  is even or odd, the ROC for  $X(z)$  is of the form  $a < |z| < 1/a$ , or else it is the entire  $z$  plane (if it exists at all).

**6.8** Prove the following properties of the  $z$  transform:

- (a) The linearity property in Eq. (6.4.1).  
 (b) The modulation property in Eq. (6.4.4).  
 (c) The time-reversal property in Eq. (6.4.6).  
 (d) The convolution property in Eq. (6.4.9).

**6.9** (*Initial-Value Theorem*) Show that for a causal sequence  $x[n]$ , the initial value  $x[0]$  is given by the following limit:

$$x[0] = \lim_{z \rightarrow \infty} X(z).$$

Determine the initial value of  $x[n]$  in each of these cases:

- (a)  $X(z) = (a - z^{-1})/(1 - az^{-1})$ ,  $|z| > |a|$ .  
 (b)  $X(z) = z^{-1}/(1 - az^{-1} + a^2z^{-2})$ ,  $|z| > |a|$ .  
 (c)  $X(z) = \log(1 - az^{-1})$ ,  $|z| > |a|$ .  
 (d)  $X(z) = e^{az}$ ,  $|z| > 0$ .
- 6.10** The following results are required to invert  $z$  transforms having multiple poles by partial-fraction expansion, as described in Appendix 6B.

(a) Using the differentiation property in Eq. (6.4.7), determine the inverse  $z$  transform of

$$X(z) = \frac{1}{(1 - az^{-1})^2}, \quad |z| > |a|.$$

Repeat for  $|z| < |a|$ .

(b) Generalize this result to the transform

$$X(z) = \frac{1}{(1 - az^{-1})^N}, \quad |z| > |a|$$

Repeat for  $|z| < |a|$ .

**6.11** Using the properties in Table 6.1, find the  $z$  transform (including the ROC) for each of the following signals.

- (a)  $a^n u[n - n_0]$ ,  $n_0 > 0$ .      (b)  $a^n u[n + n_0]$ ,  $n_0 > 0$ .  
 (c)  $\text{Od}\{a^n u[n]\}$ ,  $|a| < 1$ .      (d)  $e^{j\Omega_0 n} u[n]$ .  
 (e)  $(\cos \Omega_0 n) u[-n]$ .      (f)  $r[n] = u[n] * u[n]$ .



**6.17** Find the step response  $s[n]$  for each of the following systems:

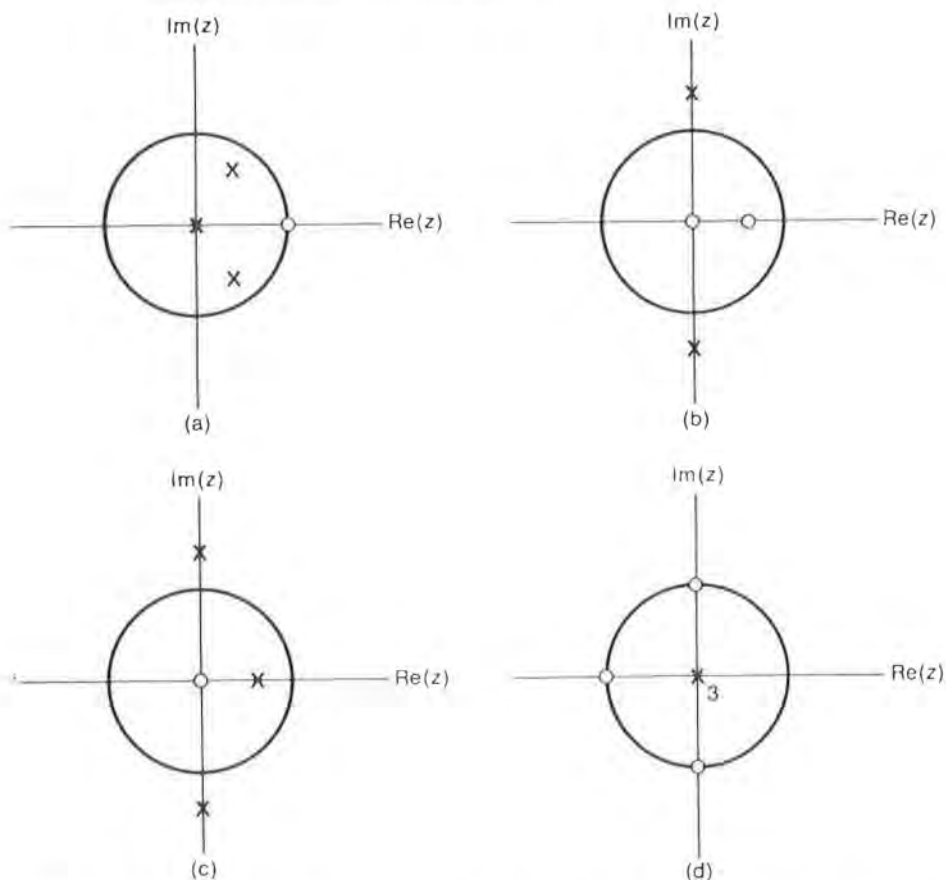
$$(a) H(z) = \frac{1}{1 + z^{-1}}, \quad |z| > 1.$$

$$(b) H(z) = \frac{2z^{-1}}{1 - 3z^{-1}}, \quad |z| < 3.$$

$$(c) H(z) = 1 - z^{-3}, \quad |z| > 0.$$

$$(d) H(z) = \frac{z^{-1} - z^{-2}}{1 - 2z^{-1} + 2z^{-2}}, \quad |z| < \sqrt{2}.$$

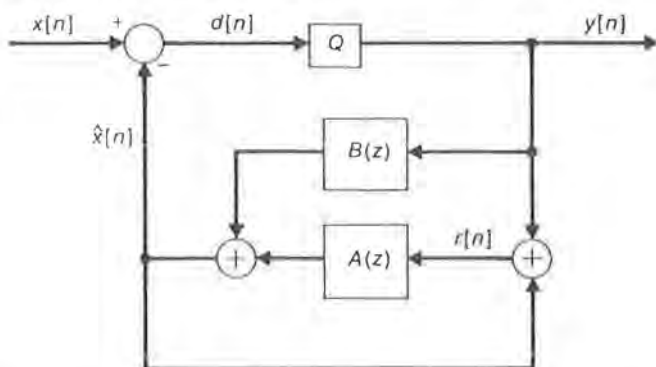
**6.18** For each of the following pole/zero plots, show the ROC for stability. Also, assuming no poles at  $z = \infty$ , identify the (stable) systems that are causal, anticausal, IIR, and/or FIR.



**6.19** For each of the following pairs of systems, determine the system function  $H_p(z)$  and the impulse response  $h_p[n]$  for the parallel interconnection of the two systems and likewise  $H_c(z)$  and  $h_c[n]$  for the cascade interconnection.

- (a)  $h_1[n] = a^n u[n]$  and  $h_2[n] = a^n u[n - 1]$ .  
 (b)  $h_1[n] = h_2[-n] = a^n u[n]$ ,  $|a| < 1$ .  
 (c)  $h_1[n] = a^n u[n]$  and  $h_2[n] = b^{n-1} u[n - 1]$ ,  $a \neq b$ .  
 (d)  $h_1[n] = (ja)^n u[n]$  and  $h_2[n] = (-ja)^n u[n]$ .  
 (e)  $h_1[n] = e^{j\Omega n} u[n]$  and  $h_2[n] = e^{-j\Omega n} u[n]$ .

**6.20** A new international standard has recently been established for digital telephone transmission at 32 kilobits per second using *adaptive differential pulse-code modulation* (ADPCM). The ADPCM encoder at the transmitter can be diagrammed as shown.



The feedback loop generates a *prediction*  $\hat{x}[n]$  of the input signal  $x[n]$ , and the difference signal  $d[n] = x[n] - \hat{x}[n]$  is quantized by an adaptive quantizer  $Q$  to produce the encoder output  $y[n]$ . The decoder at the receiver corresponds to the inverse of the encoder and produces the recovered signal  $r[n]$  that, in the absence of quantization and transmission errors, would equal the original signal  $x[n]$ . If we neglect the time-varying nature of the adaptive filters  $A(z)$  and  $B(z)$ , their system functions are given by

$$A(z) = a_1 z^{-1} + a_2 z^{-2}$$

and

$$B(z) = b_1 z^{-1} + b_2 z^{-2} + \cdots + b_6 z^{-6}.$$

The quantizer  $Q$  is also neglected in the following analysis.

- (a) Find the encoder system function  $H_e(z)$  from  $x[n]$  to  $y[n]$ .  
 (b) Show that the signal  $r[n]$  in the encoder equals  $x[n]$ , that is, that the system function  $H_r(z)$  from  $x[n]$  to  $r[n]$  is unity.  
 (c) Diagram a decoder network  $H_d(z)$  in terms of  $A(z)$  and  $B(z)$  with input  $y[n]$  and output  $r[n]$  such that  $H_d(z) = 1/H_e(z)$ .  
 (d) How many finite nonzero poles and zeros does the encoder have? The decoder?

- (e) A *minimum-phase* system has all of its zeros, as well as its poles, inside the unit circle. Why is it necessary for the encoder to be minimum phase?
- 6.21** For each of the following systems, find all of the corresponding inverse systems  $H_I(z)$ . Which inverse systems are stable? Causal? FIR?
- (a)  $h[n] = (0.9^n + 0.5^n)u[n]$ .      (b)  $h[n] = (0.9^n - 0.5^n)u[n]$ .  
 (c)  $h[n] = \delta[n] + \delta[n - 2]$ .      (d)  $h[n] = (-1)^n u[-n]$ .  
 (e)  $h[n] = 2^{-|n|}$ .      (f)  $h[n] = 16\delta[n] - \delta[n + 4]$ .
- 6.22** (a) Write difference equations relating the input  $x[n]$  and the output  $y[n]$  for the first-order LPF in Eq. (6.6.8) and HPF in Eq. (6.6.9).  
 (b) Repeat for the second-order LPF, HPF, BPF, and BSF in Eqs. (6.6.29–32).
- 6.23** Show that the conditions

$$|a_2| < 1 \quad \text{and} \quad |a_1| < 1 + a_2$$

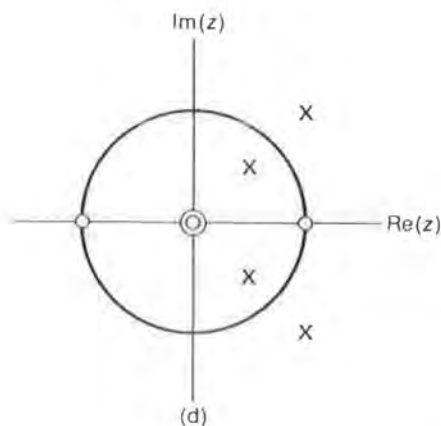
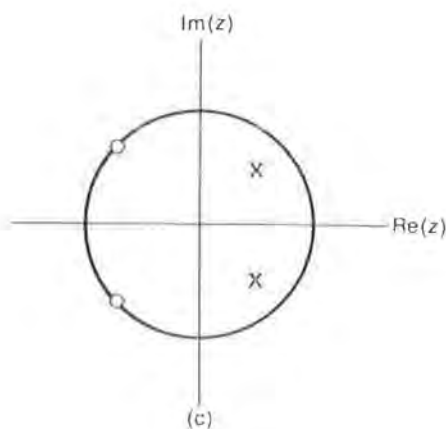
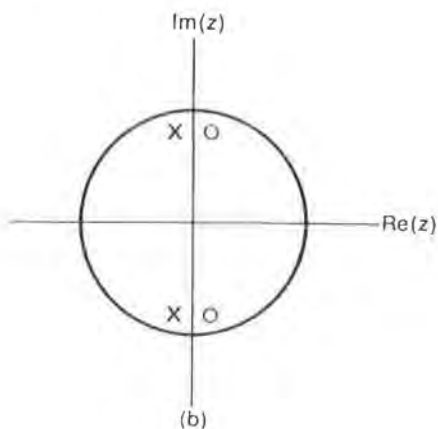
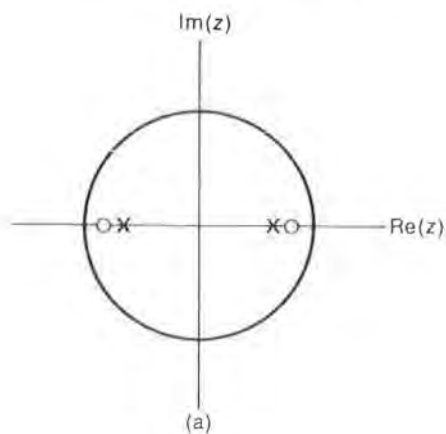
guarantee the stability of a causal, rational second-order system function with denominator  $1 + a_1 z^{-1} + a_2 z^{-2}$  for real-valued coefficients  $a_1$  and  $a_2$ . (*Hint*: For complex-conjugate poles  $p$  and  $p^*$ , we need  $|p| < 1$ , while for real poles  $p_1$  and  $p_2$ , we must have  $-1 < p_1, p_2 < 1$ .)

- 6.24** Given an  $N$ th-order *prototype* LPF design  $H_p(z)$ , a set of corresponding HPF, BPF, and BSF designs with specified cutoff frequencies can be produced by the *spectral transformation*  $H(z) = H_p[G(z)]$ , where  $G(z)$  is one of the *allpass* functions defined below. (Formulas for the parameters  $g$ ,  $g_1$ , and  $g_2$  are provided in several references noted in the Bibliography (e.g., in Jackson and in Oppenheim and Schaffer.)
- (i)  $H(z)$  is an  $N$ th-order HPF for  $G(z) = -(z - g)/(1 - gz)$ .  
 (ii)  $H(z)$  is a  $2N$ th-order BPF for  $G(z) = -(z^2 + g_1 z + g_2)/(1 + g_1 z + g_2 z^2)$ .  
 (iii)  $H(z)$  is a  $2N$ th-order BSF for  $G(z) = (z^2 + g_1 z + g_2)/(1 + g_1 z + g_2 z^2)$ .

In each of the following, let  $H_p(z)$  be the first-order LPF in Eq. (6.6.8).

- (a) Show that the spectral transformation in (i) produces a first-order HPF of the form in Eq. (6.6.9).  
 (b) Show that the spectral transformation in (ii) produces a second-order BPF of the form in Eq. (6.6.31).  
 (c) Show that the spectral transformation in (iii) produces a second-order BSF having a numerator of the form in Eq. (6.6.32).

6.25 For each of the pole/zero plots below, sketch the magnitude response  $|He^{j\Omega}|$  of the corresponding (stable) system.



6.26 (a) Using geometric analysis, show that the 3-dB bandwidth of the second-order BPF in Eq. (6.6.31) is about  $2(1-r)$  radians for  $0 \ll r < 1$ .

(b) Repeat for the second-order BSF in Eq. (6.6.32).

For each of the following denominator polynomials  $A(z)$ , give corresponding BPF and BSF systems functions  $H(z)$ , sketch the magnitude responses  $|H(e^{j\Omega})|$ , and state the approximate 3-dB bandwidth and center frequency  $\Omega_0$ .

(c)  $A(z) = 1 - 0.9z^{-1} + 0.81z^{-2}$       (d)  $A(z) = 1 + 0.98z^{-2}$

(e)  $A(z) = 1 - 1.5z^{-1} + 0.75z^{-2}$       (f)  $A(z) = 1 + z^{-1} + 0.5z^{-2}$

## 6.27 The 3-dB bandwidth of the first-order LPF

$$H(z) = C \frac{1 + z^{-1}}{1 - az^{-1}}, \quad |z| > |a|,$$

was estimated in Example 6.23 as simply  $\Omega_b \approx (1 - a)$  in the narrowband case ( $0 \ll a < 1$ ). Given a desired bandwidth  $\Omega_b$  in the general case (narrowband or wideband), the required values of the parameters  $a$  and  $C$  can be determined precisely from the magnitude-squared response  $|H(e^{j\Omega})|^2$ , as follows: First,

$$|H(e^{j\Omega})|^2 = H(e^{j\Omega})H^*(e^{j\Omega}) = \frac{1 + \cos \Omega}{f_0 + f_1 \cos \Omega},$$

where  $f_0$  and  $f_1$  are functions of  $a$  and  $C$ . Noting that  $|H(e^{j0})| = 1$  and  $|H(e^{j\Omega_b})| = 1/\sqrt{2}$  for a unity-gain LPF with 3-dB bandwidth  $\Omega_b$ , and using the above expression for  $|H(e^{j\Omega})|^2$ , write two simultaneous linear equations from which the values of  $f_0$  and  $f_1$  can be determined, given  $\Omega_b$ . Then indicate how the desired parameters  $a$  and  $C$  can be evaluated.

6.28 An allpass filter has the property that  $|H(e^{j\Omega})| = 1$  for all frequencies  $\Omega$ , that is,

$$H(e^{j\Omega}) = e^{j\theta(\Omega)},$$

where  $\angle H(e^{j\Omega}) = \theta(\Omega)$ . Such filters are used in cascade with other systems to modify (*equalize*) the phase response of the overall cascade system, as well as in certain derivations and transformations.

- (a) Given the  $N$ th-order polynomial  $A(z) = a_0 + a_1 z^{-1} + \cdots + a_N z^{-N}$ , show that the filter

$$H(z) = \pm \frac{z^{-N} A(z^{-1})}{A(z)}$$

is allpass if the coefficients  $a_k$  are real-valued.

- (b) Determine the explicit form of the numerator polynomial  $z^{-N} A(z^{-1})$ .
- (c) If the allpass filter is both stable and causal, what restriction applies to the locations of its zeros in the  $z$  plane? If the poles have values  $p_1, \dots, p_N$ , give the values of the zeros.
- (d) If  $A(z) = 1 - a^4 z^{-4}$ ,  $0 < a < 1$ , draw the corresponding pole/zero plot.
- (e) Sketch the phase response  $\angle H(e^{j\Omega})$  for

$$H(z) = \frac{z^{-1} - a}{1 - az^{-1}}, \quad 0 < a < 1.$$

- 6.29** One class of second-order LPF or HPF has double zeros at  $z = -1$  or  $z = 1$ , respectively, as shown in Eqs. (6.6.29) and (6.6.30). Another LPF/HPF class has complex-conjugate zeros on the unit circle, corresponding to system functions of the form

$$H(z) = \frac{1 - 2(\cos \Omega_1)z^{-1} + z^{-2}}{1 - 2r(\cos \Omega_0)z^{-1} + r^2z^{-2}}, \quad |z| > r,$$

where  $H(z)$  is lowpass for  $\Omega_0 < \Omega_1$  and highpass for  $\Omega_0 > \Omega_1$ . Draw the pole/zero plot for  $H(z)$  in each of the following cases, indicating the values of  $r$ ,  $\Omega_0$ , and  $\Omega_1$ , and sketch the corresponding magnitude response  $|H(e^{j\Omega})|$ .

- (a)  $H(z) = \frac{1 + z^{-1} + z^{-2}}{1 - z^{-1} + 0.5z^{-2}}$   
 (b)  $H(z) = \frac{1 - z^{-1} + z^{-2}}{1 + z^{-1} + 0.5z^{-2}}$   
 (c)  $H(z) = \frac{1 + z^{-2}}{1 - z^{-1} + 0.333z^{-2}}$   
 (d)  $H(z) = \frac{1 + z^{-2}}{1 + z^{-1} + 0.333z^{-2}}$   
 (e)  $H(z) = \frac{1 + \sqrt{3}z^{-1} + z^{-2}}{1 - 0.8z^{-1} + 0.64z^{-2}}$   
 (f)  $H(z) = \frac{1 - \sqrt{2}z^{-1} + z^{-2}}{1 + 1.5z^{-1} + 0.75z^{-2}}$

- 6.30** The zeros of linear-phase FIR filters have several interesting and useful properties relative to their locations in the  $z$  plane. In the following, assume that the  $M$ th-order FIR filter  $H(z)$  is linear-phase and that its coefficients  $b_n$  are real-valued.

- (a) Show that  $H(z)$  satisfies  $H(z) = z^{-M}H(z^{-1})$  or  $H(z) = -z^{-M}H(z^{-1})$ .  
 (b) Show that if  $z_0$  is a zero of  $H(z)$ , then  $z_0^*$ ,  $1/z_0$ , and  $1/z_0^*$  are also zeros.  
 (c) As a consequence of part (b), zeros can occur singly at  $z = \pm 1$ , in real-valued pairs, in complex-conjugate pairs on the unit circle, or in conjugate/reciprocal quadruples. Give simple examples of  $H(z)$  in each case.  
 (d) Show that for even symmetry in  $h[n]$  and  $M$  odd, there is always a zero at  $z = -1$ . [Hint: Consider Eq. (6.6.37) for  $H(-1)$  in this case.] Similarly, for odd symmetry in  $h[n]$  and  $M$  even, show that there is always a zero at  $z = -1$ .

- (e) Show that for odd symmetry in  $h[n]$  with  $M$  even or odd, there is always a zero at  $z = 1$ . [Hint: Consider Eq. (6.6.37) for  $H(1)$  in this case.]
- 6.31** A simple but useful method for smoothing a noisy data sequence is called *smoothing by 3s and 5s*. It consists effectively of the cascade of two uniform-averaging filters as defined in Eq. (6.6.43), with  $M + 1 = 3$  in one filter and  $M + 1 = 5$  in the other.
- Sketch the pole/zero plot and magnitude response for each of the cascaded averaging filters.
  - Sketch the pole/zero plot and magnitude response of the overall filter.
  - Find the impulse response of the overall filter.
  - What is the order of the overall filter?
  - What is the dc gain of the overall filter? What is the gain at  $\Omega = \pi$ ?
  - Draw block diagrams for the overall filter as the cascade of two transversal structures and as a single transversal structure.
- 6.32** Each of the following linear-phase FIR filters has its zeros on the unit circle and thus annihilates sinusoidal signals of the form  $x[n] = \sin(\Omega_0 n + \phi)$  for some frequency  $\Omega_0$  and all phase angles  $\phi$ ; that is,  $y[n] = 0$  for all  $n$ .
- $H(z) = 1 - \sqrt{2}z^{-1} + z^{-2}$ .
  - $H(z) = 1 + z^{-1} + z^{-2}$ .
  - $H(z) = 1 - z^{-1} + z^{-2}$ .
  - $H(z) = 1 + z^{-2}$ .

Match each of these filters with one or more of the sequences  $x[n]$  below that it annihilates. Carry out the convolution  $y[n] = h[n] * x[n]$  for several values of  $n$  in each case to check that  $y[n]$  is indeed zero.

- $\{\dots, A, A, -A, -A, \dots\}$
  - $\{\dots, A, -A, 0, \dots\}$
  - $\{\dots, A, 0, -A, 0, \dots\}$
  - $\{\dots, A, A, 0, -A, -A, 0, \dots\}$
  - $\{\dots, A, 2A, A, -A, -2A, -A, \dots\}$
  - $\{\dots, A, \sqrt{2}A, A, 0, -A, -\sqrt{2}A, -A, 0, \dots\}$
- 6.33** Draw direct-form-II structures for the second-order LPF, HPF, BPF, and BSF in Eqs. (6.6.29–32). If coefficients with integer values do not require actual multipliers (only binary shifts and/or sign changes), how many multiplications per output sample  $y[n]$  are required, in general, to implement each filter?
- 6.34** In general, an  $M$ th-order FIR filter requires  $M + 1$  multipliers in its

(transversal) implementation. However, for linear-phase filters, only about  $M/2$  multipliers are required if the distribution property of arithmetic is utilized. Show how this savings is accomplished for both even and odd symmetry in  $h[n]$  by drawing the corresponding transversal structures.

- 6.35** Draw direct-form-II, parallel-form-II, and cascade-form-II structures for each of the following filters, using first-order sections with real-valued coefficients wherever possible.

$$(a) H(z) = \frac{1}{1 - 0.49z^{-2}}, \quad (b) H(z) = \frac{1 + z^{-3}}{1 - 0.512z^{-3}}$$

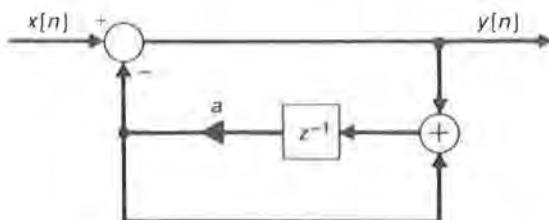
$$(c) H(z) = \frac{0.5 - 2z^{-1} + 0.8z^{-2}}{1 - 1.3z^{-1} + 0.4z^{-2}}, \quad (d) H(z) = \frac{0.25 + z^{-4}}{1 + 0.25z^{-4}}$$

- 6.36** It is possible (although usually not desirable) to implement FIR filters using recursive structures. As an example, draw a (recursive) direct-form-II structure for the uniform-averaging filter as expressed in Eq. (6.6.44). Is this structure canonical? Is it stable in the sense that the intermediate signal  $w[n]$  in Fig. 6.30, as well as the output  $y[n]$ , is bounded for all bounded inputs  $x[n]$ ?

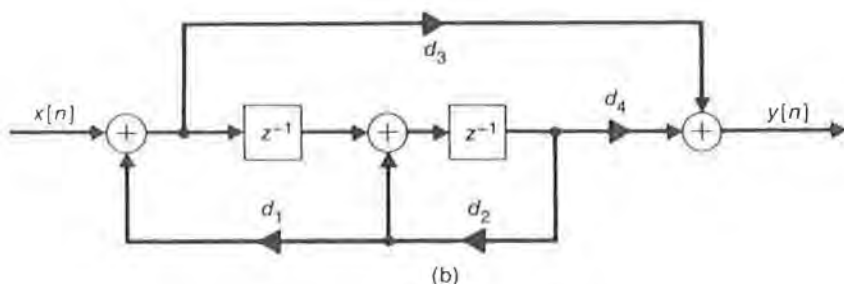
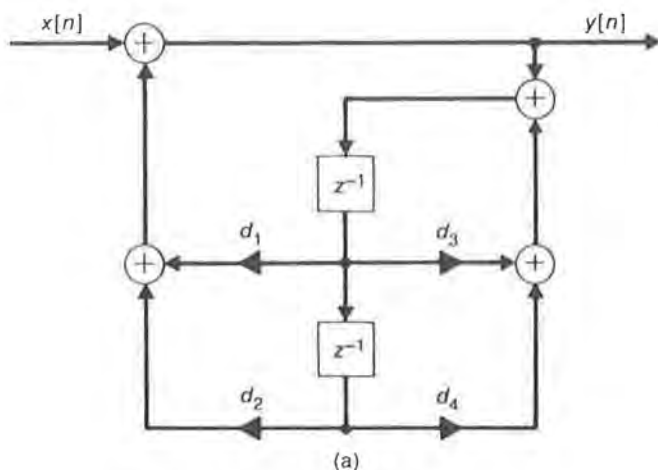
- 6.37** (a) Show that the feedback interconnection of two (causal) subsystems  $F(z)$  and  $G(z)$  depicted in Fig. 6.10 results in the overall system function

$$H(z) = \frac{F(z)}{1 - F(z)G(z)}$$

- (b) Given that  $F(z) = K$  (constant), determine  $K$  and  $G(z)$  such that  $H(z)$  is the first-order LPF in Eq. (6.6.8). Repeat for the first-order HPF in Eq. (6.6.9). Is  $G(z)$  stable in either case?
- (c) Determine  $H(z)$  for the filter shown. Is the filter FIR or IIR? Is the structure recursive or nonrecursive?



- 6.38** Determine  $H(z)$  for each of the second-order systems shown. Give conditions on the coefficients  $d_i$  for the system to be stable and *minimum-phase* (i.e., both poles and zeros inside the unit circle).



**6.39** For each of the following difference equations and initial conditions, determine the output  $y[n]$  for  $n \geq 0$  using the unilateral  $z$  transform:

- (a)  $y[n] - 0.5y[n-1] = 2$ ,  $y[-1] = 0$ .  
 (b)  $y[n] - 0.5y[n-1] = 2$ ,  $y[-1] = 2$ .  
 (c)  $y[n] - 0.5y[n-1] = 2$ ,  $y[-1] = 4$ .  
 (d)  $y[n] + 0.25y[n-2] = 0$ ,  $y[-1] = 0$ ,  $y[-2] = 4$ .

**6.40** The autocorrelation function of a discrete-time signal  $x[n]$  is defined as

$$\phi_{xx}[n] = x[n] * x^*[-n] = \sum_{k=-\infty}^{\infty} x[n+k]x^*[k].$$

- (a) Express the  $z$  transform  $\Phi_{xx}(z)$  of the autocorrelation function in terms of  $X(z)$ . Also relate the regions of convergence  $R_x$  and  $R_\phi$ . State a condition on  $X(z)$  for  $\Phi_{xx}(z)$  to exist. What must be the form of  $R_\phi$  if it exists?
- (b) Let  $y[n]$  be the output of an LTI system with system function  $H(z)$  to the input  $x[n]$ . Express the  $z$  transform  $\Phi_{yy}(z)$  of the output autocorrelation in terms of  $H(z)$  and  $\Phi_{xx}(z)$ .

- (c) Let  $H(z)$  in part (b) be an allpass filter, as defined in Problem 6.28. Express the output autocorrelation  $\phi_{yy}[n]$  in terms of  $\phi_{xx}[n]$ .
- (d) Let  $x[n] = 0.5^n u[n]$  and  $h[n] = (-0.8)^n u[n]$ . Find  $\phi_{xx}[n]$  and  $\phi_{yy}[n]$ .

**6.41** Write the following subroutines in Fortran, Pascal, Basic, etc., with the indicated arguments to implement discrete-time filters in parallel and cascade form II:

- (a) CASSEC (X1, Y1, A1, A2, B1, B2, D1, D2) to implement a second-order cascade-form-II section, where X1 is the section input, Y1 is the section output, A1 and A2 are the feedback coefficients, B1 and B2 are the feedforward coefficients, and D1 and D2 are the contents of the delays. (*Hint*: Be careful to update D1 and D2 in the correct order.)
- (b) PARSEC (X1, Y1, A1, A2, G1, G2, D1, D2) to implement a second-order parallel-form-II section as above, except that G1 and G2 are the feedforward coefficients.
- (c) CASFORM (X, Y, K, A, B, D, N, B0) to implement the overall cascade form, where arrays X and Y of dimension K contain, respectively, the input and output data  $x[n]$  and  $y[n]$  for  $n = 1, 2, \dots, K$ ; arrays A, B, and D of dimension N contain the feedback coefficients, feedforward coefficients, and delayed data, respectively; and B0 is the coefficient  $b_0$ . Assume that all arrays are initialized before the subroutine is called and make use of the subroutine CASSEC.
- (d) PARFORM (X, Y, K, A, G, D, N, G0) to implement the overall parallel form as above, except that G is the feedforward coefficient array and G0 is the coefficient  $g_0$ . Make use of the subroutine PARSEC.